

Carl von Ossietzky Universität Oldenburg

School of Mathematics and Science, Institute of Physics

European Master in Renewable Energies

Master's Thesis

Title:

**Well-to-Wake Prospective Life Cycle Assessment of Synthetics Fuels for the
Maritime Sector in the Baltic and North Seas**

Presented by: Zulma Karina Aza Pedraza

First Examiner: Dr. Urte Brand-Daniels

Second Examiner: Prof. Dr. Carsten Agert

Place, Date: Oldenburg, Germany, 17.02.2025

ABSTRACT

The utilization of synthetic fuels produced from renewable sources has been considered as an alternative solution to lowering maritime sector emissions. Nevertheless, the synthetic fuel processes involved in the supply chain from production location to bunkering port pose significant challenges due to the additional emissions generated from these processes. A prospective life cycle assessment (pLCA) is crucial for defining environmental hotspots of Well-to-Wake (WTW) and how the results can change regarding the increasing shares of renewable sources in 2030 and 2050 electricity generation scenarios comparing to base case (2019).

This study focuses on a case study using pLCA for Well-to-Tank (WTT) and WTW scopes. The WTT includes e-hydrogen, e-ammonia and e-methanol pathways produced in Wilhelmshaven, Germany and transported to Rotterdam, the Netherlands as a final bunkering port. Key processes such as e-hydrogen production, compression, e-ammonia and e-methanol synthesis, storage, transport, ammonia cracking and methanol dehydrogenation are analysed. Moreover, for the WTW scope, which integrated the WTT and the Tank-to-Wake (TTW) phases for the utilization of e-hydrogen in a Roll-on/Roll-off Ship with a Proton Exchange Membrane fuel cell (PEMFC) or Internal Combustion Engine (ICE) to produce electricity for the ship in a round trip from Rotterdam to Immingham, UK.

Results reveal that within the WTT scope, the e-methanol pathway has the highest global warming potential (GWP) impact (0.067 kg CO₂ eq /MJ_{LHV}), followed by e-ammonia (0.058 kg CO₂ eq /MJ_{LHV}), while e-hydrogen pathway has the lowest GWP impact (0.029 kg CO₂ eq /MJ_{LHV}) for the base case. By 2030, increasing photovoltaic and wind electricity shares are expected to reduce GWP emissions by 55%, 67%, and 43% for e-hydrogen, e-ammonia, and e-methanol pathways, respectively compared to the base case. By 2050, the reductions are projected to reach 59%, 66%, and 42% for e-hydrogen, e-ammonia, and e-methanol pathways, respectively. Furthermore, ICE represents the technology with the highest GWP impact (142 ton CO₂ eq /RT) compared to the PEMFC (112 ton CO₂ eq/RT) for the base case scenario. Future electricity generation scenarios show significant GWP reductions of 53% for both technologies by 2030 and 54% and 52% for PEMFC and ICE by 2050, respectively. Considering other categories, e-hydrogen shows the lowest impact in future scenarios. Decreasing trends were observed for acidification, eutrophication, and energy resources, whereas material resource demand and land use are projected to increase. This study concludes the decisive role of renewable energy integration in enhancing the environmental performance of synthetic fuel pathways, with e-hydrogen emerging as the most favourable option for the WTT scope and PEMFC. Finally, the WTW results emphasize the need to account for upstream synthetic fuel stages in environmental assessments.

ACKNOWLEDGEMENT

I would like to express my sincere gratitude to Dr. Urte Brand-Daniels and the specialist supervisor, Komal Mallesh Chougule, for their invaluable guidance, support, and insightful feedback throughout this study. I am also thankful to the German Aerospace Center (DLR), Institute of Networked Energy Systems, particularly the Energy Scenarios and Technology Assessment Group, for providing the necessary resources and a favourable environment to complete this work. Additionally, I am grateful to my family and friends, who gave me the strength and encouragement to achieve this goal.

TABLE OF CONTENT

TABLE OF CONTENT	4
1 Introduction.....	9
1.1 Background	9
1.2 Motivation and Problem Statement.....	10
1.3 Aim of the Study and Research Questions	11
1.4 Thesis Outline	11
2 Theoretical Background	12
2.1 Literature Review Criteria	12
2.2 Synthetic Fuels for Maritime transportation.....	12
2.2.1 E-hydrogen from Water Electrolysis.....	13
2.2.2 E-ammonia via Nitrogen from Air Separation Unit.....	14
2.2.3 Carbon Dioxide CO ₂ sources	15
2.2.4 E-methanol Synthesis.....	15
2.3 Maritime Supply Chains Using Synthetic Fuels.....	16
2.3.1 Compressed e-hydrogen	16
2.3.2 E-ammonia	21
2.3.3 E-methanol	23
2.4 Synthetic fuels Powertrain System in the Maritime Sector	24
2.4.1 Fuel Cells	25
2.4.2 Internal Combustion Engines.....	26
2.5 State-of-the-art of LCA and pLCA of Synthetic Fuels maritime supply chains.....	26
3 Methodology	28
3.1 Overview of Prospective Life Cycle Assessment Methodology	28
3.1.1 Goal and Scope Definition	29
3.1.2 Life Cycle Inventory -LCI	29
3.1.3 Life Cycle Impact Assessment -LCIA.....	29
3.1.4 Interpretation	30
3.1.5 Tools and software	30
3.2 Prospective Life Cycle Assessment – WTW Study	30
3.2.1 Goal and Scope definition.....	30
3.2.2 Functional Unit.....	38
3.2.3 System Boundaries.....	38
3.2.4 Life Cycle Inventory	39
3.2.5 Life Cycle Impact Assessment.....	44
3.2.6 Interpretation	45
4 Results	46

4.1	Part 1: WTT Results	46
4.1.1	Global Warming Potential (Kg CO ₂ eq) Category: WTT Scope	46
4.1.2	Impact assessment of Other Categories: WTT Scope	52
4.2	Part 2: Well-to-Wake WTW Scope Results	54
4.2.1	Global Warming Potential (Kg CO ₂ eq) Category	54
4.2.2	Impact Assessment of Other Categories – WTW Results	55
5	Discussion	56
5.1	Comparative Review of WTT GWP Results with prior Studies.	56
5.2	GWP Reduction through Compressed H ₂ in Energy Conversion Technologies 58	
5.3	Effect of GWP in WTT Phases Following H ₂ Production	59
5.4	Effect of GWP in Storage and transport phases following H ₂ Production in the WTT Scope.	60
5.5	Green Hydrogen vs. H ₂ Production from Electricity Generation scenarios	61
5.6	CO ₂ -Equivalent Contributors for the WTW Scope Using PEMFC and ICE	62
6	Limitation of the study	63
7	Conclusions	64
8	Future Work	67
9	References	69

LIST OF FIGURES

Figure 1 Literature review approach. Own plot Adapted from [10].....	12
Figure 2 General supply chain for compressed hydrogen [own figure].....	17
Figure 3 Key components of hydrogen pipeline system [30]	18
Figure 4 Pilot-scale compressed H ₂ Ship [32]	19
Figure 5 Tube trailer develop by Calvera Hydrogen [34].	19
Figure 6 General supply chain for e-ammonia [own figure]	21
Figure 7 General supply chain for e-methanol [own figure]	23
Figure 8 Powertrain configuration for PEMFC and ICE. Plot created with icons provided by DLR and adapted from [8]	25
Figure 9 WTW system boundary. Plot created with icons provided by DLR and adapted from [78]	31
Figure 10 WTT System boundary phases: e-hydrogen pathway [own figure].....	33
Figure 11 WTT System boundary phases: e-ammonia pathway [own figure].....	34
Figure 12 WTT system boundary phases: e-methanol pathway [own figure].....	36
Figure 13 System boundaries applied for the study. Own plot adapted from [8]. Grey boxes represent the foreground processes, and blue represents the background processes. Boxes with dotted lines represent future estimations.	39
Figure 14 LCI Flow diagram WTT phases.....	40
Figure 15 Flow diagram for energy conversion technologies.....	40
Figure 16 Electricity generation scenarios: Germany and Netherlands [76] [95].....	42
Figure 17 GWP of WTT synthetic fuel pathways.....	46
Figure 18 GWP of H ₂ pathway for BC, 2030 and 2050 scenarios.....	47
Figure 19 GWP of NH ₃ pathway for BC, 2030 and 2050 scenarios	49
Figure 20 GWP of CH ₃ OH pathway for BC, 2030 and 2050 scenarios.....	51
Figure 21 Environmental impacts of EF 3.1 impact categories for synthetic WTT fuels pathways	53
Figure 22 GWP for the PEMFC and ICE utilization per RT (WTW)	55
Figure 23 Environmental impacts of EF 3.1 categories using PEMFC and ICE per RT - All Scenarios.....	56
Figure 24 GWP Comparison results of WTW analysis with MFO	59
Figure 25 Impact of GWP in WTT supply chain phases for H ₂ production.....	59
Figure 26 GWP of WTT pathways considering electricity generation scenarios for H ₂ production.....	62
Figure 27 Elementary flow contribution of WTW PEMFC	63
Figure 28 Elementary flow contribution of WTW ICE.....	63

LIST OF TABLES

Table 1 Technical characteristics of electrolysis technologies. Adapted from [13, 14].	13
Table 2 Advantages and challenges for electrolysis technologies. Adapted from [13, 14]	14
Table 3 Key properties of synthetic fuels [16, 23, 24]	16
Table 4 Comparison of compressed storage tank types [27] [28]	18
Table 5 Key Characteristics Fuel Cells [49] [50] [51]	25
Table 6 Characteristics of ICE per fuel type [55]	26
Table 7 Key information of Life Cycle Assessments from the literature review	27
Table 8 Impact categories EF 3.1 [73]	29
Table 9 Key Parameters Case 1: e-hydrogen pathway [84][82][59]	33
Table 10 Key Parameters Case 2: e-ammonia pathway [4] [16] [8, 85]	35
Table 11 Key Parameters case 2: e-methanol pathway [4] [82] [8]	36
Table 13 Main specifications Magnolia Seaways [86]	37
Table 14 Operation data of one round trip	37
Table 15 Energy conversion technologies parameters	38
Table 16 EF3.1 Impact categories used in the study [72]	44

LIST OF ABBREVIATIONS

ASU	Air Separation Unit
BC	Base Case
CH ₃ OH	Methanol
CH ₄	Methane
CO ₂	Carbon Dioxide Emissions
DAC	Direct Air Capture
FC	Fuel Cell
GHG	Greenhouse Gas
GWP	Global Warming Potential
H ₂	Hydrogen
HFO	Heavy Fuel Oil
IAM	Integrated Assessment Model
ICE	Internal Combustion Engine
IMO	International Maritime Organization
km	Kilometre
LCA	Life Cycle Assessment
LCI	Life Cycle Inventory
LCIA	Life Cycle Impact Assessment
LHV	Lower Heating Value
LNG	Liquid Natural Gas
LOHC	Liquid Organic Hydrogen Carrier
LSFO	Low Sulphur Fuel Oil
MJ _{LHV}	Megajoule of the lower heating value.
MFO	Marine Fuel Oil
N ₂ O	Nitrogen Dioxides
NH ₃	Ammonia
NO _x	Nitrogen Oxides
PEMFC	Proton Exchange Membrane Fuel Cell
pLCA	prospective Life Cycle Assessment
PM	Particulate Matter
PSA	Pressure swing adsorption
PV	Photovoltaic
RCPs	Representative Combination pathways
Ro-Ro	Roll-on/Roll-off
RT	Round Trip
SMR	Steam Methane Reforming
SO _x	Sulphur oxide
SSPs	Share Socio-economic pathways
TRL	Technology Readiness level
TTW	Tank-to-Wake
WTT	Well-to-Tank
WTW	Well-to-Wake

1 Introduction

1.1 Background

While maritime transport plays an essential role in the European Union (EU) economy and is one of the most energy-efficient modes of transport, it is also a large and growing source of greenhouse gas (GHG) emissions [1]. In 2018, global maritime emissions represented 1,076 million tonnes of CO₂ and were responsible for around 2.9% of global emissions caused by human activities. According to the Fourth International Maritime Organization (IMO) Report [2], the current trend indicates that by 2030 maritime transport could account for between 85% and 105% of the 2008 reference year emissions, and between 90% and 130% by 2050. Furthermore, the FuelEU maritime initiative, which is part of the “Fit for 55 Package” established in 2023 by the Council of European Union [3], the GHG intensity limit on energy used on board by a ship, starting in 2025, a 2% reduction from the reference value (91.16 gr CO₂ eq/MJ) and a gradual increase up to 80% by 2050 [3]. In response to this challenge, The International Maritime Organization IMO has set a strategy for the reduction of GHG emissions from ships adopted on 7 July of 2023, which defines levels of ambitions to ensure technological innovation and introduction and availability of zero or near zero GHG emissions technologies, fuels and energy sources for international shipping [4]. For the European Union, the North and Baltic are the most frequented seas. More than 30,000 vessels travel the North/Baltic Sea Canal annually, and about 2,000 vessels cross the Baltic Sea each day at any time [2]. Therefore, maritime traffic results in a significant consumption of maritime fuels derived from fossil sources, which generates a considerable environmental impact, such as air pollution and GHG emissions mainly produced by marine fuels, particularly heavy fuel oil (HFO).

To address these challenges, synthetic fuels produced from renewable sources are expected to be more pivotal. The replacement of fossil-based maritime fuels with synthetic fuels derived from renewable energy sources is a promising pathway for lowering emissions in the maritime sector. One possible pathway for the production of synthetic fuels is using green hydrogen produced from water electrolysis technologies such as alkaline, proton exchange membrane and solid oxide electrolysis using renewable energy sources such as wind or photovoltaics. When methanol and ammonia are produced from hydrogen, which is produced from renewable energies, they can be called e-methanol and e-ammonia [5]. Among the synthetic fuels produced with hydrogen, e-ammonia and e-methanol are required in the maritime sector to reduce local air pollution and adhere to regulations, minimizing environmental and climatic effects of shipping due to associated emissions of GHG, nitrogen oxides (NO_x), and sulphur oxides (SO_x) [6].

For the Baltic and North Sea hydrogen production projections based on the International Energy Agency (IEA) Hydrogen Production Projects Database, the Northwest Europe's production of hydrogen from renewable energies could top 7 million tonnes (Mt) per year by 2030 if all planned projects become commercially operational, which could mean that the North Sea could become a hub for non-fossil-based hydrogen [7]. As demonstrated by the following production projections, it is imperative to emphasise the necessity of developing and using infrastructure for synthetic fuels, not solely for the purpose of production but also for the supply chain.

1.2 Motivation and Problem Statement

Regarding the feasibility of large-scale implementation of production, distribution, storage and bunkering for synthetic fuels such as e-hydrogen, e-methanol and e-ammonia for the maritime sector, the International Renewable Energy Agency (IRENA) remarks the alternatives to have realistic mitigation pathways consistent with the goal of GHG emissions reduction. In addition, for the maritime sector, the transition towards climate neutrality is complex and is accompanied by changes in the fuel supply chain, propulsion system configuration, and infrastructure. These changes can result in an increase in emissions apart from those resulting from the synthetic fuel production. Therefore, it is essential to evaluate the future environmental impacts of different synthetic fuel supply chain pathways from the production, including storage and transport as a final stage of Well-to-Tank (WTT) as well as different propulsion systems as a Tank-to-Wake (TTW). These two elements are integrated to form the WTW scope.

Kanchiralla et al. [8], investigated the environmental impact of various decarbonization options assessed from the cradle to the grave for synthetic fuels through prospective life cycle assessment (pLCA). However, their study does not account for the environmental impacts of the processes following production that are required to transport the fuel to the bunkering port. The authors of the study acknowledge that that future studies may consider the location of fuel production based on the availability of feedstock and the fuel distribution between production sites and bunkering [8]. Moreover, Akhtar et al. [9] remark in their study that the importance of large-scale energy storage and mobility infrastructures are imperative for meeting the current global energy demand [9]. Consequently, the conditioning, which includes processes such as liquefaction and storage, and the reconditioning, which includes processes such as compression and evaporation, were subjected to a life cycle assessment along with transport phases [9]. While this study offers valuable insights through the implementation of life cycle assessment methodology, it does not address prospective scenarios.

Based on the research gaps outlined above, the novelty of the present study lies in its incorporation of technologies and processes for the storage and transport of synthetic

fuels, which are currently in the early stages of development and have the potential to mature within the projected time frame for the Life Cycle Assessment (LCA). Furthermore, the pathways will be determined for the North Sea in accordance with the production sites, serving as an initial and strategic filling point prior to utilisation in a reference ship. This analysis may be considered a representation of the environmental performance of a more realistic scenario. Consequently, the results obtained may be utilised in further technical and economic feasibility studies.

1.3 Aim of the Study and Research Questions

Based on the research gaps identified, the aim of the study is to conduct a pLCA, which will evaluate the future environmental impacts of different synthetic fuels (e-hydrogen, e-ammonia, e-methanol) from production to the bunkering port and the use of e-hydrogen in the energy conversion technologies on-board. Furthermore, the emissions and environmental impacts including global warming potential (GWP), acidification, marine eutrophication, energy, and material resources, as well as land use for the synthetic fuel pathways for base case and future electricity generation scenarios are quantified. Similarly, the following research questions will be addressed in this study:

- What are the global warming potential (GWP) key environmental hotspots from Well-to-Tank (WTT) of synthetic fuels pathway cases and Well-to-Wake (WTW) hydrogen energy conversion technologies to be used in the maritime transport of the North Sea?
- How does the level of environmental impacts differ between the various synthetic fuel pathways and e-hydrogen energy conversion technologies on board?
- How does the level of environmental impacts change regarding the increasing shares of renewable sources such as wind and solar energy in future electricity generation scenarios?

1.4 Thesis Outline

The structure of the present study is outlined as follows: the first chapter corresponds to the introduction, in which the motivation of the study, the objectives and the research questions were explained. The second chapter theoretical background presents a comprehensive overview of the production, supply chain processes and energy conversion technologies using synthetic fuels for maritime applications. Additionally, a state-of-the-art review of the application of LCA in synthetic fuels in the maritime sector is presented. The methodology section details the pLCA approach used for the study, adopting the ISO 14040/44. In turn, this chapter is divided into two parts, the first offering an overview of the methodology, while the second part details how the methodology is applied to the case study. Subsequently, in the results and discussion chapters, the

findings are presented, analysed, and interpreted in relation to the research questions. Finally, the limitations of the study, conclusions and future work are outlined.

2 Theoretical Background

2.1 Literature Review Criteria

In order to include relevant scientific articles and technical reports in the theoretical background and to establish the technical basis for the case study, an approach to conduct the literature review was defined based on the procedure described by Thonemann et al. [10]. Initially, keywords were formulated in alignment with the research questions and categorized into four main groups: synthetic fuels, energy conversion technologies, propulsion systems maritime application and LCA methodological approaches. These keywords were subsequently searched across the databases depicted in Figure 1. The criteria review and the forward and backward search approach were employed to identify the relevant information and data required for the study. As a result, 41 out of the 51 identified articles and reports were selected for case study definition, data analysis and literature review, including 17 articles focused on applications for maritime supply chains and on-board energy conversion technologies. The remaining articles were excluded from this study.

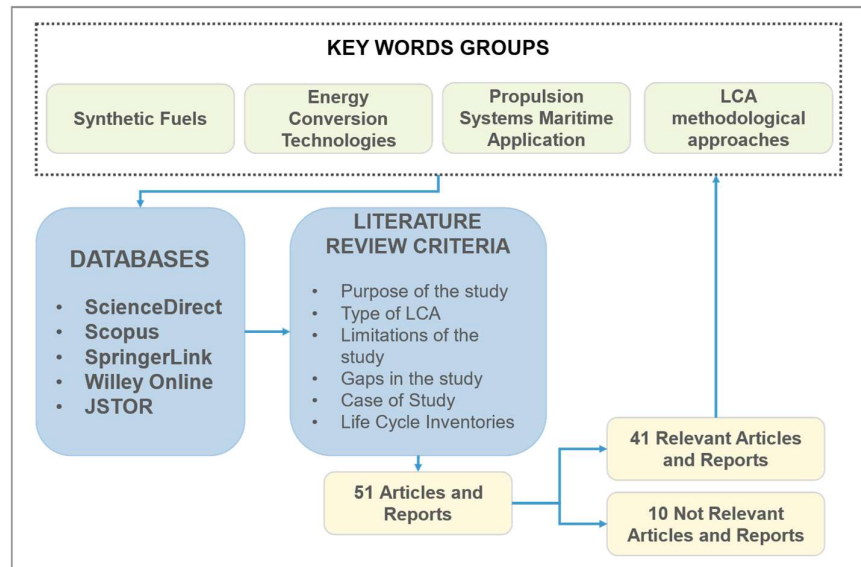


Figure 1 Literature review approach. Own plot Adapted from [10]

2.2 Synthetic Fuels for Maritime transportation

One of the strategies to decarbonize the maritime sector is to replace fossil fuels such as Marine fuel oil (MFO), Liquid Natural Gas (LNG) and Low Sulphur Fuel Oil (LSFO). However, fossil fuels produce vast amounts of CO₂ emissions and are the primary source of emissions in the maritime sector [11]. In order to achieve the goals set by the International Maritime Organization (IMO) of reducing CO₂ emissions by 50% by 2050,

it is imperative that the maritime sector explores the potential of renewable energy sources [11]. Renewable maritime fuels include a variety of alternatives, such as e-hydrogen, e-ammonia, and e-methanol. They can be classified as synthetic fuels when created from through chemical processes utilizing materials such as CO₂, water, and sustainable energy sources like wind or solar power [12]. This section outlines the electrolysis processes for hydrogen production, and subsequently, the production of e-ammonia from hydrogen and nitrogen from air separation, and the production of e-methanol from hydrogen and CO₂ by means of the direct air capture process (DAC).

2.2.1 E-hydrogen from Water Electrolysis

The water electrolysis is an electrochemical process where water is split into hydrogen and oxygen at room temperature with the help of electricity as is follow in equation 1 [13]:



The above mentioned reaction requires 1.23 V cell voltage to separate the water into hydrogen and oxygen at room temperature. However, experimentally the required cell voltage for efficient water splitting is 1.48 V [13].

This section will focus on three different types of electrolysis technologies such as alkaline, proton exchange membrane (PEM) and solid oxide electrolysis systems. Table 1 and Table 2 illustrate technical characteristics and the most relevant advantages and challenges for the water electrolysis technologies.

Table 1 Technical characteristics of electrolysis technologies. Adapted from [13, 14]

	Alkaline	PEM	Solid Oxide
Electrolyte	KOH/NaOH Alkaline Liquid	Solid polymer electrolyte (PFSA)	Yttria stabilized Zirconia (YSZ) Ceramic Electrolyte
Electrode/Catalyst (H ₂ Side)	Nickel coated perforated stainless steel	Iridium oxide	Ni/YSZ
Electrode/Catalyst (O ₂ Side)	Nickel coated perforated stainless steel	Platinum carbon	Perovskites (LSCF, LSM) (La,Sr,Co,FE) (La,Sr,Mn)
Nominal Current Density	0.2–0.8 A/cm ²	1–2 A/cm ²	0.3–1 A/cm ²
Voltage Range	1.4–3 V	0.4–2.0 V	1.0–1.5 V
Operating Temperature	70–90 ° C	50–80 ° C	700–850 ° C
Cell Pressure	< 30 bar	< 70 bar	1 bar
System Energy Consumption	4.5- 7.5 kWh Nm ⁻³	5.8- 7.8 kWh Nm ⁻³	2.5- 3.5 kWh Nm ⁻³
Efficiency	50%–78%	50%–83%	89% (laboratory)
Lifetime (stack)	60 000 h	50 000–80 000 h	20 000 h

Development Status	Mature	Commercialized	R & D
Technology Readiness Level - TRL	9	9	8

Table 2 Advantages and challenges for electrolysis technologies. Adapted from [13, 14]

	Alkaline	PEM	Solid Oxide
Advantages	<ul style="list-style-type: none"> Well established in industrial applications. It uses a cost-effective nickel catalyst. 	<ul style="list-style-type: none"> Commercialized technology. Operates higher current densities. High purity of the gases. 	<ul style="list-style-type: none"> High working temperature. High efficiency.
Challenges	<ul style="list-style-type: none"> It uses highly corrosive chemicals. Lower energy efficiency. 	<ul style="list-style-type: none"> Use of precious metals like platinum as catalysts. Requires higher purity water. High operating cost. 	<ul style="list-style-type: none"> Limited stability. Poor durability. Under development.

2.2.2 E-ammonia via Nitrogen from Air Separation Unit

E-ammonia can be produced by the Haber-Bosch process or ammonia synthesis, the most popular method from 19th century [15]. This process occurs at high pressure and temperatures and requires the presence of iron-based catalyst in an exothermic reaction [15]. Nitrogen from an air separation unit (ASU) processes such as cryogenic air separation and pressure swing adsorption (PSA) have been used to separate nitrogen from air [16]. Nitrogen is used as a reactant in conjunction with hydrogen to form ammonia, according to the following equation 2:



The reactor operates at 550° C and 200 bar in the presence of iron-based catalyst. The outlet stream is sent to a heat exchanger, followed by a flash separator to have liquefied ammonia at -33° C as a final product [16]. Recent technological advancements have focused on enhancing efficiency by decreasing temperatures through the utilisation of novel catalysts, such as ruthenium based. This can incur a significantly higher cost when compared to the utilisation of iron-based catalysts. Other methods currently under development include photocatalyzed and electrochemical ammonia generation, which have the potential to reduce energy demand by 20% [15].

Ammonia is an option for the maritime sector to achieve emission reduction targets. Accordingly, DNV has proposed that by 2050, at least 15% of long-distance ships should be fuelled by ammonia and hydrogen [15]. The latter, due to cost and storage and energy demand issues in the compression and liquefaction, it is not considered the fuel with the

highest interest [15]. Alternatively, producing ammonia from renewable sources represents a solution for large capacities given that it is more economically feasible and can be almost 16 times cheaper than hydrogen storage, which is technically challenging and consumes a lot of energy [15]. In contrast, ammonia presents safety risks due to the NO_x, NH₃ and SO_x forming fine particles and can be potentially dangerous for humans [16].

2.2.3 Carbon Dioxide CO₂ sources

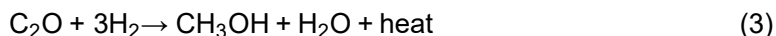
The significance of air-captured carbon dioxide (CO₂) technologies for synthetic fuels can be attributed to the fact that they serve as a feedstock for the methanol synthesis process. As reported by Papantoni et al. [17], there are several types of CO₂ sources, the most notable of which are point sources, biogenic sources, and CO₂ captured from the atmosphere. The latter corresponds to DAC, which will be the focus of this review.

2.2.3.1 Carbon Dioxide from Direct Air Capture (DAC)

Using DAC, CO₂ is captured directly from the air and permanently stored; it removes the CO₂ from the atmosphere. Two technology approaches are currently being used to capture CO₂ from the air: solid and liquid DAC. Solid DAC technology uses solid sorbent filters that chemically bind, typically with amine materials [18]. Afterwards, CO₂ can be released and captured when the filters are heated. On the other hand, liquid systems pass air through chemical solutions, typically relying on aqueous hydroxide solutions which, remove the CO₂ while returning the rest of the air to the environment [18]. Other approaches, such as electro-swing adsorption and membrane-based, are still at the prototype level, between 4 and 6 of the technology readiness level (TRL) [19].

2.2.4 E-methanol Synthesis

The non-fossil fuel alternative for e-methanol synthesis is through the utilization of carbon oxide (CO) or carbon dioxide (CO₂) and green hydrogen as a reactant, as illustrated in equations 3 and 4 [20]:



This process is usually performed in the temperature range from 250 to 300° C, and a pressure range from 5 to 10 MPa, in the presence of CuO, ZnO and Al₂O₃ as a catalyst in an exothermic reaction.

E-methanol can be used as a main fuel and also as a feedstock to produce other synthetic fuels such as e-gasoline. For maritime transport, e-methanol can be used in ship propulsion systems, especially in short-distance vessels. The clean-burning properties of e-methanol make it an attractive alternative fuel, as it lacks sulphur and

carbon-to-carbon bonds, reducing solid SO_x and particulate matter (PM) emissions, and its lower adiabatic flame temperature can limit NO_x formation during combustion [21]. The 2-stroke and 4-stroke engines are currently available with a TLR of 9 [22].

2.3 Maritime Supply Chains Using Synthetic Fuels

When considering the potential use of synthetic fuels to reduce the environmental impact of shipping, it is essential to outline the processes and technologies required for synthetic fuel production, storage, transport from production site to the point of final consumption and processes required to ensure the transfer of fuel to the ship according to its characteristics. This section provides an overview of the processes and technologies for the supply chain of three synthetic fuel forms: hydrogen, e-methanol and e-ammonia. The hydrogen can be used in three primary physical forms, compressed gaseous hydrogen, cryo-compressed hydrogen, and liquefied hydrogen. In addition, a chemical form to store and transport the hydrogen is a liquid organic hydrogen carrier (LOHC) [13]. Although, for the purpose of this study, it will be analysed in the compressed form. Table 3 presents the key properties of the synthetic fuels considered for this study.

Table 3 Key properties of synthetic fuels [16, 23, 24]

Properties	e hydrogen	e-ammonia	e-methanol
Molecular Formula	H ₂	NH ₃	CH ₃ OH
Form	Compressed	Liquid	Liquid
Density (25 ° C, 1 Bar) [kg/m ³]	0.089	682	798
Volumetric Energy Density [MJ/l]	10.8	12.7	15.7
Low Heating Value [MJ/kg]	120	18.8	19.9
Temperature [K]	298	240	175-338
Pressure [Bar]	20-700	1	1
Boiling Point (1 Bar) [° C]	-254	-33	65

Following the production of synthetic fuels, the transport and storage phases present significant economic barriers, particularly for long distances [23]. As illustrated in Table 3, the density of e-hydrogen in its compressed state is relatively low (0.089 kg/m³) in comparison to e-ammonia (682 kg/m³) and e-methanol (798 kg/m³). This results in higher infrastructure and operative requirements such as compression and, consequently, higher costs. This highlights the importance of the utilisation of alternative fuels. Nevertheless, e-ammonia and e-methanol can have a more significant impact on the environment, not only in the combustion process, but also in the supply chain phases.

2.3.1 Compressed e-hydrogen

Supply chains can have different configurations depending on the strategic fuel supply requirements and their end use (maritime, aviation, and road transportation sectors). The

general supply chain for compressed hydrogen shown in Figure 2 can be used to analyse the processes required for the WTT in the maritime sector. Yellow boxes indicate the phases called as conditioning, which are required before synthetic fuel transport. Aquamarine boxes show the means of transport, and green boxes show the required reconditioning processes to deliver the fuel to the end user.

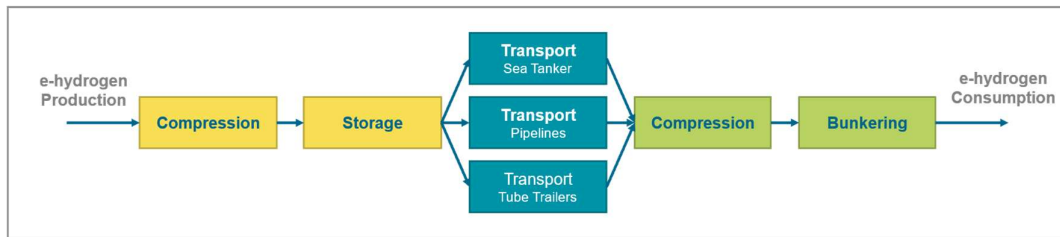


Figure 2 General supply chain for compressed hydrogen [own figure]

2.3.1.1 E-hydrogen Compression

E-hydrogen from renewable sources is typically produced at a pressure of up to 30 bar [25]. As the temperature and pressure of e-hydrogen increase, its density also rises, allowing for the storage and transportation of significant quantities in smaller spaces when compressed [26]. The most commonly used technologies for hydrogen compression are based on mechanical compression and include reciprocating, diaphragm and centrifugal compressors that have been widely used in the chemical industry [28]. Alternative compression technologies, such as electrochemical and metal hydride compression systems, are under development or in an early commercial stage. These technologies do not have moving parts, which, in principle, should increase their reliability and eliminate contamination problems due to the presence of lubricant oil [27].

2.3.1.2 Compressed Hydrogen Storage

Regarding the H₂ storage, two main options are considered: salt caverns and pressurized tanks. Salt Caverns use natural formations with limited porosity. The storage pressure can be in the range of 50-200 bar, resulting in a relatively low volumetric hydrogen storage density (approximately 10 g/L) [25]. Advantages include low hydrogen losses, large capacity and low capital cost requirements when compared to the construction of dedicated storage tanks [25]. However, the use of these formations is limited by physical constraints on the availability of salt caverns close to the supply chain corridor [25]. An alternative option is the use of pressurized tanks. Four types of compressed storage pressure tanks are classified in a commercial stage at TRL 9 [26]. Type I and II are usually used for stationary applications due to their high weight, while Type III and IV tanks are designed for portable applications, such as storage on board in ships propulsion systems [25]. This form of storage is the preferred choice when relatively

limited quantities are required and when the location has specific considerations. Table 4 presents a comparison of compressed storage tank types.

Table 4 Comparison of compressed storage tank types [27] [28]

	Type I	Type II	Type III	Type IV
Materials	Steel/Aluminium	Steel/Aluminium liner Filament windings around the cylinder part	Aluminium Steel liner Composite over-wrap (fibre glass/aramid or carbon fibre)	Composite over-wrap (carbon fibre) Polymer line
Maximum Pressure (bar)	Steel: 175 Aluminium: 200	Al/glass: 263 Steel/carbon fibre: 299	Al/glass: 305 Al/aramid: 438 Al/carbon: 700	350 (buses) 700 [30]
Applications	Stationary Storage	Stationary Storage	Vehicles	Vehicles

2.3.1.3 Compressed Hydrogen Transportation

The transport phase can be classified into two distinct categories: transmission and distribution. Transmission involves transporting large quantities of fuel over long distances from production facilities to storage sites or industrial hubs, including pipelines and sea tankers [29]. In contrast, distribution involves delivering the fuel to end final users, such as refuelling stations or small industrial facilities, where it is mainly transported by truck tankers [29].

2.3.1.3.1 Compressed Hydrogen pipelines

Pipelines carry pressurized hydrogen from the production location to the bunkering ports, with operating pressures ranging from 16 to 100 bar and diameters typically between 400 and 1,400 mm [30]. The flow velocity generally varies between 10 and 20 m/s, depending on the pipeline design. Recompression and metering stations can be placed at intervals of 8 to 30 km [30]. Figure 3 illustrates the main components a pipeline system.

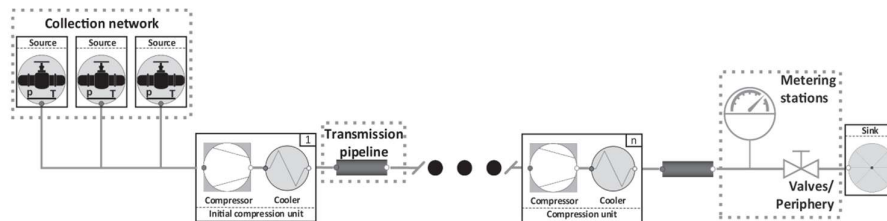


Figure 3 Key components of hydrogen pipeline system [30]

Repurposing of existing gas pipelines is considered as a feasible option for transporting compressed hydrogen. However, certain measures must be implemented to ensure safe and efficient operation, including 1) cleaning, drying and purging with inert nitrogen gas

to eliminate gaseous and other impurities, 2) pipeline monitoring and inspection to detect and localize flaws, cracks, or leaks, and 3) replacement of old equipment such as valves that have been operated for long periods. Furthermore, applying internal coating is required to avoid or mitigate hydrogen embrittlement [30].

2.3.1.3.2 Compressed Hydrogen Sea Tankers

A limited number of studies on the transportation of compressed gaseous hydrogen in sea tankers was found. However, a pilot-scale compressed hydrogen ship with a cargo capacity of 450 tonnes was developed by Global Energy Ventures, and the possibility of a scaled version with a capacity of 2,000 tonnes has been proposed (Figure 4). The design incorporates a steel tank with a stainless steel liner, surrounded by multiple high-strength steel layers to prevent hydrogen embrittlement [31]. The propulsion is planned to be an electric drive, supported by advancements in hydrogen-blended generation and hydrogen fuel cells. The pilot prototype is expected to be operational by 2025 [32].

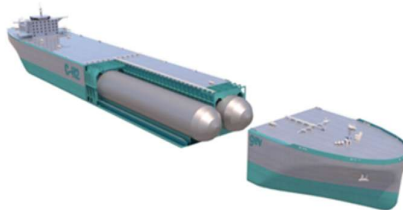


Figure 4 Pilot-scale compressed H₂ Ship [32]

2.3.1.3.3 Compressed Hydrogen tube trailers

One commonly used method for road distribution of compressed hydrogen is tube trailers. These trailers are configured with Type III or IV tanks, composed of composite materials such as carbon fibre with a non-metallic composite liner. Pressures of up to 500 to 700 bar can be withstood by these tanks, increasing the volumetric hydrogen storage density to approximately 40 g/L (at 700 bar) [33]. Figure 5 illustrates a tube trailer with a working pressure of 517 bar an storage capacity of 1 tonne developed by Calvera Industry in Zaragoza, Spain [34].



Figure 5 Tube trailer develop by Calvera Hydrogen [34].

2.3.1.4 Final Compression at Bunkering Port

Once the final transport destination for hydrogen is reached, compression or decompression processes are carried out based on the pressure requirements of the specific final user. For maritime applications, a pressure of 700 bar is required for on-board storage [8].

2.3.1.5 Bunkering

The final stage of the hydrogen supply chain is the bunkering process, during which hydrogen is transferred as fuel to onboard storage systems via a hose. Two primary methods have been identified: the cascade filling method and the direct filling method [35]. In the cascade filling method, hydrogen is stored on the platform at a pressure of 500 bar. The pressure is gradually reduced to 350 bar which is the required pressure for filling the onboard storage tank. In the direct filling method, a compressor is utilized, which is capable of accepting compressed hydrogen at an input pressure of 10 bar, assuming a direct filling from the electrolyser production on the platform, and delivering a gas output at 350 bar without requiring storage on the platform [35]. The choice of method depends on the technical and economic feasibility of the specific option. Both methods fall under the shore-to-ship or terminal-to-ship categories, where bunkering is conducted from an onshore platform. Additionally, the ship-to-ship bunkering method, where fuel is transferred between vessels, is considered a viable option for maritime applications but is beyond the scope of this literature review.

Hydrogen Purification Units

After hydrogen production, hydrogen needs to be purified before further processes for the supply chain [36]; as it is stated by Du et. al. [37], hydrogen purification units are crucial in the hydrogen supply chain. Depending on the characteristics of the storage or transport infrastructure, it is necessary to analyse their integration in each phase or at least after the hydrogen production phase and the bunkering port. The ISO 14687:2019 standard stipulates a hydrogen purity mole fraction of 99.97% for PEMFC application in road vehicles [37]. The standard also enumerates the primary impurities as CO, CO₂, H₂S, NH₃, water vapour, O₂ and CH₄ as the most important. Purification technologies in the literature include pressure swing adsorption (PSA), membrane separation, metal hydride separation and cryogenic distillation [37]. In the PSA method, adsorbents such as zeolite, activated carbon, alumina or silica gel can be used to adsorb gases in the bed of solid materials. For membrane separation, a perm-selective membrane made of novel material such as nanomaterial is used as the separation medium and under pressure differences, hydrogen purification can be achieved. Metal hydride separation uses metal hydride alloys to absorb and desorb hydrogen and purify it. Finally, in cryogenic

distillation, the hydrogen is purified by separating the gases due to their differences in volatility, making the condensation of these gases at a reduced temperature [37].

2.3.2 E-ammonia

Ammonia is a chemical molecule with many uses, such as fertiliser in agriculture, coolant, or medium for storing energy. Due to its facility to be stored and transported in liquid form [38]. Interest has recently expanded to the application of clean ammonia as a carbon-free energy carrier in future energy systems, for instance, it can function as a clean fuel for shipping vessels [39]. Additionally, it is considered well-suited for transporting renewable energy alongside its traditional industrial applications. Figure 6 is used to analyse the processes required in a supply chain for the maritime sector. Two possibilities for the supply chain have been identified based on the fuel form: gaseous and liquid ammonia. Given the advantages offered by storage and transportation in liquid form, as well as its potential for use in propulsion systems, the liquid form is regarded as the most suitable for the maritime supply chain.

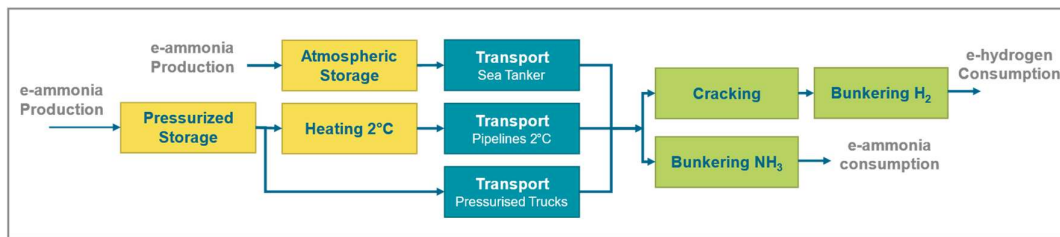


Figure 6 General supply chain for e-ammonia [own figure]

2.3.2.1 E-ammonia Storage

Currently, the primary methods for storing ammonia are: 1) Pressure storage at ambient temperature and around 15 bar in spherical or cylindrical pressure vessels with capacities up to 1,500 tonnes per vessel. 2) Semi-refrigerated storage at about 0° C in insulated, usually spherical pressure vessels for quantities up to about 2,500 tonnes. 3) Atmospheric storage at -33 ° C in insulated cylindrical tanks for around 50,000 tonnes each and 4) Solid-state storage [38]. Pressurized and atmospheric storage will be detailed below.

The most suitable method for large-scale storage is atmospheric storage, based on the above information and the fact that ammonia at atmospheric pressure is liquid at - 33.3 ° C and ambient pressure. LNG stainless steel in cryogenic vessels has great potential for ammonia storage [15]. The storage capacity for an import ammonia terminal is in the range of e 30 to 50 ktonnes of ammonia [39]. As well as liquid hydrogen, part of the ammonia in the storage tanks evaporates. It is important to note that, for liquified fuel storage, ammonia energy density (LHV) is 12.9 GJ/m³ and requires approximately 1.45 times more space than LNG to store the same amount of energy. Consequently,

changing marine fuel from LNG to ammonia means more frequent refuelling, larger storage tanks, or dual fuel solutions [15]. For small-scale storage, the most suitable method is pressurised storage, which is good for loading and unloading trucks, sea tankers and ships carrying pressurised ammonia and for entering or exiting from pipeline systems [38]. In the maritime supply chain, both cases could apply.

2.3.2.2 E-ammonia Transport

The transport of liquid ammonia can be accomplished by sea tankers, pipelines, truck tankers and barges in a liquid form [38]. Ammonia is typically transported in carbon steel pipelines with a typical diameter between 0.15 and 0.25 m in a liquid state at pressures of around 17 bar [40]. Globally, more than 7,600 km of ammonia pipelines are monitored, and 65% operated in United States. Typical capacities of such pipelines range from 120 to 14,000 tonnes of ammonia daily [39]. Pumps are used to keep up the required pressures over long distances and to prevent ammonia evaporation [39]. Furthermore, ammonia transportation by pipelines requires the ammonia to be heated to at least 2° C to avoid brittle fractures in the pipeline and transported at a minimum pressure of 20 bar to prevent gas formation [38]. Ammonia is typically transported in pressurised liquid form via pipelines over distances of up to several thousand km. However, trucks are the preferred mode of transportation for distances of approximately 150 km or less [41].

Ocean transportation of ammonia can be accomplished by sea tankers, river and coastal transportation by barges. Sea tankers are insulated and may be designed as semi-refrigerated (at 4 to 8 bar and around -10° C) or mostly as fully refrigerated vessels (at near-atmospheric pressure and between -50° C to -30° C). Ammonia is transported as a pressurised liquid at a pressure of 15 to 16 bar and provided with pressure relief devices [38].

2.3.2.3 E-ammonia Cracking

If the end user requires compressed hydrogen, the ammonia must be cracked. ammonia cracking is an endothermic reaction (See equation 5) that requires temperatures above 180° C to be thermodynamically feasible [42]. Metal nanoparticles catalyst supported on high surface area metal oxide, is used to conduct the reaction at high rates [42]. Hydrogen is the main output while nitrogen is a by-product of the reaction.



Ammonia cracking can be accomplished in the bunkering port or on board the ship before the propulsion system. The choice of the approach will depend on the application.

2.3.2.4 E-ammonia Bunkering

As with marine fuel bunkering methods, ammonia can be transferred to a vessel via three primary means: truck-to-ship, ship-to-ship, or terminal-to-ship. The latter method involves the utilisation of hoses or loading arms to establish a connection between the storage terminal and the vessel. The transfer of ammonia via hose assembly is the traditional method of bunkering fuels constituted by the hose/end fittings and connection couplings at each side. Two flexible hoses are utilised: one for liquid and the other for vapour, as applicable. Full rigid arms are provided with rigid insulated pipe sections to transfer ammonia to the receiving vessel [43]. If hydrogen is the final product, similar bunkering methods for compressed hydrogen apply in this instance.

2.3.3 E-methanol

The increasing use of renewable sources during methanol production has significantly reduced its CO₂ footprint, making it a desirable option for various types of vessels and also as a hydrogen carrier. As physical characteristics, methanol is a colourless liquid that is easier to handle and store than other fuels such as LNG, ammonia and hydrogen, which has made it more suitable as a marine fuel [21]. For e-methanol a typical supply chain as shown in Figure 7.

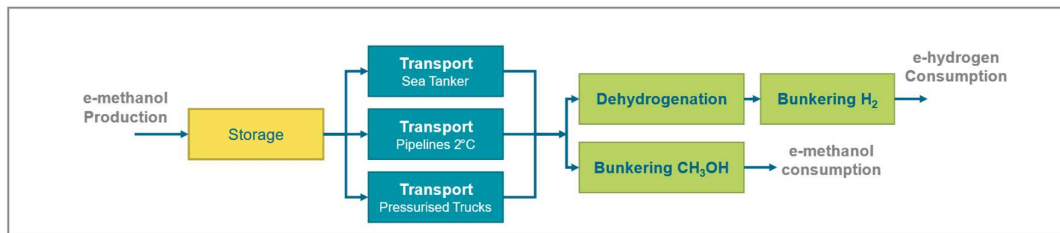


Figure 7 General supply chain for e-methanol [own figure]

2.3.3.1 E-methanol Storage

Most large-scale methanol storage is conducted in carbon steel or 300-series austenitic stainless-steel tanks, similar to the storage of flammable oil products, such as gasoline, currently in use [41]. The lower specific energy of methanol requires approximately 2.54 times more storage volume for the same energy content when compared to LNG. This factor should be counted when considering the use of fossil-fuel infrastructure as a reference.

2.3.3.2 E-methanol Transport

Methanol is a chemical commodity with a large market. Therefore, it can be transported using sea tankers, trains and truck tankers, which are suitable for transporting hazardous chemicals [44].

2.3.3.3 e-methanol Dehydrogenation

If the end user requires compressed hydrogen, the methanol must be dehydrogenated. A method that is currently in use involves the methanol-reforming or aqueous methanol dehydrogenation to hydrogen and carbon dioxide [45]. The endothermic reaction is depicted by equation 6, using copper- or metal-based catalysis at a temperature between 200 and 300° C.



As well as ammonia cracking, this process can be accomplished in the bunkering port or on board the ship before the propulsion system. The choice of the approach will depend on the application.

2.3.3.4 e-methanol Bunkering

Methanol bunkering, also referred to as refuelling, could be comparable to that of MGO or HFO bunkering. Methanol maintains its liquid state at ambient temperatures and pressures, thereby allowing the utilisation of existing infrastructure for methanol storage and bunkering, with minor modifications [46]. If the end product is hydrogen, then similar bunkering methods for compressed hydrogen apply in this instance.

2.4 Synthetic fuels Powertrain System in the Maritime Sector

Synthetic fuel-based powertrain system represents the final stage of the maritime fuel supply chain and is crucial in reducing GHG emissions in the maritime transport sector. As noted by Kanchiralla et al. [47], the powertrain system can include storage tanks, energy conversion technologies, and additional components such as an electric motor, gearbox, control unit, generator, and selective catalytic reduction (SCR) systems, particularly in configurations incorporating internal combustion engines (ICE). According to Interreg [48], various ship energy conversion technologies could be assumed to have reached a TRL suitable for market adoption by 2030. These technologies can, therefore, serve as a reference for analyzing the environmental impacts of synthetic fuel supply chains in maritime use. This section will focus on FC and ICE for maritime applications. As illustrated in Figure 8, a typical powertrain configuration for both FC and ICE.

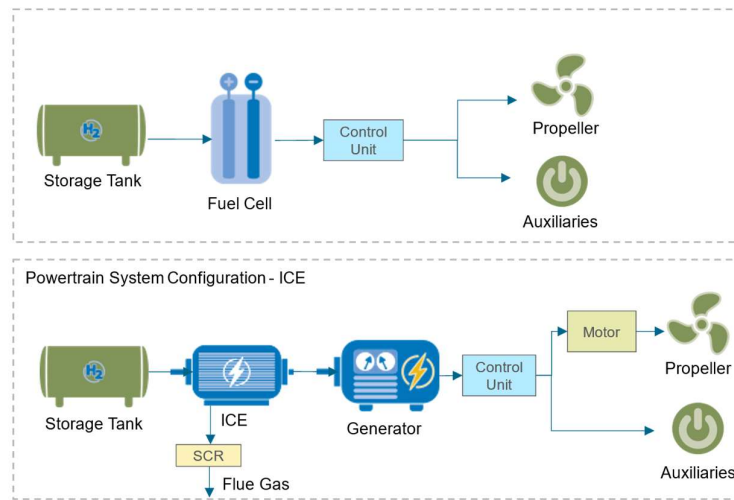


Figure 8 Powertrain configuration for PEMFC and ICE. Plot created with icons provided by DLR and adapted from [8]

2.4.1 Fuel Cells

For maritime applications, according to Xing et al. [49], Proton Exchange Membrane fuel cell (PEMFC), High Temperature Proton Exchange Membrane (HTPEMFC), Molten carbonate fuel cells (MCFC) and Solid Oxide fuel cells (SOFC) are known as technologies that can be applied to maritime transport using synthetic fuels considering energy efficiency, power capacity and sensitivity to fuel/oxidant impurities. The aforementioned technologies are distinguished based on the type of electrolyte material employed. Table 5 provides an overview of the key characteristics of FC technologies.

Table 5 Key Characteristics Fuel Cells [49] [50] [51]

Parameter	PEMFC	HTPEMFC	MCFC	SOFC
Electrolyte	Polymer membrane	PBI polymer doped with phosphoric acid	Molten carbonate salt	Porous ceramic material
Typical Fuel	Hydrogen	Hydrogen	Hydrogen, methanol and hydrocarbons	Hydrogen, methanol and hydrocarbons
Operating Temperature (° C)	65–85	160–220	650–700	500–1000
Power Capacity	≤120 kW	-	120 kW–10 MW	10 MW
Electric Efficiency	50–60%	50–60%	50–55%	50–60%
Technology Readiness Level	8	6	7	7

Ballard Power Systems has developed the FCwave™ FC module, a 200 kW system designed for maritime applications based on PEMFC [52]. This is characterised by its modularity, which allows for configurations ranging from 200 kW to multiple megawatts. Currently, this technology is employed on the Norwegian ferry Hyra, which, as of 2023, functions in conjunction with electric batteries to provide power to the ship [53].

2.4.2 Internal Combustion Engines

Another technology under development with the potential to be employed in propulsion systems to limit the GHG emissions in the TTW for ship is the hydrogen-based internal combustion engine. The working principle of the ICE follows the Otto Cycle and Diesel Cycle, which are also used with gasoline and diesel as a main fuel. In this, the engine is capable of converting the chemical energy of the fuel into mechanical energy to generate propulsion of the ship [54]. In comparison with a fossil-fuel ICE, the adaptations required to use this engine with hydrogen are the substitution of the injectors and the implementation of a hydrogen purge system as the most significant adaptations [54]. Rodriguez-Rios et al. [54], indicates that, compared to PEMFC, ICE, as an advantage, has the potential to utilise hydrogen with a lower degree of purity, thereby reducing the complexity and cost of the fuel pre-processing. Conversely, using a fossil fuel as a pilot may result in significant emission levels when the technology is operational. Table 6 indicates the TRL and the efficiency per fuel used.

Table 6 Characteristics of ICE per fuel type [55]

	Compressed Hydrogen	Ammonia	Methanol
TRL	5	3	8
Efficiency	42% - 48%	42% - 46%	41% - 45%

MAN Energy Solutions is currently developing a hydrogen-fuelled and medium speed engine under the project called HydroPoLEn, since October of 2023 [56]. By mid-2025, the company is expected to have completed the testing of a full-scale, two-stroke engine that runs on ammonia [57]. It is noteworthy that a two-stroke engine using methanol has been in service for maritime shipping since 2016. It has been reported that the use of green methanol has resulted in a 95% reduction in carbon emissions and a 99% reduction in SO_x emissions [58].

2.5 State-of-the-art of LCA and pLCA of Synthetic Fuels maritime supply chains

This state-of-the-art review comprehensively examines the most recent applications of pLCA or LCA in the context of synthetic fuel supply chain for maritime applications. Table 7 provides a detailed description of the aspects analysed from the studies available in research publications. It should be noted that some studies reviewed assets and other types of fuel; however, the table only makes references to synthetic fuels derived from renewable sources, which is a requirement for the production of synthetic fuels. Gaps were identified according to the scope of this study.

Table 7 Key information of Life Cycle Assessments from the literature review.

Authors	LCA Type	Synthetic fuels	Stages Included	Software /Database	LCI	Functional Unit	Gaps
Wulf et al. [59]	LCA	Compressed H ₂ and LOHC form for vehicle transportation.	Production, Storage, Transport by pipeline and trailers and fuelling station.	Ecoinvent 3.3	✓	1 Kg of Hydrogen at ambient temperature (15° C), 700 bar and purity of 99,9%.	They did not consider other form of hydrogen carries such as -e-methanol and ammonia. They did not consider the bunkering stage and the stage of the use in the ship (TTW).
Wulf and Zapp. [60].	LCA	Compressed H ₂ and LOHC form for vehicle transportation	Production, Storage, Transport by pipeline and trailers and fuelling station	openLCA 1.6 Ecoinvent	×	1 Kg of Hydrogen at ambient temperature (15° C), 700 bar and purity of 99,9%.	They did not consider other form of hydrogen carries such as -e-methanol and ammonia. They did not consider the bunkering stage and the stage of the use in the ship (TTW).
Tsiklios et al. [30]	LCA	Compressed H ₂ .	Transport by pipeline: repurposed and new construction.	openLCA 1.6 Ecoinvent 3.6	✓	1 Kg of Hydrogen over a distance of 500 km.	They did not consider other synthetic fuels forms. They did not consider other forms of transportations.
Alghool et al. [61]	LCA	Compressed and liquid H ₂ , methanol and ammonia.	Production, Conditioning, Storage, Transport by ships and reconditioning stages.	GaBi	✓	1 Kg of Hydrogen.	They did not consider the bunkering stage and the stage of the use in the ship (TTW).
Akhtar et al [9].	LCA	Compressed and liquid H ₂ and LOHC, and ammonia.	Production, Compression Storage, Transport by pipeline and trailers and fuelling station	SimaPro 9.1.1.1 Ecoinvent 3.6	✓	1 Kg of Hydrogen.	As the final user application is in road transportation, the bunkering stage and the use in the ship (TTW) were not considered in this analysis.
Al-Breikiet al. [62].	LCA	Compressed and liquid H ₂ , methanol and ammonia.	Production, Storage, Loading, Transport by ships and fuelling station	GREET	×	1 Kg of Hydrogen produced, transported and 1 MJ utilized in an internal combustion engine.	As the final user application is in road transportation, the bunkering stage and the use in the ship (TTW) were not considered in this analysis.
Fernandez-Rios et al. [54].	LCA	Compressed H ₂ .	Production and consumption of hydrogen in PEMFC and ICE.	openLCA 1.10.3 GaBi	✓	1 kWh of energy produced.	As the scope of the study was focussed on propulsion technologies, they did not include supply chain stages.
Kanchiralla et al. [55].	pLCA (timeframe: 2030)	Compressed H ₂ and liquid H ₂ , e-methanol and ammonia.	Production and consumption of hydrogen in PEMFC, SOFC and ICE.	Ecoinvent 3.7.1	✓	One round trip with case study ship.	As the scope of the study was focussed on propulsion technologies, they did not include supply chain stages.
Hwang et al. [63].	LCA	Liquid H ₂ .	Production, Transport, Liquefaction, Storage, Bunkering, Consumption.	GABI/CML 2021 EF 2.0 TRACI 2.1	×	1.08x10 ⁹ MJ Energy. Consumption per RT.	The objective of the study was focussed to compare Liquid H ₂ with MFO and NG; other alternative fuels were not included in the study.

Kleijne et al. [64].	LCA	Compressed H ₂ , Liquid H ₂ and NH ₃ .	Production, Compression, Transport, Regasification, NH ₃ .	Simapro 9.4.0.2/ Ecoinvent 3.8	x	1 Kg of Hydrogen.	The scope of the study did not include a particular application. However, a WTT scope is well-defined, with storage as the final phase.
----------------------	-----	---	---	--------------------------------	---	-------------------	---

The majority of life cycle assessment studies concentrate on the alternative fuel supply chain in the context of production, transportation, fuel refuelling stations and consumption applications for road mobility. A limited number of studies were identified in the literature review for maritime applications. For instance, Liu et al. [65] conducted a comprehensive literature review on the life cycle assessment of transportation alternative fuels, although this did not include aviation and maritime applications.

A lack of sufficient information on LCA studies for marine applications has resulted in insufficient studies analysing the bunkering stage in marine fuel supply chains. Additionally, there is a relatively limited scope of research available on the utilisation of propulsion technologies in ships that employ synthetic fuels. However, it is important to note that these studies do not encompass the post-production stages necessary to deliver fuels to the bunkering port, thereby omitting critical stages from a comprehensive WTW analysis. This includes studies conducted by Fernandez-Rios et al. [54] and Kanchiralla et al. [55]. Lastly, most studies conducted a traditional LCA; however, Kanchiralla et al. [55] study provides a prospective LCA with a WTW scope that places a particular emphasis on propulsion systems on ships with 2030 as a time framework.

3 Methodology

3.1 Overview of Prospective Life Cycle Assessment Methodology

LCA is a methodology defined by the principles and framework set forth by ISO 14040/44 standards [66]. The methodology assesses the potential environmental impacts of a product or system over its entire life cycle [67]. As stated by Cucurachi et al. [68], a LCA that analyses a well-defined system can be called an ex-post analysis which also refers to a traditional LCA. As stated by Brand et al. [69], the prospective view of Life Cycle Sustainability Assessment (LCSA) covers aspects such as the environmental, economic, and social consequences and impacts of technology in interaction with the surrounding system through LCA, Life Cycle Costing (LCC), and Social Life Cycle Assessment (SLCA). Additionally, it consciously incorporates changes over time in life cycle data, system/actor behavior, and/or their relationships. Based on this perspective, the definition of prospective LCA adopted for this study can be considered as the assessment of the potential environmental impacts of a system while incorporating changes in life cycle data over time, such as technological efficiencies and projected electricity generation scenarios. The LCA methodology, as defined by the ISO 14040/44

standards, consists of four steps [65] and has been adopted for this study incorporating changes in the life cycle data over time to consider the prospective view, particularly in the life cycle inventory step. Each step is described in detail in the following sections.

3.1.1 Goal and Scope Definition

In this stage, the goal and scope of this study are defined, including the system boundaries, the life cycle framework, functional unit [65] and the foreground and background systems defined for the study. As depicted by Frischknecht [70], the foreground system consists of processes which are under the control of the decision-maker for which an LCA is carried out and the background system consists of processes on which no or, at best, indirect influence may be exercised by the decision-maker.

3.1.2 Life Cycle Inventory -LCI

The subsequent stage entails the data collection within the assessment framework. This stage encompasses input information such as energy, materials and consumables requirements, as well as the construction of the plant, equipment or technologies. Output information may include the main product, by-products, emissions and waste [65]. In addition, this step collects the life cycle data projected for the prospective scenarios considered for the study, which will be detailed later.

3.1.3 Life Cycle Impact Assessment -LCIA

The third stage involves the analysis of the environmental impact categories. It is undertaken to identify the potential consequences of the scope framework [65]. There are various LCIA methods according to the focus of the study. ReCiPe 2016, Environmental Footprint (EF) 3.1 and the Intergovernmental Panel on Climate Change (IPCC) 2021 are notable among these. The ReCiPe 2016 comprises two approaches: Midpoint Indicators and Endpoint Indicators. The former focuses on 17 specific environmental impacts, while the latter shows the environmental impact at high levels, such as the impact on human health, biodiversity and resource scarcity [71]. The EF 3.1 method concentrated on the 16 midpoints categorised impact categories (Table 8), which were normalised and weighted to obtain the final impact per functional unit [72]. Finally, IPCC 2021 focuses on the climate change category over a 20-year and 100-year horizon in a midpoint approach [47].

Table 8 Impact categories EF 3.1 [73]

IMPACT CATEGORY	INDICATOR	UNIT
Climate Change	Radioactive Forcing as GWP100	kg CO ₂ eq
Ozone depletion	Ozone depletion potential (ODP)	kg CFC ⁻¹¹ eq
Human Toxicity, cancer	Comparative Toxic unit for humans	CTU _h
Human Toxicity, non-cancer	Comparative Toxic unit for humans	CTU _h

Particulate Matter	Impact on human health	Disease incidence
Ionizing Radiation, human health	Human exposure efficiency relative to U ²³⁵	kBq U ²³⁵ eq
Photochemical ozone formation, human health	Tropospheric ozone concentration increase	kg NMVOC eq
Acidification	Accumulate Exceedance (AE)	Mol H ⁺ eq
Eutrophication, terrestrial	Accumulate Exceedance (AE)	Mol N eq
Eutrophication, fresh water	Fraction of nutrients reaching freshwater end compartment (N).	kg P eq
Eutrophication, marine	Fraction of nutrients reaching marine end compartment (N).	kg N eq
Ecotoxicity, fresh water	Comparative toxic unit for ecosystems	CTUe
Resource use, fossil	Abiotic resource depletion – fossil fuels (ADP fossil fuels)	kg Sb eq
Resource use, minerals and metals	Abiotic resource depletion (ADP ultimate reserves)	MJ
Land Use	Soil Quality Index	Dimensionless
Water Use	User deprivation potential	m ³ water eq of deprived water

3.1.4 Interpretation

The final phase involves the interpretation of results and impact assessment, as well as the discussion of the key findings to draw meaningful conclusions and provide recommendations that support informed decision-making [65].

3.1.5 Tools and software

Activity Browser is a graphical user interface for advanced life cycle assessment using Brightway2 [74], which was used in this study. This software was selected because of its ability to provide a modular LCA framework, which is particularly useful for supply chains that can be broken down into individual modules, which is the case for this study [75]. Furthermore, this tool manages the projects and databases, including background databases such as Ecoinvent 3.9.1 and Biosphere3 [76]. Furthermore, it models life cycle inventories and analyses the LCA results according to the method selected [77]. Finally, graphs were generated using Python for data results visualization.

3.2 Prospective Life Cycle Assessment – WTW Study

3.2.1 Goal and Scope definition

This study aims to perform a pLCA, which will evaluate the future environmental impacts of different synthetic fuels (e-hydrogen, e-ammonia, e-methanol) from production to the bunkering port and the use of e-hydrogen in the energy conversion technologies on-

board for base case and future electricity generation scenarios are quantified. This will be evaluated in the proposed case study described below.

3.2.1.1 Case Study Description

The WTW approach was used for the case study as a framework to assess the life cycle impacts of different fuel and propulsion technologies for ships. Figure 9 illustrates the general framework of the life cycle assessment for the ship system. The WTW approach consists of two main scopes: Well-to-Tank (WTT) and Tank-to-Wake (TTW). The WTT scope encompasses all upstream processes, including the electricity generation, fuel production, conditioning processes, transportation, and reconditioning at the bunkering port. In contrast, the TTW scope focuses on the ship's operational phase, covering onboard fuel storage, energy conversion technologies, and the powertrain system that delivers energy to the propeller. The scope of this study is divided into two parts. The first part assesses the WTT assessment of e-hydrogen, e-ammonia, and e-methanol pathways. The second part of the study comprises the WTW scope, integrating the WTT and TTW phases. This section evaluates the use of compressed hydrogen as the primary fuel in two onboard energy conversion technologies: PEMFC ICE. In this context, the impacts from the WTT phase, including H₂ production, compression, storage, and transport, are fully integrated into the TTW analysis, ensuring a comprehensive WTW assessment of the overall environmental impacts from fuel production to final energy conversion onboard.

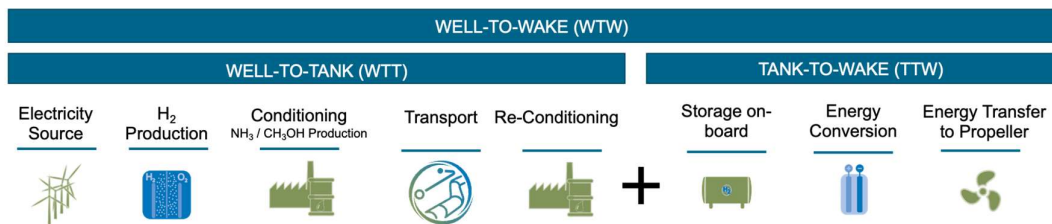


Figure 9 WTW system boundary. Plot created with icons provided by DLR and adapted from [78]

3.2.1.1.1 WTT Scope

For the first part, the production of synthetic fuels and conditioning processes for transporting e-hydrogen, e-ammonia, and e-methanol are proposed to be located in Wilhelmshaven, Germany. These fuels were selected for the case study because, according to IRENA [79], the use of hydrogen via FC and ICE is a decarbonisation option in the maritime sector, especially for short distances. However, there are problems with costs and infrastructure in their supply chain. Meanwhile methanol and ammonia are considered the most promising fuels for decarbonising the sector. Therefore, it is considered relevant to share the WTT scope for the three fuels. In the case of e-hydrogen, it is assumed that this is transported by a new hydrogen pipeline over 403 km. For e-ammonia, it is assumed it is transported by sea tanker over 457 km, while for e-

methanol, it is assumed that it is transported by truck tanker over 387 km. The selection of these transport modes was made based on the characteristics of each fuel that were explored in the preceding chapter, and also because they can be representative options for the case study.

The selection of Wilhelmshaven as a site to produce hydrogen and synthetic fuels was based on the premise that its strategic location could establish it as a national hydrogen hub for Germany according to [80], this would enable the import, production and distribution of hydrogen to consumption centres in the northern regions of the country. Additionally, the port of Rotterdam was selected because it represents the largest Europe bunkering port and also the largest methanol hub in North Western Europe [81]. On the other hand, the Port of Rotterdam in the Netherlands has been established as the final transport destination, where the reconditioning processes for each pathway take place.

The WTT is comprised of three distinct cases. The pathways under consideration are compressed e-hydrogen, e-ammonia and e-methanol.

Case 1: e-hydrogen Pathway

Figure 10 depicts the case 1 compressed e-hydrogen pathway. Key parameters for this pathway are listed in Table 9. The efficiency is assumed to be 67% for the base case (2020), increasing to 68% and 75% for the 2030 and 2050 scenarios, respectively [82]. The e-hydrogen from alkaline electrolysis is assumed to be produced at 30 bar [82]. Subsequently, reciprocating compressors are used to increase the hydrogen pressure to 85 bar, the required level for the subsequent storage phase [59]. Following that, it was considered to store the hydrogen in a salt cavern. As Chapter 2 outlines, storing compressed hydrogen in type I and II tanks is a viable option. However, for the purposes of this study, storage in salt caverns would be considered to analyse the impact of salt cavern storage on the e-hydrogen pathway. Although salt caverns are employed for long-term storage, they possess a high technical potential, with a value of 33 TWh of H₂ in northern Germany [83]. For the transport phase, a new pipeline is proposed, featuring a 48-inch diameter with four compression units, and a transport capacity of 13 GW. This infrastructure ensures a consistent operational pressure of 80 bar along the pipeline [30]. Finally, a final compression phase was considered at the bunkering port to increase the pressure to 700 bar, which is the pressure required for storage on-board [8].

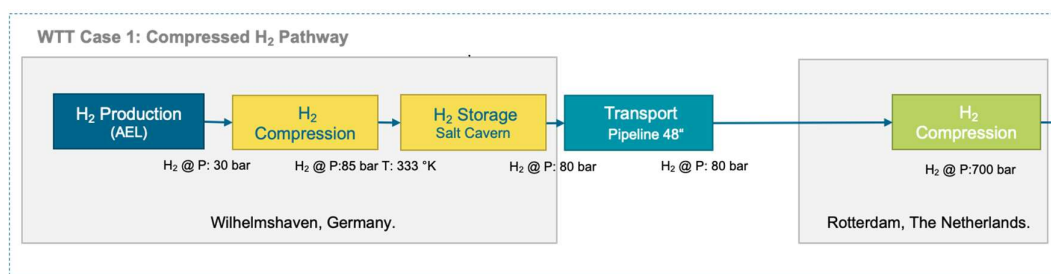


Figure 10 WTT System boundary phases: e-hydrogen pathway [own figure]

Table 9 Key Parameters Case 1: e-hydrogen pathway [84][82][59]

Phase	Process/ Technology	Location	Output Product	Electricity Consumption	Electricity Source
H₂ Production	Alkaline Electrolysis	Wilhelmshaven, DE.	H ₂ @ 30 bar	50.12 kWh/kg H ₂	Electricity from Wind source– All Scenarios
H₂ Compression	Reciprocating Compressors	Wilhelmshaven, DE.	H ₂ @ 85 bar	0.72 kWh/kg H ₂	DE Electricity Generation. BC, 2030 and 2050.
H₂ Storage	Salt Cavern	Wilhelmshaven, DE.	H ₂ @ 80 bar	0.07 kWh/kg H ₂	DE Electricity Generation. BC, 2030 and 2050.
H₂ Transport	Compressed H ₂ pipeline	DE/NL	H ₂ @ 80 bar	0.47 ¹ kWh/kg H ₂	DE/NL Electricity Generation. BC, 2030 and 2050.
H₂ Compression	Reciprocating Compressors	Rotterdam, NL.	H ₂ @ 700 bar	3.2 kWh/kg H ₂	NL Electricity Generation. BC, 2030 and 2050.

Case 2: e-ammonia Pathway

Figure 11 depicts case 2, the e-ammonia pathway. Key parameters for this pathway are listed in Table 10. The pathway starts with green hydrogen production, following the same criteria as case 1. Nitrogen is produced through Cryogenic Distillation at 200 bar and 268 K [16]. The Haber-Bosch process, using iron-based catalysis, combines nitrogen and hydrogen as primary inputs for the NH₃ synthesis [16]. A flue gas capture system was not assumed for this process. Consequently, NH₃ and NO_x are emitted into the atmosphere.

For the NH₃ storage, it was assumed that the ammonia would be stored refrigerated (given its boiling point of -33 ° C) to maintain its liquid state at ambient conditions. This requires electricity, as detailed in Table 10. Emissions during storage include a boil-off

¹ Per compression unit. The pipeline system it was assumed to have four units.

rate of 0.062%, along with CO, NO_x, and volatile organic compounds (VOC) [61]. The study assumes all previous stages occur in the same location, and thus infrastructure connections between processes are not considered. Consequently, the present study does not consider the infrastructure connected to the processes.

NH₃ transportation was assumed using a sea tanker powered by marine fuel oil. Boil-off during transport was estimated at 0.004% [61], with emissions similar to those during storage. At the bunkering port in Rotterdam, it was assumed that the NH₃ cracking process would convert ammonia back into hydrogen at 240 bar, with nitrogen as a by-product [85]. Nitrogen as a by-product was outside the scope of the study. Finally, as in case 1, the final H₂ compression to 700 bar was considered.

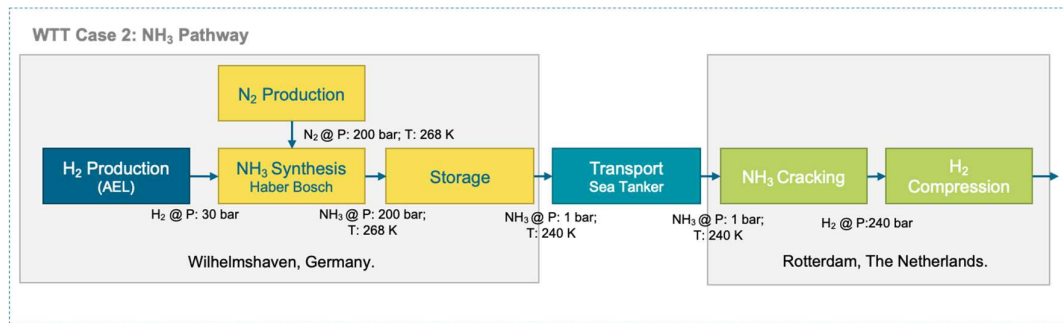


Figure 11 WTT System boundary phases: e-ammonia pathway [own figure]

Table 10 Key Parameters Case 2: e-ammonia pathway [4] [16] [8, 85]

Phase	Process Technology	Location	Output Product	Electricity Consumption	Electricity Source
H₂ Production	Alkaline Electrolysis	Wilhelmshaven, DE.	H ₂ @ 30 bar	50.12 kWh/kg H ₂	Wind Electricity – All Scenarios.
N₂ Production	Cryogenic Distillation	Wilhelmshaven, DE.	N ₂ @ 200 bar	0.105 kWh/kg N ₂	DE Electricity Generation. BC, 2030 and 2050.
NH₃ Synthesis	Haber-Bosh Process	Wilhelmshaven, DE.	NH ₃ @ 200 bar	0.105 kWh/kg NH ₃	DE Electricity Generation. BC, 2030 and 2050.
NH₃ Storage		Wilhelmshaven, DE.	NH ₃ @ 1 bar	0.068 kWh/kg NH ₃	DE Electricity Generation. BC, 2030 and 2050.
NH₃ Transport	Sea Tanker		NH ₃ @ 1 bar	NA	
NH₃ Cracking		Rotterdam, NL.	H ₂ @ 240 bar	4.86 kWh/kg H ₂	NL Electricity Generation. BC, 2030 and 2050.
H₂ Compression	Reciprocating Compressors	Rotterdam, NL.	H ₂ @ 700 bar		NL Electricity Generation. BC, 2030 and 2050.

Case 3: e-methanol Pathway

Figure 12 depicts the case 2, e-methanol pathway proposed for the study. Key parameters for this pathway are listed in Table 11. The pathway starts with green hydrogen production, employing the same criteria as those utilized in Case 1. CO₂ is assumed to be sourced from DAC with amina-based silica using a sorbent. The CH₃OH synthesis is an exothermic process with iron-based catalysis to produce hydrogen at 10 bar [85]. For the study, it was supposed that the heat would be not utilised for other processes. For the CH₃OH storage, it is anticipated that traditional storage tanks will be used for methanol produced from fossil sources. Additionally, all upstream processes were assumed to occur in the same location in Wilhelmshaven. Therefore, the study does not take into account the infrastructure required to connect to the processes.

The CH₃OH transport was modelled using truck tankers fuelled by low-sulphur marine diesel over a distance of 387 km to the bunkering port in Rotterdam. At the port, the CH₃OH dehydrogenation process and final compression were assumed to take place. During this step, methanol is converted back into hydrogen, producing emissions of CH₃OH and CO₂ [85].

Although e-methanol is synthesized using hydrogen from renewable sources, the CO₂ used in this process was assumed to originate from fossil fuels. This assumption was made to close the carbon loop, considering that the DAC process captures CO₂ from the atmosphere. Finally, as in Case 1, the hydrogen undergoes final compression to 700 bar.

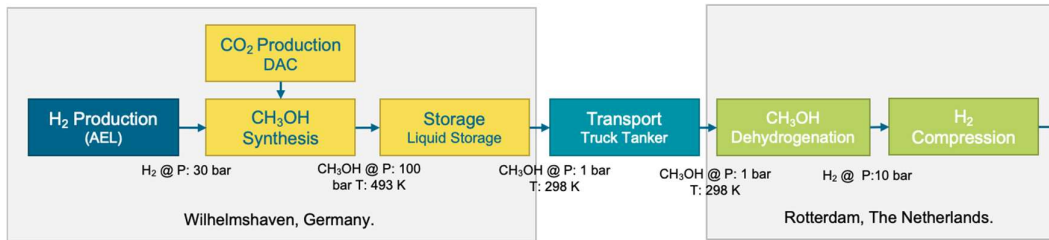


Figure 12 WTT system boundary phases: e-methanol pathway [own figure]

Table 11 Key Parameters case 2: e-methanol pathway [4] [82] [8]

Phase	Process Technology	Location	Output Product	Electricity Consumption	Electricity Source
H₂ Production	Alkaline Electrolysis	Wilhelmshaven, DE.	H ₂ @ 30 bar	50.12 kWh/kg H ₂	Wind Electricity – All Scenarios
CH₂ Production	DAC	Wilhelmshaven, DE.	N ₂ @ 200 bar	1.44 kWh/kg CO ₂	DE Electricity Generation. BC, 2030 and 2050.
CH₃OH Synthesis		Wilhelmshaven, DE.	NH ₃ @ 100 bar	0.29 kWh/kg NH ₃	DE Electricity Generation. BC, 2030 and 2050.
CH₃OH Storage		Wilhelmshaven, DE.	NH ₃ @ 1 bar	0.068 kWh/kg NH ₃	DE Electricity Generation: BC, 2030 and 2050.
CH₃OH Transport	Truck Tanker		NH ₃ @ 1 bar	NA	
CH₃OH Dehydrogenation		Rotterdam, NL.	H ₂ @ 1 bar	4.86 kWh/kg H ₂	NL Electricity Generation. BC, 2030 and 2050.
H₂ Compression	Reciprocating Compressors	Rotterdam, NL.	H ₂ @ 700 bar	3.2 kWh/kg H ₂	NL Electricity Generation. BC, 2030 and 2050.

Within the WTT scope, compressed hydrogen was selected as the final product for all three synthetic fuel pathways. This decision was made to ensure comparability of the hydrogen carriers within the WTT scope, using the same production site and bunkering location, and additionally to evaluate their potential for application in the most promising compressed hydrogen conversion technologies for ships, particularly considering hydrogen-based propulsion systems.

It is important to note that, for all synthetic fuel pathways in this case study, purification units were excluded. Similarly, oxygen treatment units were not considered within the scope of the study. Additionally, water treatment and demineralization units for water used as a feedstock in alkaline electrolysis were omitted. The impact of these units on the supply chains could be significant, and their inclusion is recommended for future research. Finally, the study considers synthetic fuel losses at each phase as a percentage of the output product within the functional unit. Details of these losses for each case in the WTT scope are provided in Appendix A.

3.2.1.1.2 WTW Scope

In the second part of the case study, WTW scope, a comparative analysis is provided of two energy conversion technologies that utilise compressed hydrogen as fuel: PEMFC and ICE. It is assumed that both technologies can be adapted to a Roll-on/Roll-off (RoRo) a vessel type commonly operating in the North Sea, which serves as the reference ship in this study. The technical parameters were established using the RoRo ship Magnolia Seaways, which has been previously examined in feasibility studies for retrofitting with a hydrogen-electric propulsion system [86]. Table 12 provides the technical specifications of the reference ship.

Table 12 Main specifications Magnolia Seaways [86]

Parameter	Value
Build year	2003
Dead Weight	23,700 ton
Propulsion Power	20 MW
Auxiliaries Power	6.8 MW

A route between Rotterdam and Immingham, UK, was selected for the study. This route was chosen because it is a currently route operated by DFDS, a European ferry and logistic company in the North Sea [87]. The route is typically served by a Roll-on/Roll-off (RoRo) ship. The calculations were based on defining a Round Trip (RT) as the journey between the departure and destination ports, including the return voyage. The operational data used for the RT calculations is provided in Table 14.

Table 13 Operation data of one round trip.

Parameter	Value	Comment / Reference
Total Power Requirement	27.9 MW	Own calculation.
Electric Motor Efficiency	95%	Taken from [8]
Round Trip Distance	776 km	Calculated using https://sea-distances.org/
RoRo average Speed	35.2 km/h	Taken from [8]
Time per Round Trip	22 hours	Own calculation.

The total power requirement of 27.9 MW was determined per RT, accounting for both propulsion power and auxiliary system demands such as hydraulics, hotel power, thrusters, and other systems [86]. For propulsion power, an electric motor efficiency of 95% was assumed [8]. This total power requirement was then used to calculate the energy demand in the form of fuel, specifically compressed hydrogen for both the PEMFC and ICE technologies. Table 14, presents the efficiencies and the calculations for electricity consumption and the corresponding amount of compressed hydrogen required per RT. It is important to note that the ICE also requires pilot fuel. For this study, MFO was used as a pilot fuel consumption was considered to be 9 gr/kWh during cruising and 30 gr/kWh during manoeuvring, with load factors of 80% and 20%, respectively [8].

Table 14 Energy conversion technologies parameters

Parameter	PEMFC	ICE	Comment / Reference
Efficiency	55%	48%	[49][8]
Electricity required per RT	615,963 kWh	615,963 kWh	Own calculation.
Hydrogen required per RT	33,598 Kg H ₂	38,498 Kg H ₂	Own calculation.
MFO Pilot fuel consumption per RT	NA	8,130 Kg	Own Calculation based on [8].

3.2.2 Functional Unit

The functional unit selected for the WTT scope is defined as one megajoule of the lower heating value (MJ_{LHV}) of the synthetic fuel across the entire supply chain. This was selected for the purpose of assessing the pLCA, by enabling the evaluation of an equivalent amount of energy delivered, regardless of the type of synthetic fuel, enhancing the comparability of the results. While for the WTW scope is defined as one round trip (RT) from Rotterdam to Immingham and back with the case study ship. This functional unit was selected to evaluate the overall impact of synthetic fuel, considering its entire lifecycle from production to consumption, under real operating conditions.

3.2.3 System Boundaries

As shown in Figure 13, the system boundaries for a WTW are divided into two main components. For the WTT component (indicated by the red dashed boundary), the synthetic fuel phases are represented as foreground systems (grey components), while electricity, infrastructure, and materials production are categorized as background systems (blue components). Conversely, the TTW component (dark blue dashed boundary) includes the energy conversion technologies and the storage on board as the foreground system, while the material production is classified as background systems. Electricity is shaded with dotted lines because prospective scenarios are considered

future estimations for the study. Similarly, H₂ production is shown with dotted lines because the study considers the estimation of future efficiencies. It is important to note that the system boundaries exclude the end-of-life phases for processes and technologies in this study. Instead, they focus solely on the construction and operational phases of the technologies and processes.

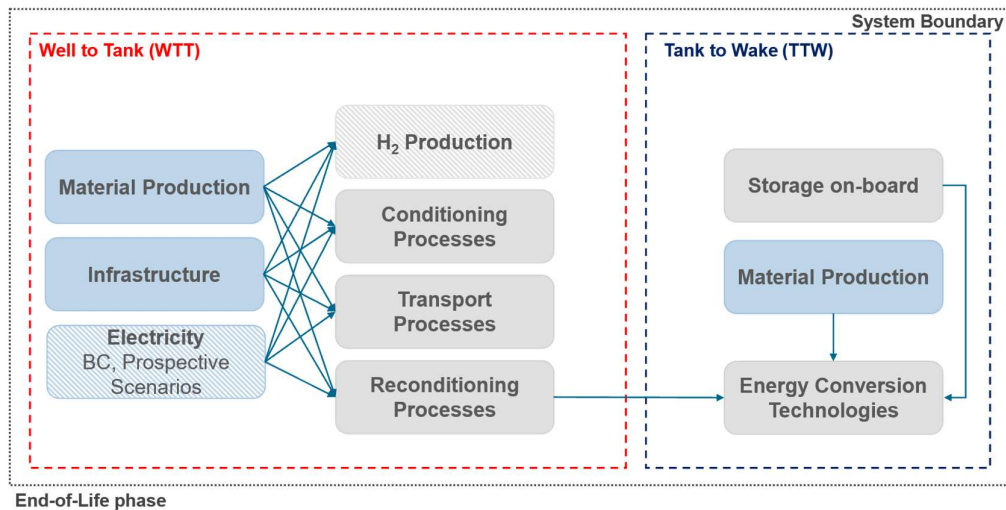


Figure 13 System boundaries applied for the study. Own plot adapted from [8]. Grey boxes represent the foreground processes, and blue represents the background processes. Boxes with dotted lines represent future estimations.

3.2.4 Life Cycle Inventory

The life cycle inventory data utilized for the modelling is presented in Appendix B. This study used foreground inventory data taken from previous scientific publications focus on supply chain application in the maritime sector. In the case of inventories of on-board energy conversion technologies, inventories for road applications were used due to the lack of available data for maritime applications. For the background inventories data, it was used Ecoinvent 3.9.1 database and the biosphere3 [76].

As mentioned previously in the case study description, for the WTT the phases are cumulative, meaning the output of one stage is the input of the next stage (change accordingly). Therefore, the outputs of each phase are the results of discounting the previous phase. This is in the case of the compressed hydrogen pathway. In the ammonia and methanol cases, the synthesis phases and the ammonia cracking and hydrogenation phases are evaluated individually, given stoichiometric of the process. Storage, transport and final compression were modelled as cumulative processes, so that the final result has to be discounted to assess individual impacts. Figure 14 illustrates the basic LCI diagram for the WTT scope, in which energy and materials are the inputs and the synthetic fuel (SF) and emissions represents the outputs.

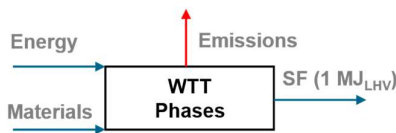


Figure 14 LCI Flow diagram WTT phases

No co-product allocation was performed in any case of the supply chains for WTT scope. All the impacts were attributed exclusively to the main product of each phase. Similarly, for this study, no cut-off criteria were applied except for those included in the inventories collected and those included in the Ecoinvent 3.9.1 database, for which the allocation cut-off by classification was used in the study. The cut-off criteria refer to the specification of the amount of material or energy flow, or the level of environmental significance associated with unit processes or product systems, to be excluded from a study [88]. Finally, for infrastructure, plant capacity plant and lifetime aspects were used to scale material requirements according to the functional unit. Specific storage durations and numbers of trips per lifetime were assumed for the storage and transport phases.

In the context of the second part of study (WTW), inventories for on-board hydrogen storage have been incorporated in conjunction with conversion technologies. For the ICE, the inventory includes the generator required to produce the propulsion power and MFO as a pilot fuel. However, all other elements of the powertrain (e.g. control unit, gear/box and propeller) system are excluded from the scope and, therefore, from the LCI. This exclusion is justified by the study focuses on manufacturing and operating energy conversion technologies and the storage on-board. Both technologies use compressed hydrogen as the primary fuel source which use the Case 1: e-hydrogen pathway, where the inventories were taken. Figure 15 shows the basic LCI diagram for energy conversion technologies, where compressed hydrogen and materials represent the inputs, and the output product represents the electricity required per RT for both technologies. In addition, MFO as an input and the emissions produced by its combustion are considered in the LCI of the ICE.



Figure 15 Flow diagram for energy conversion technologies

3.2.4.1 Data Collection

The present study is primarily based on data collected by Soler et al. [82] for the WTT scope. In particular for the case 1: compressed hydrogen pathway, with regard to hydrogen production using alkaline electrolysis technology, efficiencies and main parameters for processes such as electricity consumption, process inputs and by-

products were derived from the Schmidt et al. [82]. In addition, the inventories for the stack for electrolyser production of 1 MW were derived from Delpierre et al. [84]. For the compression phase the inventories by Soler et al. [82] were used and for the compression construction the inventory was derived from Van der Giesen et al. [89]. The inventory for the storage in a salt cavern was taken from Wulf et al. [59]. Subsequently, pipeline construction and operation inventories were derived from Tsiklios et al [30]. For the compression in the bunkering port, inventory taken for the previous compression phase is used. However, the compression design was scaled by the required final pressure. For this, electricity consumption was derived from Kanchiralla et al. [8].

Regarding the case 2: e-ammonia pathway, the inventory for the nitrogen production was derived from Mayer et al.[16], e-ammonia production from D'Angelo et al. [90]. Moreover, the inventory for the ammonia storage was derived from Alghool et al. [61]. As the e-ammonia was defined to transport by sea tanker and can be transported in the same way as LNG [61], theecoinvent activity “transport, freight, sea, tanker for liquefied natural gas” was used. At this point, it was considered to use the density ratio of liquefied natural gas to liquefy ammonia by 1.6 to calculate the fuel consumption of the liquefied ammonia tanker using the fuel consumption of HFO in kg HFO / Ton-km and the emission due to the use of heavy fuel oil. In addition, the ammonia cracking inventory were derived from Arrigorri et al. [91][Click or tap here to enter text..](#)

Finally for the case 3: e-methanol pathway, the DAC inventory was derived from Qie et al [18], e-methanol synthesis inventory from Schmidt et al. [82]. Moreover, the inventory for the e-methanol storage was derived from the Ecoinvent activity “liquid storage tank production, chemicals, organics,” due to the fact that e-methanol can be stored in as a fossil fuel product. In the same way as for the e-methanol transport, for which “market for transport, freight, lorry >32 metric ton, EURO6” was used. Finally, the e-ammonia dehydrogenation inventory was taken from Alghool et al. [61].

With regard to the second part of study (WTW), the Type IV 700 bar epoxy resin tank construction inventory was derived from Usai et al [92]. The PEMFC plant and stack inventories were taken from Stropnick et al. [93]. The ICE construction inventory was taken from Fernandez-Rios et al [54]. In addition, the low sulphur diesel inventory was used for the MFO due to its similarity in density and the Ecoinvent market group for diesel, low sulphur activity. Finally, the emission derived from the combustion of the MFO was taken from Kanchiralla et al. [8].

3.2.4.1.1 Electricity Generation Scenarios

In order to assess the potential environmental impacts depending on the electricity mix used in the several process phases after H₂ production, different future scenarios for

electricity generation in the considered countries Germany and the Netherlands (background data) are assumed and integrated into the pLCA. The selection of electricity as a key variable is justified by its central role in most phases defined within the Well-to-Tank (WTT) scope, where electricity serves as a primary input. Furthermore, IRENA mentioned that the GHG emissions of synthetic fuels are determined by the carbon intensity of the electricity utilized and carbon and the source of the CO₂ feedstock [94].

This study does not include Integrated Assessment Model (IAM) scenarios since REMIND and IMAGE models are defined for the transnational level such as Western Europe Union (WEU) and are not available for the specific countries proposed for the case study. Figure 16 illustrates the current and the projected electricity generation scenarios by source, as considered in the locations included in the study case (Germany and the Netherlands), across three scenarios: the base case (BC), 2030 and 2050 scenarios.

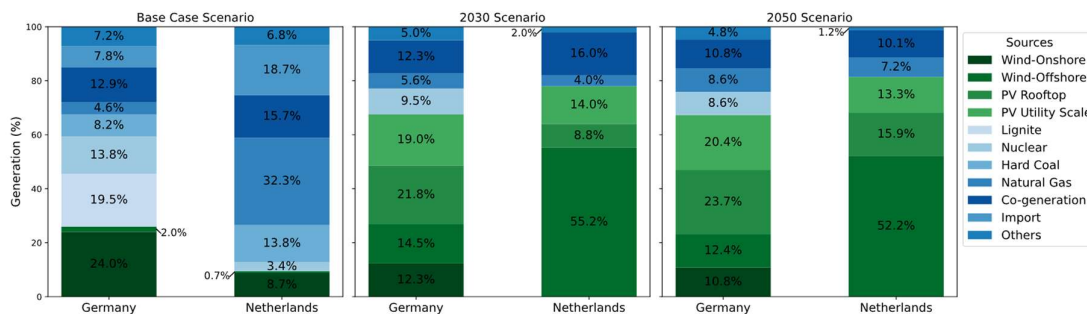


Figure 16 Electricity generation scenarios: Germany and Netherlands [76] [95]

Base Case Scenario (2019): The Ecoinvent 3.9.1 activity market for energy high voltage from Germany and the Netherlands in 2019 represents the electricity generation scenario utilized in the base case scenario. [76]. The outdated scenario (2019) represents a challenge to demonstrate the timeliness of the study, as Kanchiralla [47] claims. His study, published in 2022 [55], used the Ecoinvent 3.7 wind electricity data set. The author suggests that if the updated data is not available, it would be better to use the published background dataset for the completed framework considered in the study. The Ecoinvent 3.9.1 database for electricity generation in Germany and the Netherlands is based on 2019 data. Although Ecoinvent 3.10.1 and Ecoinvent 3.11, released in November 2024, introduced electricity mix fixed for 2020 and updated for 2023 for reference countries, respectively [96]; however, it became available only during the final phase of this study and could not be integrated. Therefore, Ecoinvent 3.9.1 was chosen to ensure reliable data and methodological consistency across all scenarios. In Germany, 26% of the power generation is accounted for by onshore and offshore wind electricity generation, respectively, representing the renewable energy component. For the remaining 74%,

which represents the non-renewable energy component, electricity generation from lignite represents the largest contributor, accounting for 19% of the non-renewable energy component. For the purposes of this case study, import sources are considered part of the non-renewable component. In contrast, in the Netherlands, 9.4% of the power generation is accounted for by onshore and offshore wind electricity generation, respectively, representing the renewable energy component. The remaining 90.6% is accounted for by the non-renewable energy component, with electricity generation from hard coal representing the largest contributor, accounting for 32% of the non-renewable energy component. For the purposes of this case study, import sources were considered part of the non-renewable component.

2030 Scenario: The 2030 electricity generation scenario employed in the study is represented by the scenario defined by Prina et al. [77]. This scenario was evaluated using a multi-objective approach to identify optimal solutions, with the objective of minimising the cost of expansion capacity while minimising annual CO₂ emissions in the intermediate scenario from the Pareto approach for seven European countries, including Germany and the Netherlands. The present study was utilised because it considers electricity mix projections for the countries in question, employs the same estimation criteria for both countries and focuses on reducing CO₂ equivalent emissions. For this scenario, In Germany, 67.5% of the power generation is accounted for by onshore and offshore wind and photovoltaic from rooftop and utility scale electricity generation, respectively, representing the renewable energy component. For the remaining 32.4%. In contrast, in the Netherlands, 78% of the electricity generation scenario is accounted for by onshore and offshore wind electricity generation, respectively. For the remaining 22%, represents the non-renewable energy component. Similarly, as in the BC scenario, import sources were considered to be part of the non-renewable component.

2050 Scenario: The same approach employed by Prina et al [77] was taken for the 2050 electricity generation scenarios for Germany and the Netherlands. In Germany, 67.2% of the power generation is accounted for by onshore and offshore wind and photovoltaic from rooftop and utility scale electricity generation, respectively. For the remaining 32.8%, represents the non-renewable energy component. In contrast, in the Netherlands, 81.4% of the electricity generation scenario is accounted for by offshore wind and photovoltaic electricity generation, respectively. For the remaining 18.6%, represents the non-renewable energy component. Similarly, as in the base case and 2030 scenario, import sources were considered to be part of the non-renewable component.

3.2.5 Life Cycle Impact Assessment

The impact assessment method employed in this study is Environmental Footprint - EF 3.1 and is focused on the categories illustrated in Table 15. The selection of this method is based on the recommendation of using this methodology by the Joint Research Centre in the document EU Commission Recommendation 2021/2079 [97]. Moreover, the European Commission has expressed support for the EF development, particularly with regard to activities such as the alignment between the Product Environment Footprint (PEF) and relevant standards (e.g. EN 15804) and the update and development of characterization models, normalization factors, and weighting factors for the life cycle impact assessment phase, among the most important contributions [97]. The selection of the six categories for presentation and analysis of the results is grounded in the premise that these categories possess the most significant impact on synthetic fuels and energy supply chains, as evidenced by preceding studies. Table 15 depicts the impact category, indicator, unit and the underlying LCIA method per impact category in the EF 3.1. The description of the categories and the unit in the context of the case study is explained below. While the category of water resources is pivotal for the analysis of the environmental impacts of hydrogen production by electrolysis, it has not been incorporated within LCIA due to the fact that the focus is oriented towards the post-production stages of the supply chains.

Table 15 EF3.1 Impact categories used in the study [72]

IMPACT CATEGORY	INDICATOR	UNIT	UNDERLYING LCIA METHOD
Climate Change	Radioactive Forcing as GWP100	kg CO ₂ eq	Bern model – GWP100 based on IPCC 2021.
Acidification	Accumulate Exceedance (AE)	Mol H ⁺ eq	Accumulate Exceedance.
Eutrophication, marine	Fraction of nutrients reaching marine end compartment (N).	kg N eq	EUTREND model as implemented in ReCiPe 2008.
Resource use, fossil	Abiotic resource depletion – fossil fuels (ADP fossil fuels)	kg Sb eq	CML 2002 method, v.4.8.
Resource use, minerals and metals	Abiotic resource depletion (ADP ultimate reserves)	MJ	CML 2002 method, v.4.8
Lan Use	Soil Quality Index	Dimensionless (pt)	Soil quality index based on LANCA model and version 2.5

Climate Change: This category assesses the impact of the GHG emissions, such as CO₂, N₂O, and CH₄ into the atmosphere as a result of human activities [47]. The consequences of this include increased average global temperatures and regional

climate change [73]. For this study, Global Warming Potential (GWP) is used as the metric to quantify climate change impacts. The unit $\text{kg CO}_2 \text{ eq/MJ}_{\text{LHV}}$ indicates the equivalent emission per unit of energy content of the synthetic fuel in the WTT while $\text{kg CO}_2 \text{ eq/RT}$ in the WTW.

Acidification: This category assesses the impact of acidifying substances in the environment, with a particular focus on soils and water bodies when hydrogen ions are released. These substances have a low capacity to be neutralized or absorbed by ecosystems without undergoing a significant change in pH. This can result in forest decline and lake acidification [73]. For this study, the unit $\text{moles H}^+ \text{ eq/MJ}_{\text{LHV}}$ indicates the quantity of hydrogen ions (H^+) in the emissions per energy content of the synthetic fuel in the WTT and $\text{H}^+ \text{ eq/RT}$ for WTW. The emission of hydrogen ions is a consequence of the mineralization of NO_x , NH_3 , and SO_x gases.

Marine Eutrophication: This category assessed the degree to which emitted substances, such as nitrogen or phosphorus, reach the sea [72]. In general, an increase in nitrogen levels has been observed to result in a significant growth of algae, which has the potential to disturb the balance of the marine environment [47]. In this study, the unit $\text{kg N eq/MJ}_{\text{LHV}}$ indicates the quantity of nitrogen equivalent per energy content of the synthetic fuel in the WTT and N eq/RT for WTW.

Resource use, fossil: This category addresses the use of non-renewable fossil natural resources, for instance, natural gas, coal and oil [73]. In this study, the unit $\text{MJ/MJ}_{\text{LHV}}$ indicates the energy content of fossil fuel per energy content of the synthetic fuel in the WTT and MJ/RT for WTW.

Resource use, minerals and metals: This category assesses the use of non-renewable abiotic natural resources, mineral and metals [73]. In this study, the unit $\text{kg Sb eq/MJ}_{\text{LHV}}$ unit indicates the quantity of non-renewable minerals and metals in kg of antimony used as a reference substance per energy content of the synthetic fuel in the WTT and $\text{kg Sb eq/MJ}_{\text{LHV}}$ for WTW.

Land Use: This category assesses land area use (occupation) and conversion (transformation) by activities related to the processes [73]. In this study, the unit $\text{pt/MJ}_{\text{LHV}}$ indicates the points per energy content of the synthetic fuel in the WTT and pt/RT for WTW.

3.2.6 Interpretation

The final stage of the methodology implies the interpretation of the results, which will be performed in the chapters Results and Discussion. respectively. Subsequent to this, the limitations, conclusions, and future work will also form part of the interpretation and will provide the key outcomes of the study and its analysis.

4 Results

4.1 Part 1: WTT Results

4.1.1 Global Warming Potential (Kg CO₂ eq) Category: WTT Scope

Figure 17 illustrates the GWP impact results for the WTT phases of synthetic fuel pathways: e-hydrogen (H₂), e-ammonia (NH₃), and e-methanol (CH₃OH). The results are presented across three scenarios: Base Case (BC), 2030 and 2050. The WTT phases of each fuel are delineated into individual phases, including e-hydrogen production, storage, transportation, and conditioning and reconditioning processes. The black dashed line indicates the total values for each pathway in each scenario. Contributions are presented in percentage (%) to the GWP result for the pathway are illustrated in stacked bars and detailed explanation will be provided subsequently. The comparison of these results with prior studies can be found in in the discussion chapter.

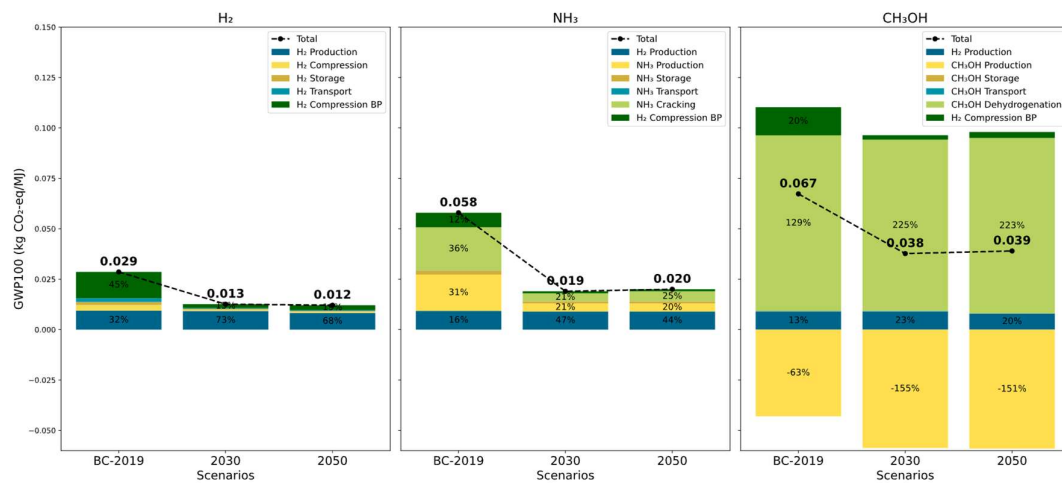


Figure 17 GWP of WTT synthetic fuel pathways

Case 1: e-hydrogen Pathway

The e-hydrogen pathway is disaggregated into specific phases, including H₂ production, compression, storage, transport, and final compression in the bunkering port. Figure 18 illustrates the results of GWP, represented by individual bars, with the final bar indicating the total per scenario. The total GWP decreases from 0.029 kg CO₂ eq/MJ_{LHV} in BC to 0.013 kg CO₂ eq/MJ_{LHV} in 2030 and subsequently to 0.012 kg CO₂ eq/MJ_{LHV} in 2050, representing a total reduction of 57% by 2030 and 61% by 2050 in comparison to the BC. The reductions are predominantly attributable to the increased share of renewables in electricity generation for supply chain phases, where electricity consumption is the primary source of CO₂ eq/MJ_{LHV}. A detailed phase-by-phase analysis follows.

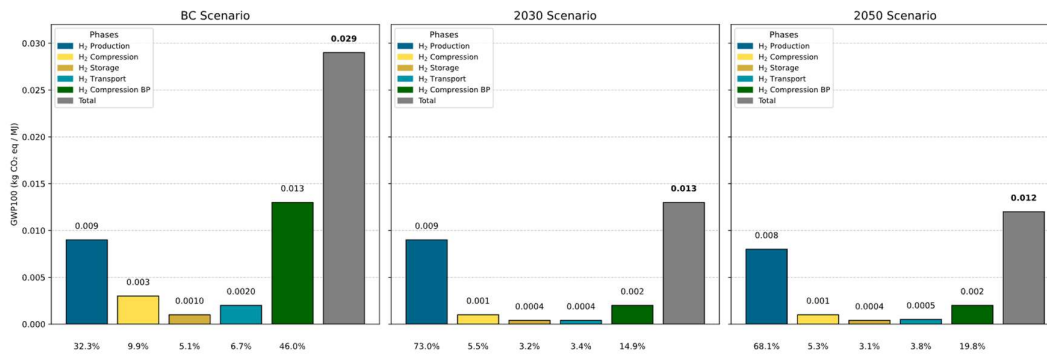


Figure 18 GWP of H₂ pathway for BC, 2030 and 2050 scenarios

The H₂ production represents a GWP of 0.0094 kg CO₂ eq/MJ_{LHV} for BC, 0.0092 kg CO₂ eq/MJ_{LHV} for the 2030 and 0.0084 kg CO₂ eq/MJ_{LHV} for the 2050. The largest contributor to this phase is the electricity production from wind electricity consumption, which accounts for 84% of the total impact. Although wind energy is considered as a non-fossil fuel source, the manufacturing of materials such as iron, fibreglass and concrete, which are required for the construction of wind turbines, generates a relevant impact. The second largest contributor is the stack used for the alkaline electrolyser, which accounts for 15% of the total impact. The observed reduction for the prospective scenarios, 2% for the 2030 and 11% for the 2050 compared to the BC, can be attributed solely to the projected decline in alkaline electrolysis technology efficiencies reported by Schmidt et al. [82], given that all scenarios were based on a wind-based electricity generation assumption. This primarily results in a reduction in electricity consumption, which subsequently leads to a slight decrease in GWP emissions. Furthermore, in consideration of prospective scenarios, the contributors to the GWP will remain consistent with the BC.

Subsequently, the e-hydrogen must be compressed from 30 to 85 bar, the required pressure for injection into the salt cavern storage facility. The impact of the H₂ compression represents a GWP of 0.003 kg CO₂ eq/MJ_{LHV} for the BC in which the main contributor is the use of electricity in Germany. It is anticipated that 76% and 78% will be reduced in comparison to BC for the 2030 and 2050, respectively. These reductions can be attributed to integrating energy scenarios that predominantly employ increase share of wind and photovoltaic energy, which account for 67.6% and 67.2%, respectively, in Germany, where the compression plant is assumed to be located. In this process, the primary contributor is the electricity consumption (0.72 kWh/kg H₂) required for the reciprocating compression units.

Following H₂ compression, it is stored in a salt cavern facility at a pressure of 85 bar. This phase contributes 0.001 kg CO₂ eq/MJ_{LHV} to the GWP in the BC. It is anticipated that 73% and 74% will be reduced in comparison to the BC for the 2030 and 2050,

respectively. Similarly to the compression phase, the reductions can be attributed to incorporating of energy scenarios that predominantly employ wind and photovoltaic electricity, which account for 67.6% and 67.2%, respectively. The main contributor to this process is the electricity consumption of the compressor and dryer utilized in the salt cavern operation before the hydrogen is injected into the pipeline.

The transport contributes 0.002 kg CO₂ eq/MJ_{LHV} to the GWP in the BC scenario. It is anticipated that 78% and 76% will be reduced in comparison to the BC for the 2030 and 2050, respectively. In accordance with the established process parameters, the optimal configuration was determined to be four compressor units per each 100 km. The initial two units are based on the German electricity generation scenario, whereas the final two are aligned with the Dutch electricity generation scenario. The GWP for the BC can be attributed to the fact that 95% of the impact can be linked to the electricity employed for the operation of the compression units, while the pipeline construction represents the second contribution, accounting for 5% for the BC. In both the 2030 and 2050, a decrease in the impact contribution from the operation of compression units was observed, reaching 80%. Conversely, the impact contribution from the pipeline construction decreased to 20%. As with the previous phases, the results for the future scenarios can be attributed to incorporating energy scenarios that predominantly employ wind and photovoltaic electricity, which account for 67% of both scenarios and 78% and 81% for the Netherlands in 2030 and 2050, respectively. By 2050, the reduction is slightly lower than in 2030 (76% vs 78%). While the share of renewables increases, the share of non-renewable natural gas sources increases from 4% to 7% in the Netherlands and from 5% to 8% in Germany, which explains the lower emission reduction.

The final phase of the e-hydrogen pathway involves compression to 700 bar. A contribution of 0.013 kg CO₂ eq/MJ_{LHV} to the GWP is made by this phase in the BC, representing the highest emission value across the entire pathway. In relation to the base case scenario, 86% and 82% reductions are observed for the 2030 and 2050, respectively. The result is primarily influenced by electricity consumption in the Netherlands, estimated at 3.2 kWh/kg H₂ and integrating energy scenarios that predominantly employ wind and photovoltaic energy, which account for 78% and 81%, respectively, in The Netherlands, where the bunkering port was assumed to be located. By 2050, the reduction is slightly lower than in 2030. While the share of renewables increases in the Netherlands, the share of non-renewable natural gas sources increases from 4% to 7%, which explains the lower emission reduction.

Case 2: e-ammonia Pathway

The e-ammonia pathway for each scenario is disaggregated into specific phases, including H₂ production, NH₃ synthesis, storage, transport by sea tanker, NH₃ cracking and final H₂ compression in the bunkering port. Figure 19 illustrates the contribution of each phase to the overall GWP which are represented by individual bars, with the final bar indicating the total for each scenario. The total GWP will decrease from 0.058 kg CO₂ eq/MJ_{LHV} in base case scenario to 0.019 kg CO₂ eq/MJ_{LHV} in 2030 and subsequently to 0.02 kg CO₂ eq/MJ_{LHV} in 2050, representing a total reduction of 66% by 2030 and 65% by 2050 in comparison to the BC. The reductions are predominantly attributable to the electricity consumption across the various phases, which constitutes the primary source of CO₂ eq/MJ_{LHV}. The detailed analysis per individual phase is presented below.

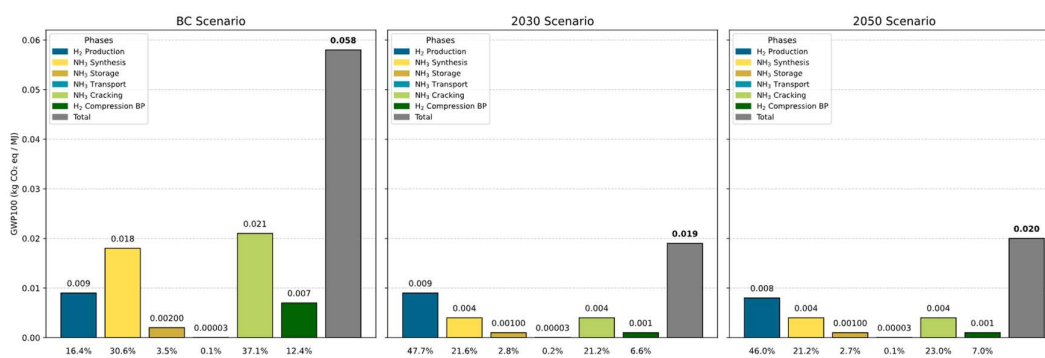


Figure 19 GWP of NH₃ pathway for BC, 2030 and 2050 scenarios

The GWP impact result for H₂ production was consistent with the result derived from Case 1. In Case 2, e-hydrogen constitutes the primary input for NH₃ synthesis via the Haber-Bosch process, in conjunction with the nitrogen derived from cryogenic distillation in a separate plant. The GWP of NH₃ synthesis reveals a value of 0.018 kg CO₂ eq/MJ_{LHV}, 0.0042 kg CO₂-eq/MJ_{LHV} for the 2030, and 0.0043 kg CO₂ eq/MJ_{LHV} for the 2050. It is anticipated that 76.2% and 75.8% will be reduced in comparison to the BC for the 2030 and 2050, respectively. These reductions can be attributed to integrating energy scenarios that predominantly employ wind and photovoltaic energy, which account for 67.6% and 67.2%, respectively, in Germany, where the Haber-Bosh and Nitrogen production plants are assumed to be located across all scenarios. In this process, the primary contributor is the electricity consumption (0.56 kWh/kg NH₃) required for the NH₃ production by 86%, followed by the electricity consumption (0.21 kWh/kg N₂) for the N₂ production by 13%, while the chemical plant materials for the process represents the 1% for the BC. In both the 2030 and 2050, the contribution will remain in the same order.

Following the NH₃ synthesis, storage phase reveals a GWP of 0.002 kg CO₂ eq/MJ_{LHV} for the BC and 0.0005 kg CO₂ eq/MJ_{LHV} for 2030 and 2050, respectively. It is anticipated

that 73.2% and 72.8% will be reduced in comparison to the BC for the 2030 and 2050, respectively. In this process, the primary contributor is the electricity consumption (0.068 kWh/kg NH₃) required to operate the compressors to maintain the ammonia refrigerated by 95% in all scenarios. The reduction in emissions will be mainly due to the electricity generation for 2030 and 2050, respectively.

For the transport phase, it was assumed to be done sea tanker. This phase contributes to 0.00003 kg CO₂ eq/MJ_{LHV} to the GWP in the BC. It is anticipated that the same result will be observed for the 2030 and 2050. This can be attributed to the fact that for this process, the impact is due to the fuel use in the ship, which in this case is heavy fuel oil (HFO). Consequently, 80% of the impact will be generated by the emissions released during the trip, mainly CO₂ with fossil origin. Furthermore, 17.7% is due to the production of the fossil-based fuel used and the remaining due to the ship tanker construction.

As soon as e-ammonia is transported to the bunkering point, it is required to be re-converted to e-hydrogen according to study. The NH₃cracking phase contributes 0.021 kg CO₂ eq/MJ to the GWP in the BC, 0.0041 kg CO₂ eq/MJ in the 2030, and 0.0046 kg CO₂ eq/MJ to the GWP in the 2050. A reduction of 81% and 78%, was observed respectively, compared to the BC. By 2050, the reduction is slightly lower than in 2030. While the share of renewables increases in the Netherlands, the share of non-renewable natural gas sources increases from 4% to 7%, which explains the lower emission reduction. These decreases are attributed to the incorporation of electricity generation scenarios, where wind and photovoltaic energy account for 78% and 81%, respectively, in The Netherlands, which is assumed NH₃ cracking plant was assumed to be located. The electricity consumption for this process represents 98% of the impact in BC and 89% in the 2030 and 2050, emphasizing the dominant role of renewable energy integration in reducing the environmental impact of NH₃ cracking.

The final phase for the e-ammonia pathway involves the H₂ compression from 240 to 700 bar. A contribution of 0.007 kg CO₂ eq/MJ_{LHV} to the GWP, 0.0013 kg CO₂ eq/MJ_{LHV} and 0.0014 kg CO₂-eq/MJ_{LHV} are made by this phase in the BC, 2030 and 2050, respectively. In relation to the BC, reductions of 81% and 79% are observed for 2030 and 2050, respectively. As the previous phase, by 2050, the reduction is slightly lower than in 2030. While the share of renewables increases in the Netherlands, the share of non-renewable natural gas sources increases from 4% to 7%, which explains the lower emission reduction. The emission results are primarily influenced by electricity consumption estimated at 1.7 kWh/kg H₂. As well as case 1, the reductions for 2030 and 2050 can be attributed to integrating energy scenarios that predominantly employ wind and photovoltaic energy, which account for 78% and 81%, respectively, in The Netherlands, where the compression plant in the bunkering port was assumed to be located.

Case 3: e-methanol Pathway

The e-methanol pathway for each scenario is disaggregated into specific phases, including H₂ production, the CH₃OH synthesis, storage, transport by truck tanker, CH₃OH dehydrogenation and final hydrogen compression in the bunkering site. The Figure 20 illustrates the contribution of each phase to the overall GWP which are represented by individual bars, with the final bar indicating the total for each scenario. The total GWP for e-methanol decreases from 0.076 kg CO₂ eq/MJ_{LHV} in BC to 0.038 kg CO₂ eq/MJ_{LHV} in 2030 and subsequently to 0.02 kg CO₂ eq/MJ_{LHV} in 2050, representing a total reduction of 43% by 2030 and 41% by 2050 in comparison to the base case scenario. The lesser reduction in 2050 is mainly due to the fact that hydrogenation represents a process with a high demand for electricity. Despite the higher proportion of electricity production from renewable sources, the proportion of electricity production from natural gas also grows from 4 to 7.2% for the Netherlands and from 5.6% to 8.6% for Germany, compared with the 2030 scenario, thus increasing the impact on the results of GWP. The reductions are predominantly attributable to the electricity consumption across the various phases of the supply chain, which constitutes the primary source of CO₂ eq/MJ_{LHV}. The detailed analysis per individual phase is presented below.

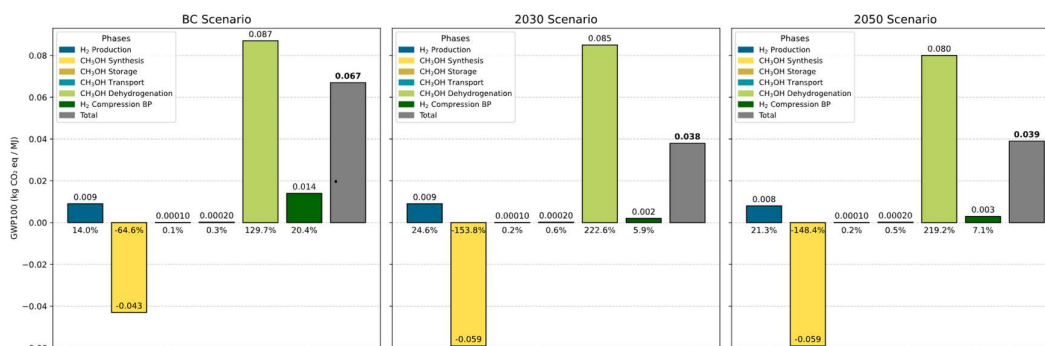


Figure 20 GWP of CH₃OH pathway for BC, 2030 and 2050 scenarios

The GWP impact result for H₂ production is consistent with the result derived from Case 1. In case 3, e-hydrogen is the primary input for the CH₃OH synthesis. CO₂ is also required, which in the case study is produced by DAC process; therefore, the GWP result includes the results of the DAC process. As the DAC process has been modelled to capture CO₂ from the atmosphere, the GWP result for this phase is -0.043 kg CO₂ eq/MJ_{LHV} for the base case scenario. For the CH₃OH synthesis, the impact caused by the electricity used for the base case was outweighed by the negative impact of the CO₂ captured. The CH₃OH synthesis reveals a GWP of -0.059 kg CO₂ eq/MJ_{LHV} and -0.059 kg CO₂ eq/MJ for the 2030 and 2050. For both will be expected to be 27% lower than the BC. These reductions can be attributed to integrating energy scenarios that predominantly employ wind and photovoltaic energy, which account for 67.6% and

67.2%, respectively, in Germany, where the e-methanol and DAC plants are assumed to be located across all scenarios. For the BC, after the impact of CO₂ captured, the electricity consumption (0.56 kWh/kg CH₃OH) required for CH₃OH synthesis represents the main contributor, followed by the heat from biomethane used in the DAC process.

Following the CH₃OH synthesis, the storage phase reveals a GWP of 0.0001 kg CO₂ eq/MJ_{LHV} for all scenarios. For this phase, it was assumed that a chemical tank used for fossil fuels can be used for e-methanol. The result obtained for all scenarios is that methanol is typically stored in ambient conditions and, therefore, does not require refrigeration [61]. Consequently, it is independent of electricity consumption.

The transport phase was assumed to be done by truck tanker, which is also independent of the electricity consumption. This phase contributes 0.0002 kg CO₂ eq/MJ_{LHV} to the GWP for all scenarios. The impact is attributable to the fuel used in the truck, which in this case is diesel with low sulphur content and which releases methane, CO₂ and NH₃ as the more significant emissions, as defined in the Ecoinvent activity.

As soon as the e-methanol is transported to the bunkering port, it is required to be re-converted to e-hydrogen according to study. The CH₃OH dehydrogenation process reveals a GWP of 0.087 kg CO₂ eq/MJ_{LHV} to in the BC, 0.085 kg CO₂ eq/MJ_{LHV} to for the 2030, and 0.080 kg CO₂ eq/MJ_{LHV} for the 2050. A reduction of 2% and 8%, respectively, compared to the BC, is observed for 2030 and 2050, respectively. For the BC, the 93% of the impact correspond to the CO₂ emissions from the process. As a second contributor, it was observed that the heat production from Natural Gas by 7%. For 2030 and 2050, the impact of the CO₂ emissions will remain the same as the BC. Following the impact of the CO₂ emissions released in the process, which are essentially offset by the emissions from CO₂ capture in the CH₃OH synthesis. The use of natural gas is associated with a significant environmental footprint. This is because the production source utilised is natural gas, which is characterised by generally high emissions, particularly CO₂, which accounts for 80% of the total emissions according to the results. The final phase of the e-methanol pathway entails H₂ compression from 10 to 700 bar, which corresponds to the identical GWP results obtained for case 1.

4.1.2 Impact assessment of Other Categories: WTT Scope

Figure 21 presents the impacts of the other environmental categories defined for the WTT scope (see also chapter 3.1.1). Each graph presents the results in the respective unit for each category on the y-axis and the synthetic fuel pathways on the x-axis. For each synthetic fuel pathway, a bar graph is provided, with each bar representing the results per scenario.

The NH₃ pathway has demonstrated consistently elevated environmental impacts within the domains of acidification and eutrophication, attributable to the emission of NO₂ and NH₃ from the Haber-Bosch process. Within the energy resources category, both the e-ammonia and e-methanol pathways exhibit analogous values in the BC; however, a substantial decline is projected for the years 2030 and 2050, attributable to the increase in the share of renewables in electricity generation. Conversely, the material resource category is projected to experience an increase in prospective scenarios for all pathways, primarily driven by the demand for nickel, copper, and silver in wind and photovoltaic energy. Similarly, the land use category is anticipated to rise in future scenarios, driven by the expansion of wind turbines and photovoltaic installations, impacting forest and industrial areas. The results for the acidification, marine eutrophication, energy resources, material resources and land use categories are elucidated in detail in Appendix C, while the results for the GWP category were previously discussed.

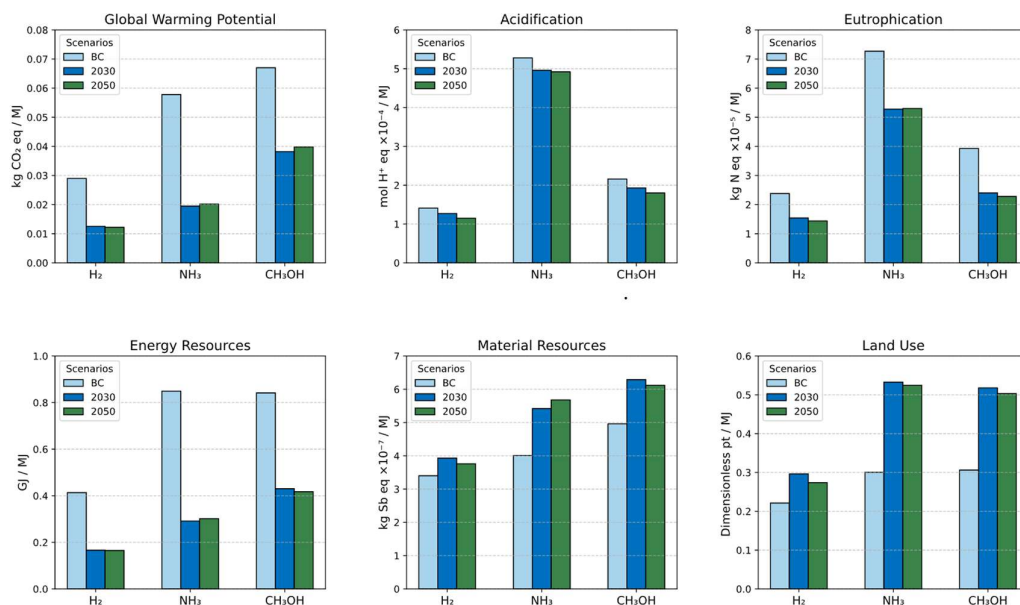


Figure 21 Environmental impacts of EF 3.1 impact categories for synthetic WTT fuels pathways

In Figure 21 for the acidification category, e-ammonia pathway consistently shows the higher acidification values across all scenarios with 5.3×10^{-4} mol H⁺/MJ_{LHV} for the BC and a decrease of 7% for 2030 and 2050. E-methanol pathway represents the second higher value in the acidification category with 2.1×10^{-4} mol H⁺/MJ_{LHV} for the BC. It will decrease by 10% and 13%, respectively, for 2030 and 2050. Finally, the e-hydrogen pathway has a value of the acidification category with 1.4×10^{-4} mol H⁺/MJ_{LHV} for the BC. It will decrease by 10% and 12%, respectively, for the 2030 and 2050.

Regarding eutrophication category, Figure 21 illustrates the e-ammonia pathway consistently exhibits the highest values across all scenarios. The BC value is 7.3×10^{-5} kg

N eq/MJ_{LHV}, while the 2030 and 2050 scenarios indicate a 27% decrease for both scenarios. E-methanol pathway represents the second-highest value in the eutrophication category, with a value of 3.9×10^{-5} kg N eq/ MJ_{LHV} for the BC. It will experience a decrease of 27% and 39%, respectively, for 2030 and 2050. Finally, the e-hydrogen pathway has a eutrophication result of 2.4×10^{-5} kg N eq/MJ_{LHV} for the BC, with a projected decrease of 35% and 40% by 2030 and 2050, respectively.

Concerning the energy resources category, In Figure 21 the e-ammonia and e-methanol pathways show the higher energy resources impact for the BC with a value of 0.84 GJ / MJ_{LHV} for the BC. It can be seen that there will be a decrease of 65% and 49% in the e-ammonia and e-methanol pathways, respectively, in 2030 and 2050. Finally, the e-hydrogen pathway a result of 0.41 GJ / MJ_{LHV} for BC, indicating a projected decrease of 60% for 2030 and 2050, respectively.

Similarly, for the material resources category in Figure 21 the e-methanol pathway shows the most significant impact for BC. This is evidenced by a value of 5×10^{-7} kg Sb eq/MJ_{LHV} for the BC, which is projected to exhibit an increase of 27% and 23% for 2030 and 2050, respectively. Subsequently, the e-ammonia pathway with a value of 4×10^{-7} kg Sb eq/MJ_{LHV} for BC will have an increase by 35% and 42%. Finally, the e-hydrogen pathway has a result of 3.4×10^{-7} kg Sb eq/MJ_{LHV} for the BC scenario and will increase of 16% and 11% for the 2030 and 2050, respectively.

Finally, for the land use category Figure 21 shows that the e-methanol pathway has the most significant impact for the BC compared to the pathways with a value of 0.31 pt/MJ_{LHV} for the BC and will have an increase of 69% and 64%. Follow by the e-ammonia pathway with a value of 0.31 pt/MJ_{LHV} for the base case scenario and will have an increase of 77% and 74%. Finally, the e-hydrogen pathway has a result of 0.22 pt/MJ_{LHV} for BC and will have an increase of 34% and 24% for 2030 and 2050, respectively.

4.2 Part 2: Well-to-Wake WTW Scope Results

4.2.1 Global Warming Potential (Kg CO₂ eq) Category

The results of the GWP for all scenarios comparing energy conversion technologies for maritime application, as defined for the study, are illustrated in Figure 22.

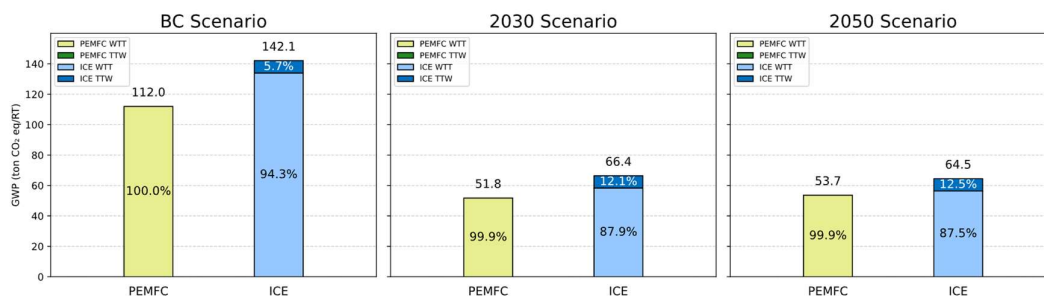


Figure 22 GWP for the PEMFC and ICE utilization per RT (WTW)

In the BC, it was found that the emissions generated by ICE were higher than those produced by PEMFC by 26%. In this study, both technologies were assumed to utilize compressed hydrogen as a main fuel, although differences in their efficiencies were evident. Additionally, it was identified that the use of MFO as a fossil fuel was a significant factor influencing the observed results in the case of ICE. Furthermore, in BC the impact from WTT corresponds to 100% and 94.3% for PEMFC and ICE, respectively. In the case of PEMFC, it can be inferred from this result that the impact on the GWP category is nil compared to the impact of the upstream stages of transporting the hydrogen from its production site to the bunkering port. Moreover, the utilization of PEMFC technology did not result in any emissions released to the atmosphere. In contrast, the utilisation of the ICE was found to contribute 5.7% of the total emissions due to the production of MFO, which was employed as a pilot fuel. Furthermore, it was determined that, for the ICE, less than 1% of the emissions were attributable to the direct release of MFO combustion emissions into the atmosphere, corresponding to 90% from CO₂ and from 9% CH₄. The results indicate that the production of materials utilised in the fabrication of both technologies does not exert an observable impact on the selected functional unit.

By the 2030, it was observed that the emission would decrease by 54% for both technologies, due to the increase in renewable sources (Wind and Photovoltaic) of electricity for that scenario. The impact of the WTT phases of e-hydrogen on PEMFC was observed to be 99.9%, while for ICE, it decreased to 87.9 and 87.5% for 2030 and 2050, respectively, compared to the BC. For PEMFC less than 1% correspond the impacts form materials used for the stack. Similarly, for ICE, the remaining 12.1% and 12.5% can be attributed to the production of MFO. The similarity of result for future scenarios is primarily due to the substantial similarity in the renewable component between them.

4.2.2 Impact Assessment of Other Categories – WTW Results

The other environmental impact categories results included in the study, for all scenarios, and both energy conversion technologies are shown in Figure 23. The comparison of energy conversion technologies across different scenarios shows a declining trend in GWP, acidification, eutrophication, and energy resource impacts, mainly due to the increase in renewable sources in electricity production. However, material resource use and land occupation show an increasing trend, particularly for PEMFC technology, due to the demand for nickel and copper in wind turbines and electrolysis stacks. Land use impacts stem from onshore wind turbines and wood chip electricity in the base case, while in 2030 and 2050, additional contributions come from photovoltaic installations in

open ground. This highlights a trade-off between emissions reduction and resource demand in the shift to renewable hydrogen production.

Notably, for the acidification category, the TTW component accounts for 37.1%, 39.6%, and 41.9% of BC, 2030, and 2050, respectively. This is primarily attributable to emissions resulting from MFO combustion during the RT. In the case of the Eutrophication category, the same component represents 61.6%, 71.1% and 72.5% for BC, 2030 and 2050, respectively, also due to emissions from MFO combustion during the RT. In the energy resources, the impact is 19.2%, 37%, and 37.1% for the BC, 2030, and 2050, respectively. This is attributable to the production of low-sulphur diesel, which is utilised in the analysis as MFO due to its similarity in physical and chemical characteristics. Finally, In the categories of material resources and land use, the WTT component largely dominates the impact, demonstrating the importance of analysing synthetic fuel from its production. The results are elucidated in detail in Appendix C, while the results for the GWP category were previously discussed.

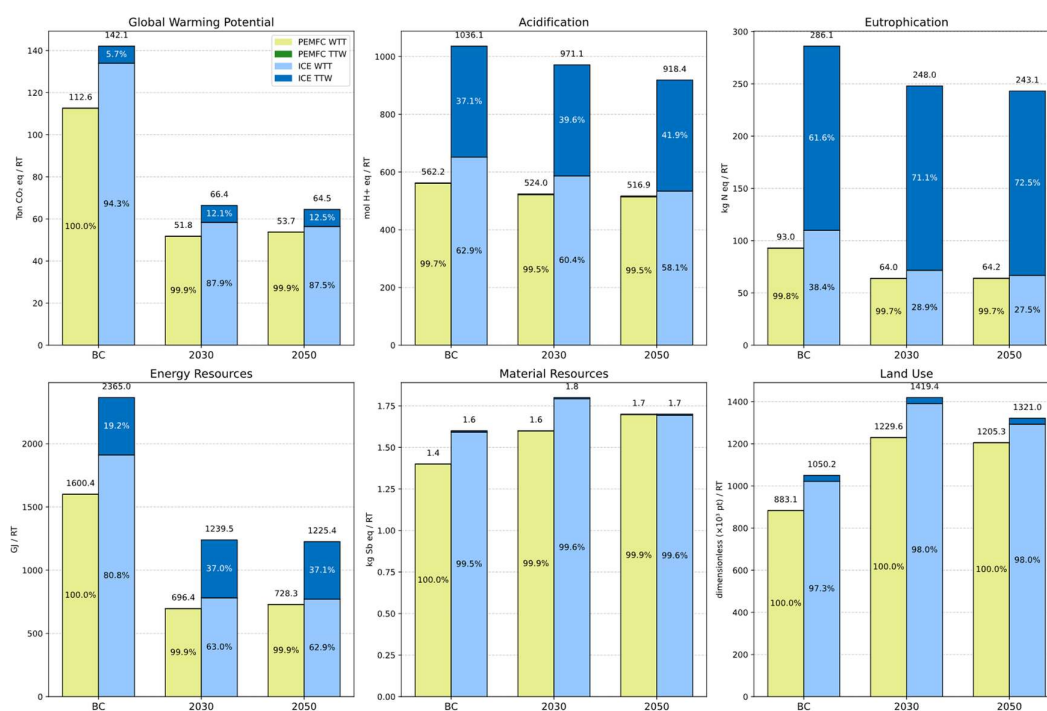


Figure 23 Environmental impacts of EF 3.1 categories using PEMFC and ICE per RT - All Scenarios.

5 Discussion

5.1 Comparative Review of WTT GWP Results with prior Studies.

This study assessed the GWP of three different synthetic fuels using one MJ of LHV as a functional unit. Some of the categories considered in this study have not been evaluated in previous studies. However, previous studies have not evaluated phases such as compression in the bunkering port and CH₃OH transport. Regarding the NH₃

and CO₃OH storage, in this instance, a comparison is not pertinent due divergent assumptions about storage time can vary between studies. This analysis offers some findings that are the result of comparison with other studies and, in the case of phases not previously explored, it may represent a starting point for future studies. Appendix D includes the results obtained for the three cases of the WTT scope for the BC and the results from prior studies, whose values were transformed to the functional unit used for the study to ensure correct comparability.

For the e-hydrogen pathway, Delpierre et al. [84] and Wulf et al. [59] reported a GWP of 0.006 and 0.009 Kg CO₂ eq /MJ_{LHV} for the H₂ production phase. Compared to the latter the results show no difference (0% variation). However, when compared to the first the emissions in this study are 34% higher. Although both references assumed exclusive wind source electricity, in the last case, PEM electrolysis technology was used, while in the first case alkaline technology was used as in the present study. Regarding the compression phase, Alghool et al. [61] reported a GWP result of 0.001 Kg CO₂ eq /MJ_{LHV}. The present study result is 67% higher than prior study. The reference value uses electricity from a 100% renewable source, while the electricity mix for the present study refers to a 9.4% renewable source (based on the BC). For the storage phase, the reference value is 0.00104 Kg CO₂ eq/MJ_{LHV} [59]. The present study is 3.85% lower than the prior study value. In this case, the same storage technology was compared. However, the reference study considered a 100% renewable source for electricity consumption. Finally, 0.0018 [40, 59] and 0.0025 kg CO₂ eq/MJ_{LHV} [30] were compared for the transport phase with the study value. The percentage difference to the results of the present study is 6% higher and 25% lower, respectively. Similarly to the previous phases, the references used renewable electricity as the electricity source.

For the e-ammonia pathway, Alghool et al. [61] and Arrigorri et al. [91] reported a GWP of 0.012 and 0.019 kg CO₂ eq /MJ_{LHV} for e-ammonia synthesis. The present study is 31% higher and 5% lower, respectively. The differences observed are due to the fact that the electricity used in the reference studies came from concentrated solar thermal power and wind power. For the transport phase by a sea tanker, a reference value of 0.00002 Kg CO₂ eq /MJ_{LHV} was reported by Alghool et al [61]., 23% higher than the value reported in prior studies. This difference can be presumed to be due to different transport assumptions between studies. Finally, 0.009 [61] and 0.01 Kg CO₂ eq /MJ_{LHV} [91] were compared for the cracking phase with the study value. The percentage difference with the present study results is 133% and 110%, higher respectively. Here, the references used renewable sources for electricity consumption, while the present study used the BC electricity generation.

For the e-methanol pathway, Alghool et al. [61] and Nizami et al. [98] reported a GWP of 0.014 and 0.016 kg CO₂ eq /MJ_{LHV} for e-methanol synthesis with similar DAC technology. The present study is 36% and 45% higher than prior study value, respectively. The differences observed are due to the fact that the electricity used in the references used renewable sources for electricity consumption. In contrast, the present study used the BC electricity generation. In this particular phase, the reference values do not consider the capture of CO₂ in the DAC process. Therefore, in order to make a comparison, the reference value was used with the inventory from the case study, but without considering the effect of capture. For the hydrogenation phase, Arrigorri et al. [91] reported a GWP value of 0.0065 kg CO₂ eq /MJ_{LHV}. The present study result is 46.1% higher than the prior study value. In this phase, the reference value does not consider the CO₂ release because it used green methanol. However, in this study, it was considered the CO₂ emitted to the atmosphere to close the loop of CO₂ capture in DAC. Therefore, to make a comparison, the reference value was used with the inventory from the case study but without considering the effect of capture.

5.2 GWP Reduction through Compressed H₂ in Energy Conversion Technologies

The present study investigates GWP emissions of a specific RT for a ship utilising a PEMFC or rather ICE with compressed hydrogen as the main fuel source. The findings indicate that the PEMFC has a GWP of 113 ton CO₂ eq /RT, while the ICE has a GWP of 142 ton CO₂ eq /RT. A comparison of the case study using an emission factor for HFO for maritime application on WTW, as defined in the 2024 LCA Guideline [99], reveals that PEMFC and ICE results represent a reduction in emissions of 73% and 66%, respectively, compared to the emissions produced by an ICE utilising MFO as the primary fuel for the round trip as indicate in Figure 24. It is important to note that for the 2030 scenario, the 99% of the PEMFC and the 88% of the ICE GWP results correspond to the cumulative environmental impact from the H₂ production and the phases required to deliver it to the bunkering port, which the selected functional unit allows considering the entire supply chain scope. Regarding the TTW part, as mentioned by Kanchiralla et al. [8], PEMFC has electrochemical combustion and high efficiencies compared with ICE. In the present case study, 55% for PEMFC and 48% for ICE. This means a key advantage for PEMFC with cleaner combustion than ICE, for which the combustion of MFO as pilot fuel still generates a carbon footprint. Despite the high impact of the WTT of hydrogen as a main fuel, compared to the GWP emissions for the MFO ICE, both technologies still significantly reduce the environmental footprint in maritime sector.

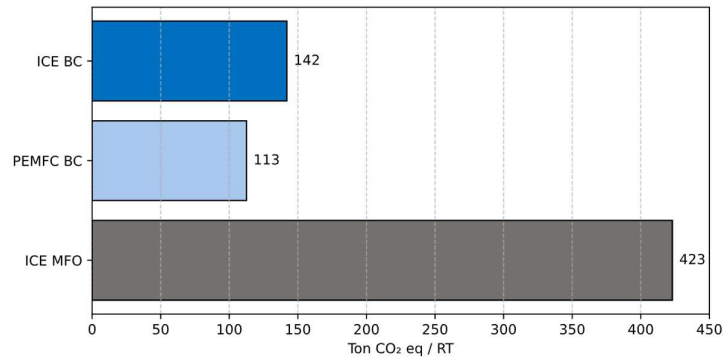


Figure 24 GWP Comparison results of WTW analysis with MFO

5.3 Effect of GWP in WTT Phases Following H₂ Production

The findings of the study indicate that H₂ production using electricity sourced from renewable sources may not be sufficient to reduce the environmental impact of hydrogen energy carriers for maritime applications. When synthetic fuel is required in a different location or involves a complex supply chain, the processes associated with delivering these fuels to the final consumer, in this case, the bunkering port, can result in additional GWP emissions. Figure 25 illustrates the contributions of the GWP emissions of hydrogen production and downstream processes in a WTT range for marine applications.

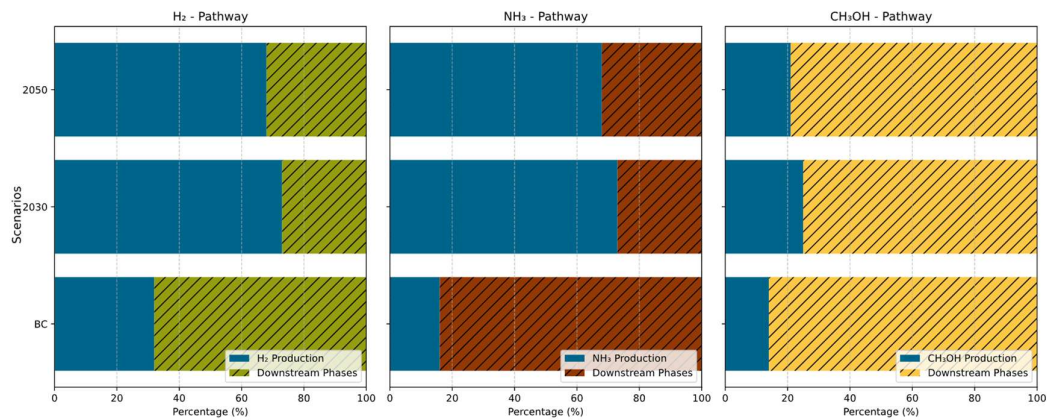


Figure 25 Impact of GWP in WTT supply chain phases for H₂ production

In e-hydrogen pathway, H₂ production contributes 32% and 68% in the downstream phases in the BC scenario. In the future scenarios 2030 and 2050, H₂ production increases to 73% and 68% respectively and decreases to 27% and 32% in the downstream phases. For the e-ammonia pathway, the H₂ production contribution is 16% and 84% for the downstream phases for the BC scenario. In the future scenarios 2030 and 2050, the H₂ production increases to 48% and 46% respectively and decreases to 52% and 54% for the downstream phases. Finally, in the e-methanol pathway, the H₂ production contribution represents the 13%, while the downstream phases represent the

87%. In the future scenarios 2030 and 2050, H₂ production increases to 23% and 20% respectively and decreases to 77% and 80% for the downstream phases.

A considerable number of studies have been conducted that analyse in detail the impacts of H₂ production, focusing on specific electrolysis technologies, as illustrated by [84]. Conversely, other studies have examined various scenarios for electricity generation, as demonstrated by [64]. This study set a wind-based source for the electricity consumption for the H₂ production with the concentrate the analysis in the downstream phases on the WTT scope. According to the case study results, for the e-hydrogen pathway, the phases with the highest effect on emissions are those required for reconditioning, specifically, the final compression to reach the pressure requirement in the ship. Only 6.7% of the GWP effect for the BC is due to pipeline transport. On the other hand, for the e-ammonia and e-methanol pathways, the conversion and reconversion processes, being energy-intensive processes, contribute more to the emissions than the transport process itself, whose contribution were less than 1% for the BC. These aspects will be analysed in detail in the following section.

Furthermore, the findings indicate that electricity consumption is the primary contributor to GWP emissions because it accounts for most processes. Also, it eclipses the environmental impact of materials utilised in process/technology manufacturing. This is presumably because the impacts can be allocated over the lifespan of the materials, which can span several decades or operational time. For instance, the electrolyser stack employed in the analysis was estimated to have a lifespan of 120,000 hours.

As considered for the case study, for e-ammonia and e-methanol pathways, reconversion to hydrogen in the bunkering port was defined for comparative purposes in the result; however, market conditions and requirements of conversion technologies under development in maritime applications allow to omit this phase on the WTT and use the fuels directly in ships. The approach employed in this study allows to demonstrate of the impact of the phases accompanying H₂ production. This is particularly relevant given the expectation that hydrogen will become an internationally traded commodity [64] . Furthermore, the results demonstrate that the downstream phases have a predominant contribution, which can be reduced by using more renewable energy sources in the electricity generation scenarios, as was observed in 2030 and 2050 GWP results.

5.4 Effect of GWP in Storage and transport phases following H₂ Production in the WTT Scope.

According to the results obtained for the case study, the storage and transport phases were found to have a small impact on the GWP of the complete pathway. As shown in Figure C1, Figure C2 and Figure C3, the contribution is less than 7% for the e-hydrogen

pathway in both phases, 3.5% for the e-ammonia pathway and 1% for the e-methanol pathway in all scenarios. For the transport phase, the contributions to the GWP category are relatively low for the whole pathway. Although ammonia and methanol use fossil fuels for transport, specifically, MFO for ammonia and low sulphur diesel for methanol, the CO₂ equivalent emissions are lower than for the other road stages. On the other hand, compressed hydrogen transport, which relies on electricity, has a higher contribution and its impact is expected to decrease in scenarios with a higher share of renewable energy sources.

Kleijne et al. [64] state that the inclusion of transport and storage capacity is critical to understanding the electricity-dependent trade-off between transport options and production sites. In their study, the distances ranged from 500 to 5,000 km for compressed hydrogen transport by pipeline and 1,000 to 20,000 km for ammonia transport by tanker. In this study, the contribution of the GWP category for hydrogen transport is 1% for a distance of 500 km and 47% for a distance of 5,000 km. For ammonia, the contribution of the transport phase is 1% for 1,000 km and 22% for the 20,000 km case in supply chains that include the same phases as in the case study. In contrast to the present study, the assumed transport distances are relatively short (403 km for pipelines and 457 km for truck tankers) compared to large logistic distances, e.g. between continents. However, the results are comparable to the distances in the lower range of the reference study. Similarly, this study assumed that the amount of fuel needed for the RoRo ship operation per year would be stored, which is a relatively small amount when compared to large scale storage of hydrogen carriers. Therefore, the impact on the GWP category for storage is small compared to other phases.

5.5 Green Hydrogen vs. H₂ Production from Electricity Generation scenarios

As defined in the case study, the analysis was conducted using wind-based electricity exclusively for H₂ production for all cases and scenarios within the WTT scope. In contrast, other phases of the supply chain were modelled with the electricity generation scenarios specified per scenario. This approach was based on the premise of ensuring green H₂ production. However, it is important to analyse the impact of using the same electricity generation scenarios for all synthetic fuel pathways, including H₂ production.

Figure 26 illustrates the results for the GWP category for the synthetic fuel pathways with H₂ production using electricity generation scenarios. It is notable that H₂ production phase constitutes the predominant contribution of the e-hydrogen and e-ammonia pathways, accounting for over 70% in the BC and 80% in the 2030 and 2050. Moreover, a comparison of the GWP results for the synthetic fuels pathways with the results displayed in Figure 17 reveals a notable increase, ranging from three to seven times that observed for all synthetic fuels pathways in all scenarios.

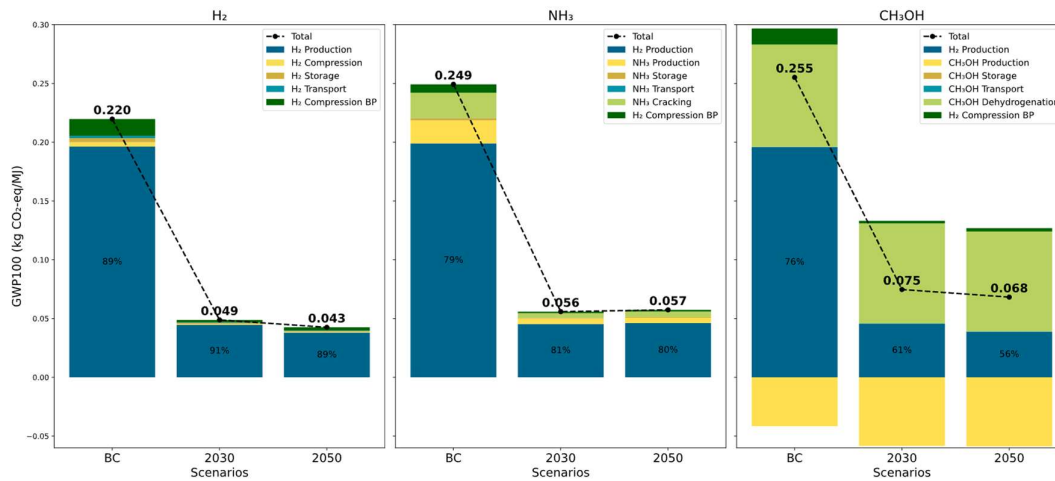


Figure 26 GWP of WTT pathways considering electricity generation scenarios for H₂ production.

Focusing on the GWP for H₂ production, using the same assumptions of electricity generation scenarios for the whole pathways, reveals a GWP of 0.19 kg CO₂ eq/MJ_{LHV}, 0.045 kg CO₂ eq/MJ_{LHV} and 0.038 kg CO₂ eq/MJ_{LHV} for the base case, 2030 and 2050, respectively. A comparison can be made with the European Union taxonomy threshold of 3 kg CO₂ eq/ kg H₂ [85], or 0.025 kg CO₂ eq/MJ_{LHV} using the functional unit of the study. This value represents the upper limit for sustainable investment in H₂ production and can serve as a reference level for assessing the GWP impact category. The outcomes for all scenarios exceed the stipulated threshold, despite the optimistic projections for electricity generation in 2030 and 2050. This reinforces the significant challenge of aligning H₂ production with renewable electricity generation. This finding is consistent with the target vision set forth in the German National Hydrogen Strategy, which aims to produce between 5 and 10 GW of green hydrogen by 2030 [100].

5.6 CO₂-Equivalent Contributors for the WTW Scope Using PEMFC and ICE

In addition to the results obtained in the environmental impact categories, it is considered essential to analyse the contribution of CO₂ equivalent emissions in the result obtained for the GWP category for the WTW scope. As illustrated in Figure 27 and Figure 28, the relative decomposition of the emissions for the functional unit of the WTW scope is demonstrated in BC and 2030 for the energy conversion technologies PEMFC and ICE, respectively.

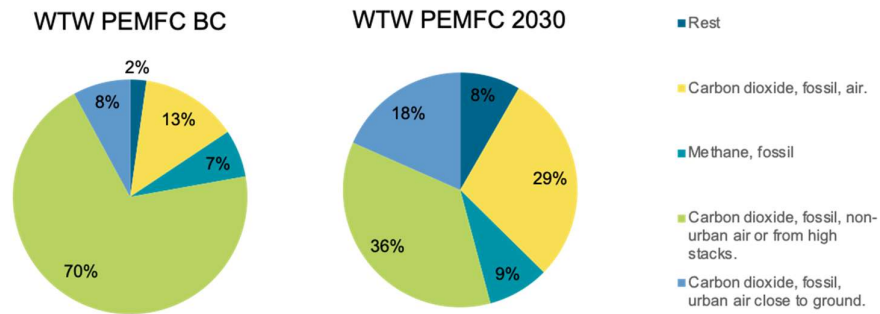


Figure 27 Elementary flow contribution of WTW PEMFC

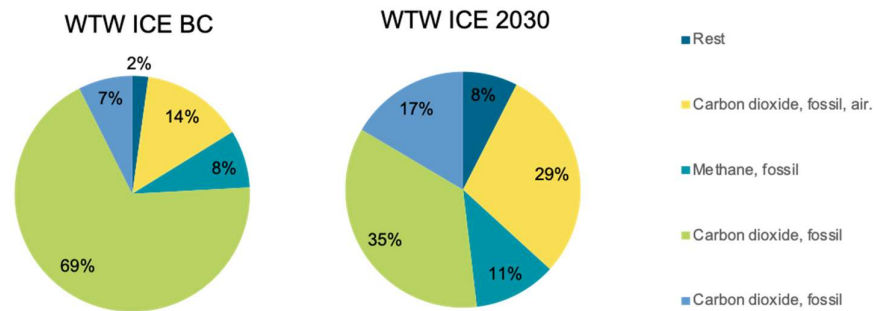


Figure 28 Elementary flow contribution of WTW ICE

The contribution of CH₄ to the CO₂ equivalent emissions is estimated to be 7% and 9% for WTW using PEMFC for BC and 2030, respectively and 8% and 11% when using ICE for the same scenarios. Despite this absolute contribution being comparatively low when considered against the total CO₂ emissions, its impact could be amplified due to its very high WGP. It is estimated that the contribution from CH₄ to the GWP emissions could be as high as 84 times the GWP caused by CO₂ emissions within a horizon of less than 20 years [101]. This is a point that should be studied further in the future, since, according to the results, when introducing future electricity generation scenarios with a higher share of renewable sources for offshore applications, the methane emissions share tends to increase, although the equivalent GWP emissions decrease as demonstrated in this study.

6 Limitation of the study

The limitations encountered in the study are described below.

- There is a lack of available data on inventories for the bunkering phase and propulsion powertrain for energy conversion technologies. In the case of the former, despite the significance of the bunkering phase within the supply chain of synthetic fuels for the maritime sector, the infrastructure has not been the subject of life cycle assessments, as evidenced by the literature review for this study. It is presumable

that this phase exerts a minimal impact on the WTT pathways, given that it does not require significant energy consumption and potential impacts may arise from the materials used for compressed storage and compressor in the case of compressed hydrogen, pumps and hoses, such as steel and concrete production to name the most relevant. In the latter case, in addition to the storage on-board and energy conversion technologies, the powertrain configuration includes elements such as control units, electric motor and SCR units in the case of the ICE. As with the former, it can be assumed that these elements exert a minimal impact on the WTW scope.

- The case study focused on the production of synthetic fuels in Wilhelmshaven, Germany and their subsequent transportation and reconditioning processes in the Netherlands, specifically in Rotterdam, The Netherlands, where is considered the bunkering port. In the prospective assessment, the IAMs scenarios were not taken into consideration due to the necessity of projected scenarios per country. This aimed to approximate the prospective study to possible scenarios for each country concerning its electricity generation context. Regarding the BC, data was drawn from the electricity generation scenarios of Ecoinvent 3.9.1, which utilises data from 2019. Despite its lack of currency, it was utilised as a reference point for the comparative study to prioritising data consistency by sourcing data from a single, designated standardized database – Ecoinvent 3.9.1 – for the two countries under consideration and to ensure reliable data and methodological consistency across all scenarios.
- Finally, as the scope of the study included the analysis of different synthetic fuels and their processes in the WTT scope and two energy conversion technologies for the WTW scope, data inventories were obtained from research publications to collect the information for the LCI. The approach used in this study is grounded in collecting the data inventories from scientific publications but ensuring its scientific origin, traceability, and scalability relative to the functional units used in the study. Future work could benefit from integrating real operational data to validate and refine modelled assumptions to improve the accuracy of prospective life cycle assessment.

7 Conclusions

This study evaluates the environmental performance of e-hydrogen, e-ammonia, and e-methanol pathways under different electricity generation scenarios. It examines their entire lifecycle, from production to bunkering and onboard energy conversion, particularly in applications using e-hydrogen. Special emphasis is placed on GWP hotspots and other environmental impacts, including how these evolve with higher shares of wind and solar sources in future scenarios.

In response to the first research question on key GWP hotspots in synthetic fuel pathways, the results of this study identified the most critical contributors within the WTT scope. Among the three pathways analysed for BC, e-hydrogen has the lowest GWP impact, with compression at the bunkering port as the main hotspot (45%), followed by H₂ production (32%), which is powered by wind electricity. Despite being a non-fossil energy source, wind power still contributes to GWP due to the manufacture of materials such as iron, fiberglass, and concrete required for wind turbine production. In the e-ammonia pathway, the main hotspots are NH₃ synthesis (22%) and cracking (21%), both driven by high electricity consumption (86% and 98% within each phase, respectively). For the e-methanol pathway, CH₃OH dehydrogenation is the most significant contributor (93% of its impact comes from CO₂ emissions as considered to close the CO₂ capture loop in DAC), followed by natural gas-based heat production use in the process (7%). In terms of GWP, for the WTW scope, the analysis of the two energy conversion technologies reveals that the ICE result is 26% higher than PEMFC. Since hydrogen is the primary fuel, the hotspots from the WTT phase remain consistent, contributing 100% of PEMFC and 94.3% of ICE total GWP. Additionally, ICE combustion as a pilot fuel adds 5.7% to its total impact.

Regarding the second research question, for acidification and marine eutrophication categories for the BC, the e-ammonia pathway presents the highest impact across all pathways. The e-ammonia pathway has an acidification impact 4 times higher and a eutrophication impact three times higher than e-hydrogen, primarily due to NH₃ and NO_x emissions from NH₃ synthesis. Similarly, e-methanol exhibits 1.4 times higher acidification and 1.6 times higher eutrophication, mainly driven by NO_x emissions from biomethane- and natural gas-based heat generation used in CH₃OH synthesis and dehydrogenation. In the energy resources category, e-ammonia and e-methanol have more than twice the impact of e-hydrogen, primarily due to the high electricity demand of NH₃ and CH₃OH synthesis, NH₃ cracking, and CH₃OH dehydrogenation, all of which rely on fossil-based electricity sources, including lignite, hard coal, and natural gas. Conversely, the e-methanol pathway presents a higher impact on material resources, which is 1.5 higher than the e-hydrogen pathway. Followed by the e-ammonia pathway, which is 1.14 higher than the e-hydrogen pathway. As was assumed for all synthetic pathways, the electricity consumption for H₂ production would be sourced from wind source, consequently, nickel and copper are the metals most affected by electricity from wind sources. The utilisation of nickel and zeolite as catalysts for NH₃ synthesis and amine-based silica production employed in the DAC and copper production used as a catalyst in the dehydrogenation phase, also have a notable impact, along with the use of lignite for German electricity mix and wind source used the electricity mix for both

countries. or land use, e-ammonia and e-methanol have 1.5 times higher impact than e-hydrogen, mainly due to forest land occupation and industrial land conversion for wind turbine installations. Additionally, biomethane co-generation, which uses wood chips in Germany's electricity mix, further contributes to land use impacts in these pathways. In the WTW scope, ICE exhibits higher environmental impacts than the PEMFC by 84% in acidification, 208% in eutrophication, and 48% in energy resource depletion for the BC. MFO as a pilot fuel contributes 37.1% and 61.6% of the total impact in the acidification and eutrophication categories, respectively, within the TTW component. In the energy resources category, TTW accounts for 19.2% of the total impact, primarily due to the production of low-sulphur diesel, used as MFO in this analysis. Conversely, differences in material resources (20% higher in ICE) and land use (16% higher in ICE) are minor, mainly linked to the WTT phase, as previously analysed.

Finally, to address the third research question regarding to the increasing share of wind and photovoltaic sources in future electricity scenarios, considering GWP in the WTT scope, the e-methanol pathway has the highest impact in BC, with reductions of 43% in 2030 and 42% in 2050. Meanwhile, the e-ammonia and e-hydrogen pathways show reductions of 67% and 65%, and 55% and 58%, respectively. A similar trend is observed for acidification, where the e-ammonia pathway, which has the highest impact in BC, decreases by 7% in both 2030 and 2050, while e-methanol and e-hydrogen decrease by 10% and 13%, and 10% and 12%, respectively. For eutrophication, e-ammonia sees a 27% reduction in both future scenarios, while e-methanol and e-hydrogen decrease by 39% and 42%, and 35% and 39%, respectively, by 2030 and 2050. The energy resources category follows the same pattern, with e-ammonia and e-methanol decreasing by 65% and 64%, and 49% and 50%, respectively, by 2030 and 2050, while e-hydrogen decreases by 60% in both scenarios. However, material resource impacts increase over time, with e-methanol rising by 27% and 23%, e-ammonia by 35% and 42%, and e-hydrogen by 16% and 11% in 2030 and 2050. Similarly, land use impacts increase across all pathways due to the expansion of wind energy infrastructure, with e-methanol and e-ammonia rising by up to 69% and 77%, and e-hydrogen increasing by 34% and 24% in 2030 and 2050, respectively. These findings highlight that while higher shares of wind and solar power significantly reduce GWP, acidification, eutrophication, and energy resource categories. However, future scenarios introduce trade-offs, as it increases material resource consumption and land use impacts due to the growing demand for renewable energy infrastructure. In the WTW scope, in terms of GWP, both PEMFC and ICE experience substantial declines compared to BC. PEMFC shows a 53% and 53% decline by 2030 and 2050 compared to BC for the GWP category. Similarly, ICE shows a 53% and 55% decline by 2030 and 2050 compared to BC. Similar reductions are observed for acidification, eutrophication, and energy resource

categories, with a further decline for the latter due to the use of MFOs as pilot fuel. However, decreasing impacts are evident in some categories, the transition also increases impacts on material resources and land use categories, as the demand for critical materials and infrastructure for renewable energy technologies grows. The trends observed on WTW scope are consistent e-hydrogen pathway, considering the high impact of this in the WTW analysis.

In summary, this study highlights the essential role of integrating renewable energy sources in improving the environmental performance of synthetic fuel pathways in the maritime sector. E-hydrogen emerges as the most favourable option among the analysed pathways due to its reduced impacts across multiple categories, particularly in future scenarios with a highly environmentally friendly electricity grid. The comparative analysis of PEMFC and ICE technologies highlights the importance of considering the preceding synthetic fuel stages when assessing the environmental performance of the technology operation. While PEMFC is shown to have a comparatively lower impact, the use of fossil-based pilot fuels in ICEs has been identified as a significant source of additional impact. However, this can be mitigated to a certain extent by adopting synthetic fuels.

8 Future Work

This study recommends conduct future work on the following aspects:

Firstly, this study focuses exclusively on the environmental aspects the synthetic fuel supply chains and hydrogen energy conversion technologies. Therefore, a more comprehensive holistic assessment such as a Life Cycle Sustainability Assessment (LCSA), which incorporates safety, economic and social aspects, is suggested to provide thorough recommendations applicable to the maritime sector.

Secondly, it was identified that material production represents an important contributor to GWP emissions. Consequently, it is recommended to include prospective scenarios for material production, such as steel, nickel, and copper production.

With regard to heat production, biomethane was used for processes located in Germany, and natural gas was used for processes located in the Netherlands across all scenarios. Thus, it is recommended for future studies the use of inventories of sustainable heat production technologies such as waste heat recovery systems.

Additionally, given the early stages of development of energy conversion technologies for powertrain ship propulsion, specifically for e-ammonia, it is recommended that future studies include a WTW pLCA using prototype data inventories and the projected efficiencies of the technology.

Furthermore, considering the significant short-term impact of CH₄ emissions, it is advisable to conduct a more detailed LCA with precise data and loss assessments at all stages of synthetic fuel pathways. This approach will help in understanding the complete effect and its relation to overall CO₂ equivalent emissions in the maritime sector.

Moreover, while the present study concentrated on categories with a more significant impact on synthetic fuel supply chains, literature on fuel chains involving ammonia and methanol, particularly concerning human toxicity, may offer relevant findings. Therefore, it is recommended that future work be completed with the analysis of this category.

In addition, future studies may conduct a sensitivity or scenario analysis to evaluate the impact of varying transport distances and storage capacities on the GWP of synthetic fuel supply chains, including a wide range of distances that reflect both regional and intercontinental logistics. Furthermore, the analysis may account for varying losses quantities, storage scales and technologies, considering future scenarios and energy conversion technologies efficiencies evolution for maritime application. A special focus can be placed on synthetic fuel supply chain losses. Kleijne et al. [64] state that minimizing hydrogen losses can greatly reduce life-cycle emission, which depends on transport modes, distance and storage time.

Finally, the scope of the study does not include an uncertainty analysis of the results obtained. Due to the uncertainty of some parameters of the technologies used in the study, it is recommended that this has to be included to identify key data collection that needs improvement and also to obtain valid results for the use in decision-making.

9 References

- [1] Reducing emissions from the shipping sector. [Online]. Available: https://climate.ec.europa.eu/eu-action/transport/reducing-emissions-shipping-sector_en (accessed: Jul. 27 2024).
- [2] International Maritime Organization, Fourth IMO Greenhouse Gas Study.
- [3] European Parliament and the Council of the European Union, "Regulation EU 2023 of the European Parliament and of the Council of on the use of renewable and low-carbon fuels in maritime transport and amending Directive 2009/16/EC," 2023. [Online]. Available: <https://www.consilium.europa.eu/en/press/press-releases/2023/07/25/fueleu-maritime-initiative-council-adopts-new-law-to-decarbonise-the-maritime-sector/>
- [4] International Maritime Organization, ANNEX 15 RESOLUTION MEPC.377(80) (adopted on 7 July 2023): 2023 IMO STRATEGY ON REDUCTION OF GHG EMISSIONS FROM SHIPS.
- [5] V. Papantoni, Short Literature Review on Life Cycle Inventory Data for PxX technologies.
- [6] J. Gomez and K. Chougule, Project MaTroSe – Milestone 3: Criteria, goals and scope of the study for the economic, ecological and multi-criteria analysisProject MaTroSe – Milestone 3: Criteria, goals and scope of the study for the economic, ecological and multi-criteria analysis.
- [7] International Energy Agency, Northwest European Hydrogen Monitor 2024. [Online]. Available: Northwest European Hydrogen Monitor 2024," 2024. [Online]. Available: <https://iea.blob.core.windows.net/assets/b8ba8ad3-f135-4002-9e21-b8cbd213fb36/NorthwestEuropeanHydrogenMonitor2024.pdf>
- [8] F. M. Kanchiralla, S. Brynolf, T. Olsson, J. Ellis, J. Hansson, and M. Grahn, "How do variations in ship operation impact the techno-economic feasibility and environmental performance of fossil-free fuels? A life cycle study," *Applied Energy*, vol. 350, p. 121773, 2023, doi: 10.1016/j.apenergy.2023.121773.
- [9] M. S. Akhtar, R. Dickson, and J. J. Liu, "Life Cycle Assessment of Inland Green Hydrogen Supply Chain Networks with Current Challenges and Future Prospects," *ACS Sustainable Chem. Eng.*, vol. 9, no. 50, pp. 17152–17163, 2021, doi: 10.1021/acssuschemeng.1c06769.
- [10] N. Thonemann, A. Schulte, and D. Maga, "How to Conduct Prospective Life Cycle Assessment for Emerging Technologies? A Systematic Review and Methodological Guidance," *Sustainability*, vol. 12, no. 3, p. 1192, 2020, doi: 10.3390/su12031192.
- [11] International Renewable Energy Agency (IRENA), "A pathway to decarbonise the shipping sector by 2050," Abu Dhabi, 2021.
- [12] J. Benajes, A. García, J. Monsalve-Serrano, and M. Guzmán-Mendoza, "A review on low carbon fuels for road vehicles: The good, the bad and the energy potential for the transport sector," *Fuel*, vol. 361, p. 130647, 2024, doi: 10.1016/j.fuel.2023.130647.
- [13] S. Shiva Kumar and H. Lim, "An overview of water electrolysis technologies for green hydrogen production," *Energy Reports*, vol. 8, pp. 13793–13813, 2022, doi: 10.1016/j.egy.2022.10.127.
- [14] A. Lahrichi, Y. El Issmaeli, S. S. Kalanur, and B. G. Pollet, "Advancements, strategies, and prospects of solid oxide electrolysis cells (SOECs): Towards enhanced performance and large-scale sustainable hydrogen production," *Journal*

- of Energy Chemistry, vol. 94, pp. 688–715, 2024, doi: 10.1016/j.jechem.2024.03.020.
- [15] K. Machaj et al., "Ammonia as a potential marine fuel: A review," *Energy Strategy Reviews*, vol. 44, p. 100926, 2022, doi: 10.1016/j.esr.2022.100926.
- [16] Patricia Mayer et al., "Blue and green ammonia production: A techno-economic and life cycle assessment perspective," *iScience*, vol. 26, no. 8, p. 107389, 2023, doi: 10.1016/j.isci.2023.107389.
- [17] Veatriki Papantoni, "Short literature review on Life Cycle Inventory data for PtX technologies," DLR, 2023.
- [18] Y. Qiu et al., "Environmental trade-offs of direct air capture technologies in climate change mitigation toward 2100," *Nature communications*, vol. 13, no. 1, p. 3635, 2022, doi: 10.1038/s41467-022-31146-1.
- [19] International Energy Agency, "Direct Air Capture_ A key technology for net zero - DirectAirCapture_Akeytechnologyfornetzero," [Online]. Available: https://iea.blob.core.windows.net/assets/78633715-15c0-44e1-81df-41123c556d57/DirectAirCapture_Akeytechnologyfornetzero.pdf
- [20] N. J. Azhari et al., "Methanol synthesis from CO₂: A mechanistic overview," *Results in Engineering*, vol. 16, p. 100711, 2022, doi: 10.1016/j.rineng.2022.100711.
- [21] O. Oloruntobi et al., "Assessing methanol potential as a cleaner marine fuel: An analysis of its implications on emissions and regulation compliance," *Cleaner Engineering and Technology*, vol. 14, p. 100639, 2023, doi: 10.1016/j.clet.2023.100639.
- [22] Methanol Institute, "Marine_Methanol_Report_Methanol_Institute," 2023.
- [23] X. Hong et al., "Techno-enviro-economic analyses of hydrogen supply chains with an ASEAN case study," *International Journal of Hydrogen Energy*, vol. 46, no. 65, pp. 32914–32928, 2021, doi: 10.1016/j.ijhydene.2021.07.138.
- [24] A. Sánchez, M. A. Martín Rengel, and M. Martín, "A zero CO₂ emissions large ship fuelled by an ammonia-hydrogen blend: Reaching the decarbonisation goals," *Energy Conversion and Management*, vol. 293, p. 117497, 2023, doi: 10.1016/j.enconman.2023.117497.
- [25] T. Zhang, J. Uratani, Y. Huang, L. Xu, S. Griffiths, and Y. Ding, "Hydrogen liquefaction and storage: Recent progress and perspectives," *Renewable and Sustainable Energy Reviews*, vol. 176, p. 113204, 2023, doi: 10.1016/j.rser.2023.113204.
- [26] A. Boretti, "Technology readiness level of hydrogen storage technologies for transport," *Energy Storage*, 2023, doi: 10.1002/est2.546.
- [27] M. R. Usman, "Hydrogen storage methods: Review and current status," *Renewable and Sustainable Energy Reviews*, vol. 167, p. 112743, 2022, doi: 10.1016/j.rser.2022.112743.
- [28] Q. Cheng, R. Zhang, Z. Shi, and J. Lin, "Review of common hydrogen storage tanks and current manufacturing methods for aluminium alloy tank liners," *International Journal of Lightweight Materials and Manufacture*, vol. 7, no. 2, pp. 269–284, 2024, doi: 10.1016/j.ijlmm.2023.08.002.
- [29] TUV SUD, Hydrogen, Storage, Transportation and Distribution. [Online]. Available: <https://www.tuvsud.com/en/themes/hydrogen/explore-the-hydrogen-value-chain/hydrogen-storage-and-distribution>
- [30] C. Tsiklios, M. Hermesmann, and T. E. Müller, "Hydrogen transport in large-scale transmission pipeline networks: Thermodynamic and environmental assessment of

- repurposed and new pipeline configurations," *Applied Energy*, vol. 327, p. 120097, 2022, doi: 10.1016/j.apenergy.2022.120097.
- [31] H2TECH, GEV's Pilot C-H2 ship to be operable by mid-2020s. Accessed: Jul. 9 2024. [Online]. Available: <https://www.h2-tech.com/news/2021/01-2021/gev-s-pilot-c-h2-ship-to-be-operable-by-mid-2020s/>
- [32] H2TECH, GEV's Pilot C-H2 ship to be operable by mid-2020s. Accessed: Jul. 9 2024. [Online]. Available: <https://www.h2-tech.com/news/2021/01-2021/gev-s-pilot-c-h2-ship-to-be-operable-by-mid-2020s/>
- [33] Calvera Hydrogen, CALVERA HYDROGEN develops the largest ever hydrogen transport tube trailer model for Shell Hydrogen. [Online]. Available: <https://www.calvera.es/calvera-hydrogen-develops-the-largest-ever-hydrogen-transport-tube-trailer-model-for-shell-hydrogen/> (accessed: Jul. 9 2024).
- [34] Calvera Hydrogen, CALVERA HYDROGEN develops the largest ever hydrogen transport tube trailer model for Shell Hydrogen. [Online]. Available: <https://www.calvera.es/calvera-hydrogen-develops-the-largest-ever-hydrogen-transport-tube-trailer-model-for-shell-hydrogen/> (accessed: Jul. 9 2024).
- [35] Offshore-Green-H2-Production-and-Bunkering-Technology: Interreg North Sea Region, 2022.
- [36] A. Peschel, "Industrial Perspective on Hydrogen Purification, Compression, Storage, and Distribution," *Fuel Cells*, vol. 20, no. 4, pp. 385–393, 2020, doi: 10.1002/fuce.201900235.
- [37] Z. Du et al., A Review of Hydrogen Purification Technologies for Fuel Cell Vehicles.
- [38] International-PtX-Hub_202401, "Ammonia-transport-and-storage," 2024.
- [39] Institut for Sustainable Process Technology, "Clean-Ammonia-Roadmap-report_online-versie," Institut for Sustainable Process Technology, 2024. [Online]. Available: <https://ispt.eu/>
- [40] T. Galimova, M. Fasihi, D. Bogdanov, and C. Breyer, "Feasibility of green ammonia trading via pipelines and shipping: Cases of Europe, North Africa, and South America," *Journal of Cleaner Production*, vol. 427, p. 139212, 2023, doi: 10.1016/j.jclepro.2023.139212.
- [41] European Commission: Joint Research Centre, "Assessment of Hydrogen Delivery Options: Feasibility of Transport of Green Hydrogen within Europe," Publications Office of the European Union, Luxembourg, 2022. [Online]. Available: <https://data.europa.eu/doi/10.2760/869085>
- [42] K. Trangwachirachai, K. Rouwenhorst, L. Lefferts, and J. A. Faria Albanese, "Recent progress on ammonia cracking technologies for scalable hydrogen production," *Current Opinion in Green and Sustainable Chemistry*, vol. 49, p. 100945, 2024, doi: 10.1016/j.cogsc.2024.100945.
- [43] ABS, "AMMONIA BUNKERING Technical and operational advisory," 2024.
- [44] J. Ellis and K. Tanneberger, "Study on the use of ethyl and methyl alcohol as alternative fuels in shipping," Final Report Version 20151204.5, European Maritime Safety Agency, 2015.
- [45] E. Alberico and M. Nielsen, "Towards a methanol economy based on homogeneous catalysis: methanol to H2 and CO2 to methanol," *Chemical communications (Cambridge, England)*, vol. 51, no. 31, pp. 6714–6725, 2015, doi: 10.1039/c4cc09471a.
- [46] Methanol Institute, "Marine_Methanol_Report_Methanol_Institute," 2023.
- [47] F. M. Kanchiralla, "Life cycle navigation through future energy carriers and propulsion options for the energy transition in shipping," THESIS FOR THE

- DEGREE OF LICENTIATE OF ENGINEERING, Department of Mechanics and Maritime Sciences, CHALMERS UNIVERSITY OF TECHNOLOGY, CHALMERS UNIVERSITY OF TECHNOLOGY, 2023. [Online]. Available: https://research.chalmers.se/publication/534684/file/534684_Fulltext.pdf
- [48] Interreg Not h-West Europe H2SHIPS, Comparative report on alternative fuels for ship propulsion: System-Based Solutions for H2-Fuelled Water Transport in North-West Europe. [Online]. Available: https://vb.nweurope.eu/media/14694/210225_h2ships_t232_compassesmtaltfuels-02.pdf
- [49] H. Xing, C. Stuart, S. Spence, and H. Chen, "Fuel Cell Power Systems for Maritime Applications: Progress and Perspectives," *Sustainability*, vol. 13, no. 3, p. 1213, 2021, doi: 10.3390/su13031213.
- [50] O. Z. Sharaf and M. F. Orhan, "An overview of fuel cell technology: Fundamentals and applications," *Renewable and Sustainable Energy Reviews*, vol. 32, pp. 810–853, 2014, doi: 10.1016/j.rser.2014.01.012.
- [51] IEA Technology Collaboration Programme, "TECHNOLOGY READINESS LEVEL (TRL) - 2023: T091," [Online]. Available: <https://www.ieafuelcell.com/fileadmin/TRL/T091.pdf>
- [52] Ballard Power Systems, Fuel Cell Power Module for Marine Applications. [Online]. Available: https://www.ballard.com/wp-content/uploads/2024/11/FCwave_20241008.pdf
- [53] Ships monthly, "First hydrogen-powered ferry Hydra enters service," *Ships monthly*, 2024, 2024. <https://shipsmonthly.com/news/first-hydrogen-powered-ferry-hydra-enters-service/>
- [54] A. Fernández-Ríos et al., "Environmental sustainability of alternative marine propulsion technologies powered by hydrogen - a life cycle assessment approach," *The Science of the total environment*, vol. 820, p. 153189, 2022, doi: 10.1016/j.scitotenv.2022.153189.
- [55] F. M. Kanchiralla, S. Brynolf, E. Malmgren, J. Hansson, and M. Grahn, "Life-Cycle Assessment and Costing of Fuels and Propulsion Systems in Future Fossil-Free Shipping," *Environmental science & technology*, vol. 56, no. 17, pp. 12517–12531, 2022, doi: 10.1021/acs.est.2c03016.
- [56] MAN Energy Solutions, MAN to Investigate Engine Concepts for Maritime Hydrogen Applications: MAN Energy Solutions to partner with industry and academia in developing hydrogen concepts optimised for maritime applications. [Online]. Available: https://www.man-es.com/docs/default-source/press-releases-new/pr-hydropolen_en.pdf?sfvrsn=bf6ca196_2
- [57] MAN Energy Solutions, A new chapter – ammonia two-stroke engines. [Online]. Available: <https://www.man-es.com/marine/products/two-stroke-engines/ammonia-engine>
- [58] MAN Energy Solutions, Methanol-ready four-stroke engines. [Online]. Available: <https://www.man-es.com/marine/products/four-stroke-engines/methanol-ready-engines>
- [59] C. Wulf et al., "Life Cycle Assessment of hydrogen transport and distribution options," *Journal of Cleaner Production*, vol. 199, pp. 431–443, 2018, doi: 10.1016/j.jclepro.2018.07.180.
- [60] C. Wulf and P. Zapp, "Assessment of system variations for hydrogen transport by liquid organic hydrogen carriers," *International Journal of Hydrogen Energy*, vol. 43, no. 26, pp. 11884–11895, 2018, doi: 10.1016/j.ijhydene.2018.01.198.

- [61] D. Alghool, M. Haouari, and P. Trucco, "It is not the same green: A comparative LCA study of green hydrogen supply network pathways," *International Journal of Hydrogen Energy*, 2024, doi: 10.1016/j.ijhydene.2024.06.346.
- [62] M. Al-Breiki and Y. Bicer, "Comparative life cycle assessment of sustainable energy carriers including production, storage, overseas transport and utilization," *Journal of Cleaner Production*, vol. 279, p. 123481, 2021, doi: 10.1016/j.jclepro.2020.123481.
- [63] S. S. Hwang et al., "Life Cycle Assessment of Alternative Ship Fuels for Coastal Ferry Operating in Republic of Korea," *JMSE*, vol. 8, no. 9, p. 660, 2020, doi: 10.3390/jmse8090660.
- [64] K. de Kleijne et al., *Worldwide greenhouse gas emissions of green hydrogen production and transport*, 2024.
- [65] F. Liu, M. Shafique, and X. Luo, "Literature review on life cycle assessment of transportation alternative fuels," *Environmental Technology & Innovation*, vol. 32, p. 103343, 2023, doi: 10.1016/j.eti.2023.103343.
- [66] ISO 14040:2006. [Online]. Available: <https://www.iso.org/standard/37456.html> (accessed: Sep. 29 2024).
- [67] European Commission, *European Platform on LCA | EPLCA*. [Online]. Available: <https://eplca.jrc.ec.europa.eu/lifecycleassessment.html> (accessed: Sep. 29 2024).
- [68] S. Cucurachi, C. van der Giesen, and J. Guinée, "Ex-ante LCA of Emerging Technologies," *Procedia CIRP*, vol. 69, pp. 463–468, 2018, doi: 10.1016/j.procir.2017.11.005.
- [69] U. Brand et al., "Sustainability and Future Trajectories: How is Prospectivity Integrated into Life Cycle Sustainability Assessment?," *EDP Sciences*, vol. 349, 2022. [Online]. Available: https://www.e3s-conferences.org/articles/e3sconf/abs/2022/16/e3sconf_lcm2022_02006/e3sconf_lcm2022_02006.html
- [70] R. Frischknecht, "LIFE CYCLE INVENTORY ANALYSIS FOR DECISION-MAKING," *Doctoral Thesis*, Swiss Federal Institute of Technology Zurich, Zurich, Switzerland, 1998. [Online]. Available: https://treeze.ch/fileadmin/user_upload/downloads/Publications/Methodology/Life_Cycle_Inventories/frischknecht-1998-PHD.pdf
- [71] RIVM Committed to health and sustainability, *LCI: The ReCiPe model*. [Online]. Available: <https://www.rivm.nl/en/life-cycle-assessment-lca/recipe>
- [72] JRC Technical Report, *Updated characterisation and normalisation factors for the Environmental Footprint 3.1 method*. [Online]. Available: <https://doi.org/10.2760/798894> (accessed: 27.12.24).
- [73] European Commission, *Commission Recommendation (EU) 2021/2279: on the use of environmental footprint methods to measure and communicate the life cycle environmental performance of products organisations*. [Online]. Available: <https://eur-lex.europa.eu/legal-content/EN/TXT/PDF/?uri=CELEX:32021H2279>
- [74] Brightway, *LCA-ActivityBrowser/activity-browser*. [Online]. Available: <https://github.com/LCA-ActivityBrowser/activity-browser>
- [75] B. Steubing, D. de Koning, A. Haas, and C. L. Mutel, "The Activity Browser — An open source LCA software building on top of the brightway framework," *Software Impacts*, vol. 3, p. 100012, 2020, doi: 10.1016/j.simpa.2019.100012.
- [76] Ecoinvent Centre, *Ecoinvent Database version 3.9.1*. [Online]. Available: <https://ecoinvent.org/>
- [77] B. Steubing, D. de Koning, A. Haas, and C. L. Mutel, "The Activity Browser — An open source LCA software building on top of the brightway framework," *Software Impacts*, vol. 3, p. 100012, 2020, doi: 10.1016/j.simpa.2019.100012.

- [78] Bureau Veritas, What Well-to-Weak decarbonization means for ship owners. [Online]. Available: <https://marine-offshore.bureauveritas.com/insight/business-insights/what-well-wake-decarbonization-means-shipowners>
- [79] International Renewable Energy Agency (IRENA), "A pathway to decarbonise the shipping sector by 2050," Abu Dhabi, 2021.
- [80] Gasunie, Von Wilhelmshaven zu den Industriezentren in Niedersachsen und NRW: Unternehmensallianz verbindet Projekte für Wasserstoffimport, -produktion, -transport und -verbrauch. [Online]. Available: <https://www.gasunie.de/news/von-wilhelmshaven-zu-den-industriezentren-in-nrw-und-niedersachsen-unternehmensallianz-verbindet-projekte-fuer-wasserstoffimport--produktion--transport-und--verbrauch>
- [81] Port of Rotterdam., Port of Rotterdam, Explanatory notes to the bunker license for bunker fuel transporter:Port of Rotterdam. [Online]. Available: <https://www.portofrotterdam.com/sites/default/files/2022-06/bunker-license-fuel-transporter.pdf>
- [82] P. Schmidt, E-Fuels: Techno-economic assesment of European domestic production and import towards 2050 - Update. [Online]. Available: <https://www.concawe.eu/download/?id=32133>
- [83] Hendrik Kondziella aKarl Specht a, "The techno-economic potential of large-scale hydrogen storage in Germany for a climate-neutral energy system,"
- [84] M. Delpierre, J. Quist, J. Mertens, A. Prieur-Vernat, and S. Cucurachi, "Assessing the environmental impacts of wind-based hydrogen production in the Netherlands using ex-ante LCA and scenarios analysis," *Journal of Cleaner Production*, vol. 299, p. 126866, 2021, doi: 10.1016/j.jclepro.2021.126866.
- [85] European Commission: Joint Research Centre, "Assessment of Hydrogen Delivery Options: Feasibility of Transport of Green Hydrogen within Europe," Publications Office of the European Union, Luxemburgo, 2022. [Online]. Available: <https://data.europa.eu/doi/10.2760/869085>
- [86] H2 Energy AG, DFDS A/S, Retrofit of an Existing RoRo Ferry with a Hydrogen-Electric Propulsion System: Feasibility Study.
- [87] DFDS, Rotterdam - Immingham freight shipping. [Online]. Available: <https://www.dfds.com/en-gb/freight-shipping/routes-and-schedules/rotterdam-immingham>
- [88] European Commission, KNOWLEDGE FOR POLICY: Supporting policy with scientific evidence. [Online]. Available: https://knowledge4policy.ec.europa.eu/glossary-item/cut-criteria_en
- [89] C. van der Giesen, R. Kleijn, and G. J. Kramer, "Energy and climate impacts of producing synthetic hydrocarbon fuels from CO(2)," *Environmental science & technology*, vol. 48, no. 12, pp. 7111–7121, 2014, doi: 10.1021/es500191g.
- [90] "Planetary Boundaries Analysis of Low-Carbon Ammonia Production Routes," vol. 9, 9740/9749, 2021.
- [91] ARRIGONI Alessandro et al., "Environmental life cycle assessment (LCA) comparison of hydrogen delivery options within Europe," 2024. [Online]. Available: doi.org/10.2760/5459
- [92] L. Usai, C. R. Hung, F. Vásquez, M. Windsheimer, O. S. Burheim, and A. H. Strømman, "Life cycle assessment of fuel cell systems for light duty vehicles, current state-of-the-art and future impacts," *Journal of Cleaner Production*, vol. 280, p. 125086, 2021, doi: 10.1016/j.jclepro.2020.125086.
- [93] R. Stropnik, A. Lotrič, A. Bernad Montenegro, M. Sekavčnik, and M. Mori, "Critical materials in PEMFC systems and a LCA analysis for the potential reduction of

- environmental impacts with EoL strategies," *Energy Science & Engineering*, vol. 7, no. 6, pp. 2519–2539, 2019, doi: 10.1002/ese3.441.
- [94] International Energy Agency, The Role of E-fuels in Decarbonising Transport.
- [95] M. G. Prina, G. Barchi, S. Osti, and D. Moser, "Optimal future energy mix assessment considering the risk of supply for seven European countries in 2030 and 2050," *e-Prime - Advances in Electrical Engineering, Electronics and Energy*, vol. 5, p. 100179, 2023, doi: 10.1016/j.prime.2023.100179.
- [96] Ecoinvent, ecoinvent v3.11. [Online]. Available: <https://ecoinvent.org/ecoinvent-v3-11/>
- [97] European Commission, European Platform on LCA | EPLCA: Environmental Footprint. [Online]. Available: <https://eplca.jrc.ec.europa.eu/EnvironmentalFootprint.html> (accessed: 27.12.4).
- [98] Muhammad Nizami, Slamet, and Widodo Wahyu Purwanto, "Solar PV based power-to-methanol via direct CO₂ hydrogenation and H₂O electrolysis: Techno-economic and environmental assessment," *Journal of CO₂ Utilization*, vol. 65, p. 102253, 2022, doi: 10.1016/j.jcou.2022.102253.
- [99] International Maritime Organization, 2024 Guidelines on Life Cycle GHG Intensity of Marine Fuels: Annex 10. Resolution MEPC.391(81). [Online]. Available: www.cdn.imo.org
- [100] Federal Ministry for Economic Affairs and Climate Action, National Hydrogen Strategic Update. [Online]. Available: www.bmwk.de
- [101] European Commission, Methane Emission: Carbon Management and Fossil Fuels. [Online]. Available: https://energy.ec.europa.eu/topics/carbon-management-and-fossil-fuels/methane-emissions_en
- [102] S. Kolb, J. Müller, N. Luna-Jaspe, and J. Karl, Renewable hydrogen imports for the German energy transition – A comparative life cycle assessment, 2022.
- [103] S. C. D'Angelo et al., "Planetary Boundaries Analysis of Low-Carbon Ammonia Production Routes," *ACS Sustainable Chem. Eng.*, vol. 9, no. 29, pp. 9740–9749, 2021, doi: 10.1021/acssuschemeng.1c01915.

DECLARATION

I hereby confirm that this thesis is entirely my own work. I confirm that no part of the document has been copied from either a book or any source – including the internet – except where such sections are clearly shown as quotations and the sources have been correctly identified within the text or in the list of references. Moreover, I confirm that I have taken notice of the 'Leitlinien guter wissenschaftlicher Praxis' of the University of Oldenburg.

Zulma Karina Aza

Place, Date: Oldenburg, 17.02.2025

APPENDIX A: WTT pathways losses

Table A1 Efficiencies considered for the e-hydrogen WTT pathways

Phase	Input	Output	Losses	Comment	Reference
H₂ Production		1.020	0.00%	No losses are considered, according to the literature.	[84]
H₂ Compression	1.020	1.015	0.50%		[102]
H₂ Storage	1.015	1.005	1.00%	1%/year	[85]
H₂ Transport	1.005	1.005	0.00%	No losses are considered, according to the literature.	[30]
H₂ Compression BP	1.005	1.000	0.50%		[102]

Table A2 Efficiencies considered for the e-ammonia WTT pathways

Phase	Input	Output	Losses	Comment	Reference
H₂ Production		1.006	0.000%	No losses are considered, according to the literature.	[84]
NH ₃ Synthesis	1.006	1.006	0.016%		[103]
NH ₃ Storage	1.006	1.005	0.062%	Mass Losses.	[61]
NH ₃ Transport	1.005	1.005	0.040%	0.04% ton/day. Only one tanker trip, lasting one day, is needed to transport the mass of ammonia required to operate the ship in one year. Thus, the percentage mass loss per kg of ammonia is 0.04%.	[61]
NH ₃ Cracking	1.005	1.005	0.0001%	Mass Losses.	[73]
H₂ Compression BP	1.005	1.000	0.500%		[102]

Table A3 Efficiencies considered for the e-methanol WTT pathways

Phase	Input	Output	Losses	Comment	Reference
H₂ Production		1.030	0.000%	No losses are considered, according to the literature.	[84]
CH ₃ OH Synthesis	1.030	1.030	0.005%		[61]
CH ₃ OH Storage	1.030	1.030	0.005%	Mass Losses.	[61]
CH ₃ OH Transport	1.030	1.030	0.002%	0.005% ton/day. It is assumed a loss value for ship tanker transportation for truck tanker transportation.	[61]
CH ₃ OH Dehydrogenation	1.030	1.005	2.470%	Mass Losses.	[61]
H₂ Compression BP	1.005	1.000	0.500%		[102]

APPENDIX B: Life Cycle Inventories

This section presents the LCI data for each phase of the synthetic fuel pathways analysed with 1 MJ_{LHV} as a functional Unit. As well as the PEMFC and ICE operation with RT as a functional unit, considering the following aspects:

- Each LCI comprise energy, materials or emission which represents the references flows per phase. In addition to this, the operation of PEMFC and ICE with RT as a functional unit is also covered.
- The values presented in the inventories were calculated in functional units, considering the lifetime of the processes and technologies and assumptions for the storage and transport of synthetic fuels.
- Specific reference flows can be consulted on the literature source indicated in each LCI. H₂ production and H₂ compression at bunkering port inventories applicable to the e-ammonia and e-methanol pathways.
- The inventories presented in this section for electricity comprise the reference flows for the base case of electricity generation scenarios. For future scenarios.
- The inventories presented in this section for electricity comprise the reference flows for the base case of electricity generation scenarios. The value remains the same for future scenarios, but the reference flow area is defined as shown in Section 3.2.4.1.1.

WTT – Case 1: e-hydrogen pathway

Pathway / Phase	H ₂ production		
Functional Unit	1 MJ		
Sources	Delpierre et al. [84]		
Input / Output	Energy/Materials/Emissions	Unit	Value
Output	Hydrogen production, alkaline electrolysis	MJ	1.02
Input	Electricity production, wind, 1-3MW turbine, onshore	kWh	4.18x10 ⁻⁰¹
Input	Market for water, deionised	kg	1.43x10 ⁻⁰¹
Input	Oxygen	Kg	6.67x10 ⁻⁰²
Input	Market for potassium hydroxide	Kg	2.08x10 ⁻⁰⁵
Input	Electrolyser production, 1Mwe, AEL, Stack	Unit	1.25x10 ⁻⁰⁵

Pathway / Phase	H ₂ compression		
Functional Unit	1 MJ		
Sources	Van der Giesen et al. [89]		
Input / Output	Energy/Materials/Emissions	Unit	Value
Output	Hydrogen compression, from 30 to 85 bar	MJ	1.015
Input	Hydrogen compression construction	Unit	8.47x10 ⁻¹³
Input	market for electricity, high voltage	kWh	6.02x10 ⁻³
Input	Hydrogen production, alkaline electrolysis	MJ	1.02
Output	Hydrogen	Kg	4.17x10 ⁻⁰⁵

Pathway / Phase	H ₂ storage		
Functional Unit	1 MJ		
Sources	Wulf et al. [59]		
Input / Output	Energy/Materials/Emissions	Unit	Value
Output	Geological Hydrogen Storage	MJ	1.01
Input	market for electricity, high voltage	kWh	2.87x10 ⁻³
Input	Solution mining for geological hydrogen storage	kg	1.81x10 ⁻¹⁰
Input	Hydrogen compression, from 30 to 85 bar	MJ	1.015
Output	Hydrogen	kg	8.33x10 ⁻⁵

Pathway / Phase	H ₂ transport		
Functional Unit	1 MJ		
Sources	Tsiklios et al. [30]		
Input / Output	Energy/Materials/Emissions	Unit	Value
Output	Hydrogen Pipeline System	MJ	1.01
Input	Pipeline, hydrogen, high pressure transmission	Km	4.43x10 ⁻¹¹
Input	compressor assembly for hydrogen pipeline	Unit	8.84x10 ⁻¹³
Input	compressor operation for hydrogen pipeline	Unit	8.84x10 ⁻¹³
Input	Geological Hydrogen Storage	MJ	1.01

Pathway / Phase	H ₂ Compression BP		
Functional Unit	1 MJ		
Sources	Van der Giesen et al. [89] and Kanchiralla et al. [8]		
Input / Output	Energy/Materials/Emissions	Unit	Value
Output	Hydrogen compression BP	MJ	1
Input	Hydrogen Pipeline System	Km	1.01
Input	market for electricity, high voltage	Unit	2.67x10 ⁻²
Input	Hydrogen compression BP construction	Unit	3.11x10 ⁻¹²
Input	Hydrogen	MJ	4.16x10 ⁻⁵

WTT – Case 2: e-ammonia pathway

Pathway / Phase	NH ₃ production		
Functional Unit	1 MJ		
Sources	D'angelo et al. [103]		
Input / Output	Energy/Materials/Emissions	Unit	Value
Output	ammonia production	MJ	1.1
Input	NH ₃ synthesis catalysts	Kg	2.96x10 ⁻⁶
Input	market for chemical factory, organics	unit	8.47x10 ⁻¹³
Input	market for electricity, high voltage	kWh	3.23x10 ⁻²
Input	nitrogen, from cryogenic distillation, gaseous	kg	4.41x10 ⁻²
Input	Hydrogen production, alkaline electrolysis	MJ	9.62 x10 ⁻³
Output	Ammonia, air	kg	8.76 x10 ⁻⁵
Output	Hydrogen, air	kg	4.12 x10 ⁻⁵
Output	Nitrogen oxides, air	kg	5.38 x10 ⁻⁵
Output	Water, air	m ³	2.56 x10 ⁻¹
Output	Water, water	m ³	5.43 x10 ⁻²
Output	Water, cooling, unspecified natural origin	m ³	8.01x10 ⁻³

Pathway / Phase	NH ₃ storage		
Functional Unit	1 MJ		
Sources	Alghool et al. [61]		
Input / Output	Energy/Materials/Emissions	Unit	Value
Output	Ammonia Storage	MJ	1.1
Input	ammonia production	MJ	1.1
Input	market for electricity, high voltage	kWh	4.00x10 ⁻³
Input	Ammonia Storage construction	unit	3.33 x10 ⁻²
Output	Ammonia, air	kg	1.21 x10 ⁻⁷
Output	Carbon monoxide, non-fossil, air	kg	1.13 x10 ⁻⁵
Output	Particulate Matter, > 10 um, air	kg	2.69 x10 ⁻⁶
Output	Particulate Matter, < 2.5 um, air	kg	2.15 x10 ⁻⁶
Output	Nitrogen dioxide, air	kg	2.15 x10 ⁻⁵
Output	VOC, volatile organic compounds, air	kg	5.38 x10 ⁻⁶

Pathway / Phase	NH ₃ transport		
Functional Unit	1 MJ		
Sources	Alghool et al. [61]		
Input / Output	Energy/Materials/Emissions	Unit	Value
Output	Ammonia Transport	MJ	1.1
Input	Ammonia Storage	MJ	1.1
Input	market for tanker, for liquefied natural gas	unit	1.77x10 ⁻¹⁴
Input	market for port facilities	unit	2.30x10 ⁻¹⁹
Output	market for maintenance, tanker, for liquefied natural gas	unit	1.77x10 ⁻¹⁴
Output	market group for heavy fuel oil	kg	7.24x10 ⁻⁶
Output	Ammonia	kg	9.93x10 ⁻⁷
Output	Arsenic ion	kg	2.73x10 ⁻¹²
Output	Cadmium II	kg	1.77x10 ⁻¹³
Output	Carbon dioxide, fossil	kg	2.26x10 ⁻⁵
Output	Carbon monoxide, fossil	kg	1.94x10 ⁻⁸
Output	Chromium III	kg	1.13x10 ⁻¹²
Output	Copper ion	kg	2.73x10 ⁻¹²
Output	Dinitrogen monoxide	kg	1.15x10 ⁻⁹
Output	Dioxins, measured as 2,3,7,8-tetrachlorodibenzo-p-dioxin	kg	7.25x10 ⁻¹⁸
Output	Hydrochloric acid	kg	4.24x10 ⁻¹⁰
Output	Hydrogen fluoride	kg	4.24x10 ⁻¹¹
Output	Lead II	kg	1.25x10 ⁻¹²
Output	Mercury II	kg	2.05x10 ⁻¹³
Output	Methane, fossil	kg	3.89x10 ⁻¹⁰
Output	NM VOC, non-methane volatile organic compounds	kg	1.94x10 ⁻⁸
Output	Nickel II	kg	1.58x10 ⁻¹⁰
Output	Nitrogen oxides	kg	5.32x10 ⁻⁷
Output	PAH, polycyclic aromatic hydrocarbons	kg	1.45x10 ⁻¹¹
Output	Particulate Matter, < 2.5 um	kg	1.27x10 ⁻⁸
Output	Particulate Matter, > 10 um	kg	1.81x10 ⁻⁸

Output	Particulate Matter, > 2.5 um and < 10um	kg	1.45x10 ⁻⁸
Output	Selenium IV	kg	2.50x10 ⁻¹²
Output	Sulfur dioxide	kg	3.30x10 ⁻⁷
Output	Zinc II	kg	5.73x10 ⁻¹²
Output	Copper ion	kg	7.88x10 ⁻¹³
Output	Fungicides, unspecified	kg	7.55x10 ⁻¹⁴
Output	Hydrocarbons, unspecified	kg	9.41x10 ⁻¹¹
Output	Thiocyanate	kg	1.26x10 ⁻¹⁴
Output	Tributyltin compounds	kg	1.15x10 ⁻¹³

Pathway / Phase	NH ₃ Cracking		
Functional Unit	1 MJ		
Sources	European Commission [85]		
Input / Output	Energy/Materials/Emissions	Unit	Value
Output	Ammonia Cracking	MJ	1.01
Input	Ammonia transport	MJ	4.75x10 ⁻²
Input	market for electricity, high voltage	kWh	4.05x10 ⁻²
Input	magnesium oxide production	kg	1.13 x10 ⁻⁵
Output	market for nickel, class 1	kg	7.24 x10 ⁻⁷
Output	market for zeolite, powder	kg	5.61 x10 ⁻⁵
Output	market for chemical factory, organics	unit	8.47x10 ⁻¹³
Output	ammonia	kg	1.67x10 ⁻⁶
Output	market for nitrous oxide	kg	-4.08x10 ⁻⁸
Output	Nitrogen oxides	kg	1.18 x10 ⁻⁷
Output	Nitrogen dioxide	kg	1.70x10 ⁻⁸

WTT – Case 3: e-methanol pathway

Pathway / Phase	CH ₃ OH Synthesis		
Functional Unit	1 MJ		
Sources	Schmidt et al. [82]		
Input / Output	Energy/Materials/Emissions	Unit	Value
Output	Methanol synthesis, hydrogen from electrolysis, CO ₂ from DAC	MJ	1.03
Input	market for electricity, high voltage	kWh	1.49x10 ⁻²
Input	Hydrogen production, alkaline electrolysis	MJ	9.70x10 ⁻³
Input	Direct Air capture	unit	7.04x10 ⁻²
Input	market for chemical factory, organics	unit	8.47x10 ⁻¹³
Output	Water	m ³	2.98x10 ⁻²
Output	Heat, waste	MJ	8.64x10 ⁻²
Output	Methanol	kg	2.66x10 ⁻⁶

Pathway / Phase	CH ₃ OH Storage		
Functional Unit	1 MJ		
Sources	Ecoinvent [76]		
Input / Output	Energy/Materials/Emissions	Unit	Value
Output	Methanol Storage	MJ	1.03

Input	Methanol synthesis, hydrogen from electrolysis, CO ₂ from DAC	MJ	1.03
Input	market for liquid storage tank, chemicals, organics	ton-km	6.08x10 ⁻¹¹

Pathway / Phase	CH ₃ OH Transport		
Functional Unit	1 MJ		
Sources	Ecoinvent [76]		
Input / Output	Energy/Materials/Emissions	Unit	Value
Output	Methanol Transport	MJ	1.03
Input	Methanol Storage	MJ	1.03
Input	market for transport, freight, lorry >32 metric ton, EURO6	ton-km	2.17x10 ⁻⁰³

Pathway / Phase	CH ₃ OH Transport		
Functional Unit	1 MJ		
Sources	Alghool et al. [61]		
Input / Output	Energy/Materials/Emissions	Unit	Value
Output	Dehydrogenation	MJ	1.01
Input	Methanol Transport	MJ	4.42x10 ⁻²
Input	market for electricity, high voltage	kWh	3.08x10 ⁻³
Input	heat production, natural gas, at industrial furnace low-NO _x >100kW	MJ	8.33x10 ⁻²
Input	iron sulfate production	kg	2.66x10 ⁻⁶
Input	chromium oxide production, flakes	kg	2.75x10 ⁻⁷
Input	copper oxide production	kg	3.03x10 ⁻⁶
Input	zinc oxide production	kg	3.21x10 ⁻⁶
Input	zeolite production, powder	kg	7.33x10 ⁻⁶
Output	Water, cooling, unspecified natural origin	m ³	14.4
Input	market for water, deionised	kg	1.67x10 ⁻¹
Input	market group for concrete, normal strength	m ³	7.86x10 ⁻¹⁰
Input	market for metal working, average for copper product manufacturing	kg	6.91x10 ⁻⁷
Input	steel production, electric, chromium steel 18/8	kg	2.76x10 ⁻⁶
Input	market for steel, low-alloyed	kg	1.07x10 ⁻⁵
Output	Carbon dioxide, fossil	kg	8.08x10 ⁻²
Output	Methanol	kg	2.06x10 ⁻⁴

WTW Scope: PEMFC

Pathway / Phase	PEMFC Electricity Production		
Functional Unit	RT		
Sources	Stropnik et al [93]		
Input / Output	Energy/Materials/Emissions	Unit	Value
Output	PEMFC	RT	1.00
Input	PEMFC electricity production, 1kWe, Stack	unit	7.13x10 ⁻⁴
Input	PEMFC electricity production, 1kWe, Balance of plant	unit	7.13x10 ⁻⁴
Input	Heat, waste	MJ	2.43x10 ⁶
Input	Hydrogen compression BP	MJ	4.03x10 ⁶

Input	Tank Type IV 700 bar carbon fiber/epoxy resin tanks	unit	8.17x10 ⁻⁷
-------	---	------	-----------------------

WTW Scope: ICE

Pathway / Phase	ICE Electricity Production		
Functional Unit	RT		
Sources	Fernandez-Rios et al. [54]		
Input / Output	Energy/Materials/Emissions	Unit	Value
Output	ICE	RT	1.00
Input	Hydrogen compression BP	MJ	4.62 x10 ⁶
Input	ICE Construction	unit	2.45 x10 ⁻⁴
Input	Tank Type IV 700 bar carbon fiber/epoxy resin tanks	unit	5.23 x10 ⁻⁶
Input	generator production, 200kW electrical	unit	1.23 x10 ⁻⁴
Input	market group for diesel, low-sulfur	kg	8.13 x10 ³
Output	Methane, fossil	kg	7.39 x10 ⁻¹
Output	Nitrogen oxides	kg	4.31 x10 ²
Output	Particulate Matter, > 10 um	kg	8.62
Output	Sulfur Oxides	kg	1.58x10 ¹

APPENDIX C: DETAILED ANALYSIS OF OTHER ENVIRONMENTAL IMPACTS.

Figure C1, Figure C2 and Figure C3 present the environmental contribution in normalized impact in percentage (%) by phase for all the cases WTT scope. The environmental impacts included in the graphs are GWP, Acidification, Marine Eutrophication, Energy Resources Material Resources and Land Used for the BC, 2030 and 2050 scenarios. For Figure C3, the GWP category was excluded.

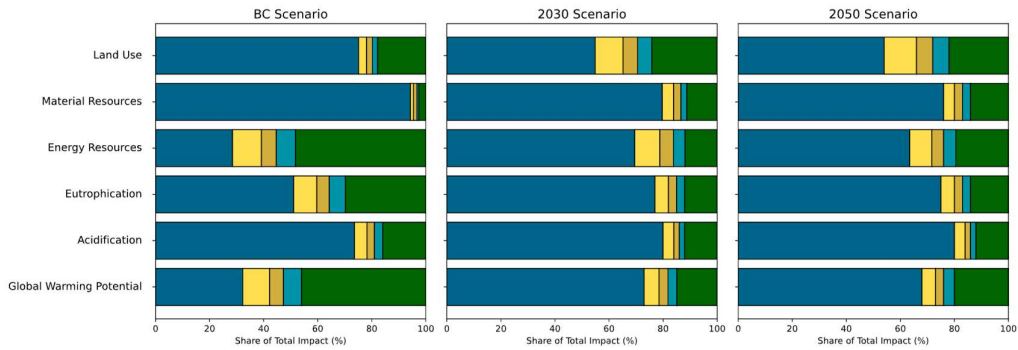


Figure C1 Environmental impacts contribution (%) by phase. WTT e-hydrogen pathway. All scenarios

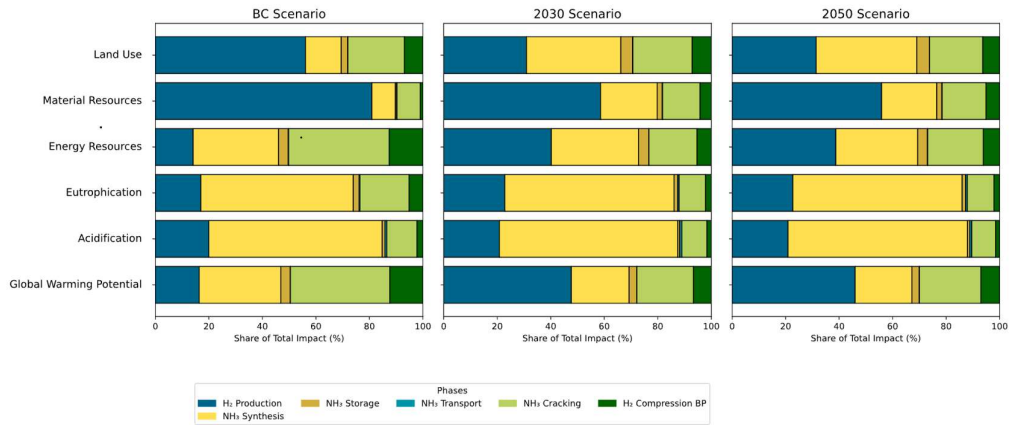


Figure C2 Environmental impact contribution (%) by phase. WTT e-ammonia pathway. All scenarios.

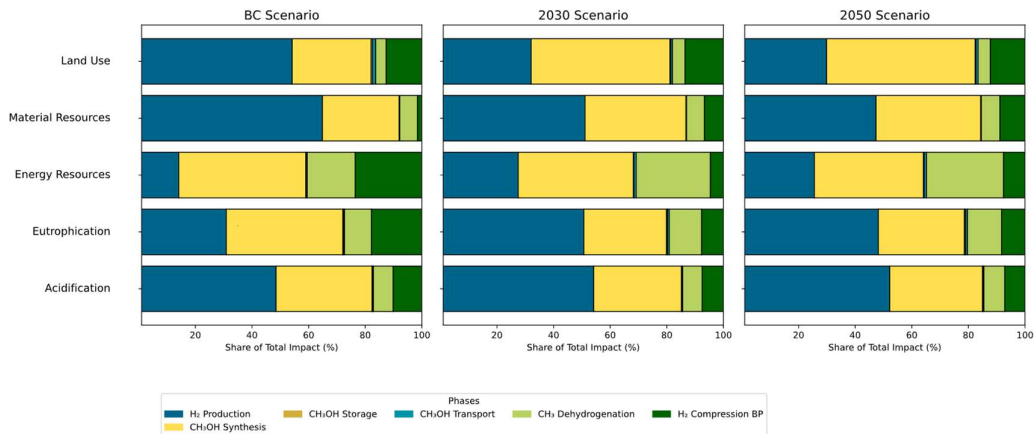


Figure C3 Environmental impact contribution (%) by phase. WTT e-methanol pathway. All scenarios.

Acidification (mol H⁺ Eq) Category Results WTT Scope.

Regarding the e-hydrogen pathway in the BC, the phase with the highest acidification impact for all scenarios is the H₂ production. The electrolyser manufacturing process is responsible for 53% of the impact of this phase. The production of the stack is dominated by nickel production, which has the potential to contribute to the emission of SO_x. For the study, it was assumed that the electricity consumption would be sourced from wind-based electricity; furthermore, the construction of the wind turbines involved steel and copper, which contributed primarily to the emissions of SO_x. As illustrated in Figure C1, the results for H₂ production represent 74%, 80% and 81% for the base case, 2030 and 2050 scenarios. The final compression at the bunkering port was identified as a second contributor to this category, representing 16%, 12% and 11% for the BC, 2030 and 2050 scenarios. This is due to the use of coal and natural gas and, to a lesser extent, the lignite in the electricity production for the BC; this can generate the potential to contribute to the emissions of SO_x. However, for future scenarios, a slight decrease will be due to the 85 process 85e in the share of renewable sources for electricity generation. Finally, for the H₂ compression, storage and transport, the impact contributions are less than 5%. For the BC scenario, the contribution is predominantly attributable to the electricity generation from lignite and hard coal, which are employed in the electricity generation in Germany. Consequently, CO₂, CO and SO_x emissions are produced. Also in these phases, for the 2030 and 2050 scenarios, the contribution is predominantly attributable to the emission in the generation of electricity from biogas and the material production of copper and silicon for electricity generation from PV in Germany and the Netherlands.

Regarding the e-ammonia pathway in the BC, the phase with the highest acidification impact across all scenarios is NH₃ synthesis by the Haber Bosh process. As illustrated in Figure C2, the results for this phase represent a contribution to the pathway of 65% for the BC, 80% and 67% for 2030 and 2050, respectively. The process has NH₃ emissions (0.00163 kg NH₃/kg NH₃) and NO₂ emissions (0.001 kg NO_x /kg NH₃) [90], which results in the highest amount H⁺/MJ_{LHV} in the e-ammonia pathway. The results indicate for BC, the process emissions represent 89% and 92% for the 2030 and 2050 scenarios and are the primary contributor to this category. H₂ production phase represents the second contribution, with a value of 20% for the base case and 21% for the 2030 and 2050 scenarios, respectively. The source for these results is consistent with what was presented for the e-hydrogen pathway. The impact contributions for the storage and transport phases are less than 1% across all scenarios and can be considered negligible. For the NH₃ cracking phase, the impact contribution for the BC corresponds to 11% and will decrease to 9% for the 2030 and 2050, respectively. For the BC, the impact is caused by the emission of NO_x from the process itself and the

emission from the electricity generation from hard coal. In contrast, for future scenarios, it is caused by the emissions of nitrogen oxides from the process itself and the emission from the electricity generation from biogas for the Netherlands. Finally, for H₂ compression at the bunkering port, the impact contribution is less than 2%. As previously stated, the contribution follows the same analysis exposed for the e-hydrogen pathway.

Regarding the e-methanol pathway in the BC, the phase with the highest acidification impact across all scenarios is H₂ production. As illustrated in Figure C3, the results for H₂ production represent a contribution to the pathway of 48% for the BC, 54% and 52% for the 2030 and 2050, respectively. Similarly, as observed in the e-hydrogen pathway, the effect on acidification is attributable to the electrolyser manufacturing process. The CH₃OH synthesis was identified as a second contributor, with a value of 34% for the BC, 31% for the 2030 scenario, and 33% for the 2050 scenarios, respectively. The results are attributable to the heat generated by biomethane, the electricity produced from lignite, and the NO_x emissions associated with the DAC process. In all scenarios, the impact contribution for CH₃OH dehydrogenation was found to be 7%. Given that this process demands heat and as was assumed, the heat generated from natural gas results in the emission of NO_x and SO_x, the latter of which contributes to the acidification impact. Subsequently, the impact contribution of H₂ compression at the bunkering port is 10% for the base case and is projected to decline to 7% in the 2030 and 2050. The results of this analysis are consistent with those previously presented for the e-hydrogen pathway. The storage and transportation phases also contribute to the impact of acidification to a lesser extent, representing less than 1% and can thus be considered negligible.

Marine Eutrophication (Kg N Eq) Category Results WTT Scope.

Regarding the e-hydrogen pathway in the BC, the phase with the highest eutrophication impact for all scenarios is that of H₂ production. As illustrated in Figure C1, the results for this phase represent 52% for the BC and 80% for the 2030 and 2050 scenarios. It was determined that the H₂ production phase resulted in NO_x emissions, which subsequently affected marine eutrophication. In the prospective scenarios, a notable decrease was observed, which can be attributed to the reduction in fossil fuel dependency for the electricity generation that source the other phases. Conversely, H₂ production from wind-based electricity remains consistent across all scenarios. It can thus be concluded that a reduction in the proportion of fossil fuels used in electricity generation will result in a related reduction in NO_x emissions, which will in turn lead to a decrease in the impact on marine eutrophication. H₂ compression at bunkering port was identified as a second contributor, with a value of 30% for the base case and 12% for the 2030 and 13% for the 2050, respectively. The impact of this category can be attributed to NO_x emissions resulting from the electricity generation from natural gas and hard coal

in the Netherlands, in 2030 and 2050. Finally, the impact contributions for the compression, storage, and transportation phases are less than 8% for the BC and less than 5% for the prospective scenarios. These contributions are primarily derived from the NO_x emissions from non-renewable sources for the electricity generation.

Regarding the e-ammonia pathway in the BC, the phase with the greatest value of eutrophication impact across all scenarios is the e-ammonia synthesis. As illustrated in Figure C2, the results for NH₃ synthesis represent 57% for BC and 63% for 2030 and 2050. The impact can be attributed primarily due to the NO_x emissions, with NH₃ emissions representing a secondary impact. Collectively, these two factors account for 69% of the impact in the BC. Moreover, it was observed that the generation of electricity from hard coal and lignite also exerts an influence on the eutrophication category during this phase. For the BC, the NH₃ cracking phase represents the second contribution to this category by 18%. The predominant impact is attributable to the utilisation of hard coal, lignite and natural gas for electricity production, representing 18% of the contribution. Nevertheless, in future scenarios, this impact is projected to decline to 10% as a consequence of the reduction in shares of these sources, as illustrated in Figure C2. H₂ production phase represents the third contributor to the pathway by 17% of the total impact. This contribution is projected to increase to 23% for 2030 and 2050. The analysis of the impact contribution is consistent with that previously outlined for this category in relation to the e-hydrogen pathway. The impact of NH₃ storage on this category is less than 2% in all scenarios and is therefore almost negligible, despite the release of NH₃ emissions during storage. This is due to the assumption of a relatively short storage period made for the case study, which results in a low value and therefore a non-relevant impact on the supply chain. Similarly, the results for NH₃ transport indicate a low value and, consequently, a non-relevant impact on the supply chain across all scenarios. The direct impact of this phase is attributable to the emission of NO₂ resulting from the utilisation of HFO by the sea tanker. Finally, it can be observed that the final compression at the bunkering port represents a value of less than 5% in all scenarios.

Regarding the e-methanol pathway in the base case scenario, the phase with the greatest value of eutrophication impact is that of CH₃OH synthesis. As illustrated in Figure C3, the results for CH₃OH synthesis represent 41% of the total impact for the BC, and it will increase by 30% for the 2030 and 2050 scenarios. In the BC, the marine eutrophication impacts were primarily attributable to the electricity consumption associated with the process itself, as well as the electricity consumption associated with the process. In the 2030 and 2050, the H₂ production will become the primary contributor to this category. This is due to the incorporation of electricity generation scenarios that increase renewable sources in comparison to the BC for subsequent

phases. For the H₂ production, it was assumed that wind-based electricity would be used in all scenarios. Nevertheless, due to the considerable amount of electricity that will be required, it will remain the primary contributor. The CH₃OH dehydrogenation phase accounts for 9% off the BC and is projected to increase by 12% in the 2030 and 2050 scenarios. The primary impact is derived from the electricity consumption required for the process. In all scenarios, the predominant impact can be attributed to the utilisation of natural gas for heat production which resulted in the release of NO_x emissions. Finally, it can be observed that the final compression at the bunkering port represents a value of 18%, 7% and 9% for the BC, 2030 and 2050, respectively. The impact contribution is essentially derived from the NO_x emissions from the non-renewable sources for the electricity generation scenarios. The impact of CH₃OH storage on this category is almost negligible across all scenarios, given that e-methanol does not require special conditions for storage. Similarly, the results for CH₃OH transport indicate a low value despite the use of diesel with low sulphur content in the truck tanker, and thus the impact on the supply chain is non-relevant across all scenarios.

Energy Resources (MJ) Category Results WTT Scope.

Regarding the e-hydrogen pathway in the base case scenario, the phase with the highest value of energy resources impact for the base case scenario is the H₂ compression in the bunkering port, accounting for 48% of the total. This value will decline in the 2030 and 2050, reaching 12% and 19%, respectively. The impact in the compression at the bunkering point can be attributed to the fossil fuels used for electricity generation in the Netherlands in the BC, with coal and natural gas representing the primary contributors. In 2030 and 2050, the impact will be due to uranium production for electricity generation (34%), electricity generation from natural gas (15%), and the market for electricity generation used for photovoltaic cell multi-silicon wafer components for PV electricity generation. The phase with the second contribution to the BC is the H₂ production, which accounts for 28% according to Figure C1. For H₂ production, it was observed that the contribution will be increased to 69% and 63% for the 2030 and 2050, respectively. The influence of fossil fuels on H₂ production can be attributed to the production of steel and, to a lesser extent, the manufacture of carbon fibre, both of which are indispensable for the construction of wind turbines across all scenarios. The increasing contribution of this phase in future scenarios will be due to the use of electricity generation scenarios in subsequent phases, with a significant increase in the share of renewable energy. Finally, for the compression, storage and transport by pipeline, it was observed that for the 2030 and 2050, there was a reduction in the impact contribution as a result of the use of the electricity generation for Germany and the Netherlands, which were exclusively applied to the last two compression units in the transport phase.

Regarding the e-ammonia pathway in the BC, after the H₂ production, the NH₃ production and cracking are the phases with a more significant impact on the energy resource with a contribution of 32% and 38%, respectively, in the BC according to the Figure C2. In this scenario, the electricity generation for Germany was employed for NH₃ synthesis. It was observed that for 2030 and 2050, the contribution will remain almost similar, with a value of 32%, despite the significant reduction indicated in Figure C2. This is due to the fact that, in the BC, the majority of electricity generated in the energy mix is derived from lignite, hard coal, and natural gas. Conversely, in the 2030 and 2050 scenarios, the utilization of renewable sources in electricity generation increases, resulting in a notable reduction in the impact category associated with this phase. Similarly, the NH₃ cracking was observed to contribute 37%, 18% and 20% respectively for BC, 2030 and 2050, respectively. Given the high electricity consumption inherent to the process, the impact decreases with the future electricity generation scenarios for the Netherlands. Finally, in the storage and transport by sea tanker, similar contribution was observed across all scenarios, with value less than 4%. In the case of e-ammonia transport, the impact stems from the use of heavy fuel oil in the ship tanker. However, this is not a significant factor in the overall result, given the assumptions made for the functional unit.

Regarding the e-methanol pathway in the BC, the phase with the greatest impact on energy resources is the e-methanol synthesis, which accounts for 45% of the total. This value will decline in the 2030 and 2050, reaching 40% and 38%, respectively. In the base case scenario, the electricity generation for Germany was employed for methanol production. In this case, the electricity consumption for the process represented 28% of the impact, while the consumption for the direct air capture process represented 38% of the impact on the energy resource, non-renewable category. As previously stated, the electricity generation is primarily composed of light, hard coal, and natural gas. In contrast, in the 2030 and 2050, the proportion of renewable sources in the electricity mix increases, resulting in a significant reduction in the impact category for future scenarios.

Similarly, with a lesser degree of impact, CH₃OH dehydrogenation also contributes to the overall effect, essentially through the utilisation of natural gas used for the production to the heat required for the process, which represents 71% of the phase for the BC and 86% for the 2030 and 2050 as illustrated in Figure C3. For the storage phase, methanol can be stored in a liquid form; therefore, it does not require electricity for the process. Furthermore, the impact of the materials on the construction is insignificant for this category. Regarding the CH₃OH transport, the impact arises from the use of diesel low sulphur in the truck tanker. However, this is inconsequential in terms of the outcome, given the assumptions made by the functional unit. Finally, the compression phase in the bunkering port was observed to contribute 23%, 4%, and 7% for the BC, 2030 and

2050, respectively. Given the considerable electricity consumption inherent to the process, the impact is expected to decrease with the future electricity generation for the Netherlands.

Material Resources (kg Sb Eq) Category Results WTT Scope.

Regarding the e-hydrogen pathway in the BC, the phase with the highest value of material resources impact is H₂ production, accounting for 94%. This value will decline in the 2030 and 2050, reaching 80% and 75% respectively, as illustrated in Figure C1. As was assumed for all synthetic pathways, the electricity consumption for H₂ production would be sourced from wind power. Consequently, nickel and copper are the metals most affected by electricity from wind source. In terms of electrolyser stack construction, copper, steel, and the metals used in the electronics for the control units are the metals production most required by the construction of the stack. In the 2030 and 2050, the same assumption that the electricity consumption would be sourced from wind power was applied; therefore, the result was only affected by the reduction of electricity consumption due to the projected efficiencies. Subsequently, the phase with the second impact contribution for the pathway is the compression at the bunkering point, which is observed to be 3% for the base case scenario and 11% and 15% for the 2030 and 2050, respectively. As the proportion of electricity generated from photovoltaic and wind sources in the Netherlands scenarios increased, the impact increased five- and six-fold in comparison to the BC. This increase is attributable to the utilisation of electricity generation with a greater proportion of renewable sources, namely photovoltaic and wind power. This has the effect of increasing the production of copper and silver, which are employed in the manufacture of multi-Silicon wafers PV panels, as well as nickel and copper, which are used in the production of wind turbines. A similar trend was observed with regard to compression, storage and transport, although in this instance, the electricity mix used for Germany was based on the 2030 and 2050.

Regarding the e-ammonia pathway in the base case scenario, the phase with the highest value of material resources impact in the BC is H₂ production which accounts for 81% of the total. According to Figure C2, this value will decrease for the 2030 and 2050 to 58% and 56%, respectively. This decline can be attributed to the same factors that were identified in the e-hydrogen pathway. Subsequent to this, the synthesis and cracking of NH₃ are the phases with a more significant impact on the material resources. In the BC scenario, for NH₃ production, metals such as silver, copper and steel predominate in electricity production and the material for the construction facilities, with energy production having the most significant impact at 8% for both phases in the BC. It was observed that for the 2030 and 2050, the impact would be increased mainly due to the increase in the use of photovoltaic and wind energy, which in turn increases the use of

metals such as tellurium, aluminium and steel. In the context of NH₃ cracking, it is imperative to acknowledge the significance of not only the impact on energy consumption but also the utilisation of nickel and zeolite, which are crucial catalysts, in the production of which cobalt is a primary constituent. With regard to the storage and transport phases, the impact contributions are less than 2% across all scenarios and can be considered negligible. Finally, the compression at the bunkering port shows an impact contribution of 1% for the base case, which is expected to rise to 4% and 6% for the 2030 and 2050, respectively. This increase can be attributed to the increased electricity consumption required in this phase, as well as the projected growth in the share of wind and photovoltaic power in the prospective scenarios.

Regarding the e-methanol pathway in the BC, the phase with the highest value of material resources impact is H₂ production with a contribution of 65%. This value is expected to decrease for the 2030 and 2050, reaching 51% and 47%, respectively, as illustrated in Figure C3. This decline can be attributed to the same factors that were identified in the e-hydrogen pathway. Subsequent to this, CH₃OH production is identified as the phase with the more significant impact on material resources, contributing 27% for the BC. Within this phase, the amine-based silica production employed in the DAC process exhibits an impact of 82% in this category. In addition, the utilisation of sodium silicate and the heat generation of from biomethane, which in turn employs zinc in its production. The impact of electricity consumption for NH₃ synthesis and the DAC is also less significant, with a contribution of 12%. It is observed that the impact contribution is expected to increase by 35% and 37% in 2030 and 2050, respectively. This is attributable to the projected rise in the utilisation of photovoltaic sources within the electricity generation for Germany in 2030 and 2050, consequently leading to an escalation in the production of copper and the materials required for the photovoltaic multi-SI production. With reference to the storage and transport phases, the impact contributions are less than 1% across all scenarios and can be considered negligible. For the CH₃OH dehydrogenation process, the factor that causes most of the impact is the copper production required for the process catalyst, followed by copper used for the heat production of natural gas used in the process for the BC. While electricity consumption does not significantly influence this category, it is projected to have a growing impact in the 2030 and 2050, attributable to an escalated utilisation of electricity from photovoltaic and wind sources in the Netherlands. Finally, the compression at the bunkering port shows an impact contribution of 1%, which is expected to rise to 6% and 8% for the 2030 and 2050, respectively. This increase could be attributed to the higher electricity consumption required during this phase.

Land Use (Dimensionless pt) Category Results WTT Scope.

With regard to the hydrogen pathway in the BC, the phase exhibiting the most significant land use impact is H₂ production, accounting for 75% of the total impact for the base case. This value is predicted to decrease for the 2030 and 2050, reaching 55% and 53%, respectively (Figure C1). As was assumed the electricity required for the process comes from wind power in onshore production; the impact is due to the occupation of forest land and the conversion of industrial areas due to the installation of wind turbines. In the context of the compression, storage, and transport process, it was observed that the BC required significant electricity consumption, resulting in an intensive occupation of the forest. This is due to the land surface being occupied by electricity generation from wood chips, which are used as a source. For the 2030 and 2050, an increase in land occupation is projected due to the increased PV generation on open ground and the land used for wind-based electricity production. Finally, for the compression at the bunkering port has an impact contribution of 18% for the BC. The 2030 and 2050 demonstrate an increase in photovoltaic generation on open ground of 14% and 13%, respectively, a requirement for greater land occupation and, consequently, an increase in the impact contribution of 24% and 22% for the 2030 and 2050, respectively.

With regard to the e-ammonia pathway in the BC, the phase exhibiting the most significant land use impact is H₂ production, accounting for 56% of the total impact for the base case. This value will decrease for the 2030 and 2050 scenarios to a value of 31% for both scenarios according to the Figure C2. This decline can be attributed to the same factors that were identified in the e-hydrogen pathway. After the e-hydrogen is produced, the NH₃ synthesis is the phase with a second significant impact on the land use category with an impact contribution of 13% for the BC. This will rise by 35% and 37% for the 2030 and 2050, respectively. The predominant factor contributing to this impact is the electricity utilised for the process itself, along with the requirement for the DAC in the BC. In this scenario, the land occupation employs wood chips to co-generate heat and power from wood chips, accounting for 40% of the total impact for this phase. It is projected that the impact will increase for 2030 and 2050 due to the incorporation of photovoltaic electricity sources on open ground within the projected electricity generation scenarios. For the NH₃ storage, an impact contribution of 2% for the BC and 4% for the 2030 and 5% for 2050 were observed. Given that ammonia requires electricity to maintain its refrigerated state, the greatest impact is attributable to the land used due to electricity consumption associated in Germany. As well as the area of industrial transformation is utilized for the storage of the fuel in liquid form. For the transport phases, the impact contributions are less than 1% across all scenarios and can be considered negligible. It is observed that the impact contribution remains almost constant at a value of 20% across all scenarios. The impact for the BC is attributable to the use of land for wood chip production used as source of electricity production, while for future

scenarios, the major impact originates from land use for photovoltaic electricity production. A similar observation can be made regarding compression at the bunkering port, where the impact remains at almost the same value of 7%, which is affected by the land use to produce wood chips in the BC and the land use for photovoltaic farms in 2030 and 2050.

With regard to the e-methanol pathway in the BC, the phase with the highest value of land use impact is H₂ production, accounting for 54% of the total impact. This value is predicted to decrease for the 2030 and 2050, reaching 32% and 30% respectively (Figure C3). This decline can be attributed to the same factors that were identified in the e-hydrogen pathway. After the e-hydrogen is produced, the CH₃OH synthesis is the phase with the second more significant impact on the land use category with an impact contribution of 28% for the BC. This will rise by 50% and 52% for the 2030 and 2050, respectively. In this phase, the effect was primarily attributed to the utilisation of heat produced by biomethane co-generation, which use wood chips from biomethane production, thereby increasing the impact of land occupation. Furthermore, the consumption of electricity for the CH₃OH synthesis and the DAC has been shown to have a significant impact due to the utilisation of wood chips for the generation of heat and electricity. Projections for future scenarios indicate that the incorporation of photovoltaic sources in the German electricity generation, anticipated in the 2030 and 2050, is likely to result in an escalation in the occupation of forest and industrial areas.

For the storage and transport phases, the impact contributions are less than 1% across all scenarios and can be considered negligible. For the dehydrogenation phase, the contribution for the BC represents 3%, and for the future scenarios, 4% will be represented by this phase. The impact for the BC is primarily attributed to the land utilised for the production of wood chips, while the land employed for photovoltaic farms in the 2030 and 2050 is the most significant contributing factor to this category. A similar observation can be made with regard to compression at the bunkering port, where the impact remains at almost the same value of 12%. This is affected by the land use for the production of wood chips for the BC and the land use for the photovoltaics farms in 2030 and 2050.

Impact assessment Other Categories: WTW Scope.

Acidification (mol H⁺ Eq) Category Results – WTW Scope

For PEMFC, the acidification result is 532 mol H⁺ eq/RT for the BC, which will decline by 7% and 8% for 2030 and 2050, respectively as illustrate in Figure 23 Environmental impacts of EF 3.1 categories using PEMFC and ICE per RT - All Scenarios. The decline can be attributable to the rising proportion of renewable sources in in the electricity

generation used for the hydrogen in the WTT, in turn reducing the NO_x emissions. Conversely, the acidification result for the ICE is 1036 mol H⁺ eq/RT for the BC, which will decline by 6% and 11% for 2050 and 2050, respectively. This decline can be attributed due to the emissions of the pilot fuel, as well as the reduction of the NO_x emissions due to the rising proportion of renewable sources in in the electricity generation used for the hydrogen in the WTT. For this category, the predominant substant emitted by the WTW for both technologies is the NO_x in 81% for all scenarios in the PEMFC utilization and 87% in the ICE utilization for the BC and 90% for the 2030 and 2050.

Eutrophication Category Results – WTW Scope

For PEMFC, the eutrophication result is 93 kg N eq/RT for the BC, which will decline by 31% for 2050 and 2050, respectively as illustrated in Figure 23. This decline can be attributed primarily to the NO_x emissions from the use of steel production used in the wind turbine construction, which is employed in generating electricity for H₂ production. Conversely, the eutrophication result for the ICE is 286 Kg N eq/RT for the BC, with a projected decline of 13% for the 2030 and 15% for the 2050, respectively. The primary contributor to this category is the direct NO_x emissions resulting from pilot fuel in the ICE operation. The slight decline observed for 2030 and 2050 can be attributed to the decrease of electricity from hard coal for the future electricity generation, thereby reducing NO_x emissions that affect the eutrophication category.

Energy Resources Category Results – WTW Scope

For PEMFC, the energy resources result is 1600 GJ / RT for the BC, which will decline by 56% and 54% for 2050 and 2050, respectively as illustrated in Figure 23. This decline can be attributed primarily to the increasing use of renewable sources for electricity generation used in the WTT hydrogen pathway, resulting in a reduction in the dependence on fossil fuels for energy production. Conversely, ICE demonstrates a substantially higher energy resources result of 2365 GJ/RT for the base case scenario. This value is projected to decline by 48% for 2030 and 2050. This decline is attributable to the increasing use of renewable energy sources for electricity generation in the WTT hydrogen pathway, leading to a reduction in the reliance on fossil fuels for energy production. However, in the specific case of the ICE, the impact of the production of MFO from fossil fuels remains a predominant factor within this category. In the baseline, it accounts for 20% of the total value of the category, while in 2030 and 2050, it represents 37% of the total.

Material Resources Category Results – WTW Scope

For PEMFC, the material resources result is 1.4 kg Sb eq/RT for the BC, this will increase by 16% and 18% for 2030 and 2050, respectively as illustrated in Figure 23. The results indicates that the primary impact is derived from the production of copper and steel (69.4%) for wind turbine construction, followed by nickel (25%) utilised in the alkaline electrolyser stack as part of the hydrogen as a main fuel. In 2030 and 2050, it was observed that due to the increase in the share of renewable sources, there will be a greater requirement for material production, particularly for the electricity production from photovoltaics, where the utilisation of PEMFC will represent 20% (silver and copper), reducing the percentage of materials required for wind turbine production and AEL stack to 59% and 21% respectively. It is also notable that the materials utilised for MFO production account for less than 1% of all scenarios. Similarly, the material resources result for the ICE is 1.6 kg Sb eq/RT for the base case, which is projected to increase by 14% and 10% for 2030 and 2050, respectively, compared to the BC. The findings reveal that the explanation provided for PEMFC is also applicable to ICE; however, due to the efficiency of ICE, a greater quantity of hydrogen is necessary, thereby resulting in a more significant impact in comparison to PEMFC. In addition, of the materials used for the MFO production which represent less than 1% for all the scenarios.

Land Use Category Results -WTW Scope

For PEMFC, the land use impact result is 883×10^3 pt / RT for the base case scenario as illustrated in Figure 23. This result will increase by 28% for 2030 and by 27% for 2050 scenario. For the base case scenario, the impact can be attributed mainly by two factors, the land used for the onshore wind turbine require to the electricity generation for hydrogen production by 75% and secondly, the land used for the production of the wood chips as a feedstock to produce electricity as part of the market of electricity in the Netherlands for the compression in the bunkering point by 12%. While for the 2030 and 2050 scenarios, the increasing can be attributed in addition to the land used for the onshore wind turbine require to the electricity generation for H₂ production by 64%, and land used for the photovoltaic installation panel in open ground by 29% according to the share of this source for future scenarios. It can be demonstrated that the utilisation of PEMFC has no impact on any of the scenarios within this category. For the ICE, the land use impact result is 1050×10^3 pt / RT for the BC. This result will increase by 26% and 20% for 2030 and 2050 scenario, respectively. The impact can be attributed similarly for all scenarios, in a manner comparable to the PEMFC, but with the distinction that the utilization of an ICE has an effect, amounting to 2.7% and 2.1% for 2030 and 2050, respectively, because of the land used for the MFO production.

APPENDIX D: Comparison between GWP results with prior studies

Table C1 Comparison between GWP results with prior studies

Synthetic Fuel	Phase	Present Study Kg CO ₂ /MJ	Prior Studies Kg CO ₂ /MJ	Percentage of difference %	Reference	Comment
H ₂	H ₂ Production	0.009	0.006; 0.009	0% -34%	[84];[59]	The reference studies used renewable energy as an electricity source.
H ₂	Compression	0.003	0.001	67%	[61]	Reference study use 100% renewable electricity. The present study results use the electricity mix for the BC scenario.
H ₂	Storage	0.001	0.00104	3.8%	[59]	Reference study use 100% renewable electricity. The present study results use the electricity mix for the BC scenario.
H ₂	Transport	0.002	0.0018; 0.0025	6%- 25%	[59];[30]	Reference studies use 100% renewable electricity. The present study results use the electricity mix for the BC scenario.
H ₂	Compression	0.013	N.A	N.A		For reference assumptions, no previous studies were found.
NH ₃	H ₂ Production	0.009	0.006; 0.009	0% -34%	[84];[59]	The reference studies used renewable energy as an electricity source.
NH ₃	Synthesis	0.018	0.012; 0.019	31% - 5%	[61]; [91]	The electricity used for the reference studies was taken from a Concentrated Photovoltaic Thermal Collectors (PVT-C) Plant and Wind Power.
NH ₃	Storage	0.0020	N.A	N.A		The reference study used renewable energy as the electricity source. Divergent assumptions about storage time can vary between studies.
NH ₃	Transport	0.00003	0.00002	23%	[61]	Reference result sea tanker transportation.
NH ₃	Cracking	0.021	0.009; 0.01	133% - 110%	[61]; [91]	The reference studies used renewable energy as an electricity source. Different values of electricity consumption.
NH ₃	Compression	0.013	N.A	N.A		For reference assumptions, no previous studies were found.
CH ₃ OH	H ₂ Production	0.009	0.006; 0.009	0% -34%	[84];[59]	The reference studies used renewable energy as an electricity source.
CH ₃ OH	Synthesis	-0.043	0.016; 0.014	36% 45%	[98]; [61]	The results were compared without prior studies the CO ₂ capture in DAC.
CH ₃ OH	Storage	0.00010	N.A	N.A	[61]	Different scaling value for case study. Differences in assumption for LCI
CH ₃ OH	Transport	0.00021	N.A	N.A		No prior studies were found to have a reference for the result value.
CH ₃ OH	Dehydrogenation	0.087	0.0065	46.1%	[91]	This result was compared with results with non-fossil CO ₂ emissions (0.0065 kg CO ₂ eq/MJ _{LHV})
CH ₃ OH	Compression	0.013	N.A	N.A		For reference assumptions, no previous studies were found.